Technical Report

TR-02-22

Pitting corrosion of copper

An equilibrium – mass transport study

Claes Taxén

Swedish Corrosion Institute

August 2002

Svensk Kärnbränslehantering AB
Swedish Nuclear Fuel
and Waste Management Co
Box 5864
SE-102 40 Stockholm Sweden
Tel 08-459 84 00
+46 8 459 84 00
Fax 08-661 57 19
+46 8 661 57 19

Pitting corrosion of copper

An equilibrium – mass transport study

Claes Taxén

Swedish Corrosion Institute

August 2002

Key words: copper, pitting corrosion, mathematical model, equilibrium, mass transport

Abstract

A mathematical model for the propagation of corrosion pits is described and used to calculate the **potentials below which copper is immune to pitting.** The model uses equilibrium data and diffusion coefficients and calculates the stationary concentration profiles of 26 aqueous species from the bulk water outside a corrosion pit to the site of the metal dissolution. Precipitation of oxides and salts of copper is considered. Studied conditions include water compositions from tap waters to seawater at the temperatures 25°C and 75°C.

Carbonate and sulphate are aggressive towards copper because of complex formation with divalent copper. Carbonate is less aggressive in a corrosion pit than outside at the pH of the bulk. Carbonate carries acidity out from the pit, favours oxide formation and may prevent the initiation of acidic corrosion pits.

The concentration profiles are used to estimate the maximum propagation rates for a corrosion pit. **A high potential is found to be the most important factor for the rate of propagation.** The levels of potential copper can sustain, as corrosion potentials are discussed in terms of the stability of cuprous oxide as a cathode material for oxygen reduction relative to non-conducting cupric phases.

Sammanfattning

En matematisk modell för propagering av frätgropar beskrivs och används till att beräkna de **potentialer under vilka koppar är immun mot gropfrätning.** Modellen använder jämviktsdata och diffusionskonstanter och beräknar stationära koncentrationsprofiler för 26 lösta species från det ostörda vattnet utanför en frätgrop till platsen för upplösningen av metallen. Utfällning av oxider och salter beaktas. Undersökta miljöer innefattar vatten med samman-sättningar från kranvatten till havsvatten vid temperaturerna 25°C och 75°C.

Karbonat och sulfat är aggressiva gentemot koppar på grund av komplex-bildning med tvåvärd koppar. Karbonat är mindre aggressivt gentemot koppar i en frätgrop än utanför vid pH-värdet hos det ostörda vattnet. Karbonat transporterar aciditet ut ur frätgropen, gynnar oxidbildning och kan förhindra att sura frätgropar uppstår.

Koncentrationsprofilerna används till att uppskatta de maximala hastigheterna för propagering av en frätgrop. **En hög potential befinns vara den avgörande faktorn för tillväxthastigheten.** De potentialnivåer koppar kan upprätthålla som korrosionspotentialer diskuteras i termer av stabiliteten hos koppar(I)oxid relativt oledande koppar(II)faser.

Summary and conclusions

A mathematical model for the propagation of corrosion pits on copper is described. The model is used to predict the potentials below which copper is immune to pitting. The criteria used for immunity against pitting is that the volume of the cuprous oxide formed at the site of the metal oxidation at the bottom of a corrosion pit must be smaller than the volume of the oxidised metal. Equal volumes would give a complete coverage of the metal in a pit by adherent cuprous oxide and propagation would not be possible. For potentials where copper is not immune to pitting an estimate of the maximum growth rate is given. The model uses equilibrium data and diffusion coefficients and calculates the stationary concentration profiles from the bulk water outside a corrosion pit to the site of the metal dissolution at the bottom a corrosion pit. Precipitation of oxides as well as of basic salts of copper is considered. A total of 26 aqueous species are considered in waters with compositions ranging from those of tap waters to that of seawater. Calculations are made for the temperatures 25°C and 75°C. The following conclusions may be drawn from the results:

- There is a minimum potential for pitting corrosion of copper. The composition of the bulk water has a big influence on the value of the minimum pitting potential.

- For propagation of a corrosion pit to be possible, there must be a cathode material, which is stable at potentials where pitting is possible. The stability of cuprous oxide relative to the solid cupric phases defines an upper potential above which the anodic dissolution of copper metal in a corrosion pit cannot be driven by a reduction process on cuprous oxide.

- The pH of the bulk water outside a corrosion pit has a small influence on the minimum potential where pitting is possible. The stability of the cuprous oxide against oxidation decreases with increasing pH. The potential window where reduction at a cuprous oxide surface can drive the anodic dissolution in a corrosion pit decreases with increasing pH. Pitting of copper is less likely to occur at high pH values.

- Expressing the difference between the minimum potential for propagation of a corrosion pit and the upper potential for stability of cuprous oxide as a margin against pitting, we find that for a water with given composition, the value of this margin increases with temperature. Pitting is less likely to occur at higher temperatures.

- Of the common anions, chloride is the most aggressive species towards copper. A strong complex formation of chloride with monovalent copper allows high copper concentrations in contact with corroding copper metal. The chloride concentration is decisive for the value of the minimum pitting potential of copper. Using the margin against pitting as a criterion, we find that the value of this margin decreases with increasing chloride concentration. Pitting is, according to these criteria, more likely to occur in waters with high chloride concentrations.

- Carbonate forms strong complexes with divalent copper. Carbonate is more aggressive at the higher pH of the bulk than at the lower pH in a corrosion pit. A high carbonate concentration may facilitate the anodic reactions in a general corrosion. The buffering capacity of hydrogen carbonate at moderately low pH values facilitates the transport of acidity out from the pit. An increased transport rate for protons, in the form of carbonic acid, favours the formation of cuprous oxide in the pit rather than the competing formation of aqueous copper species. A high carbonate concentration may increase the value of the minimum pitting potential and decrease the value of the upper stability potential for cuprous oxide. Pitting is less likely to occur in water with high carbonate concentrations.

- Sulphate forms a complex with divalent copper. Sulphate is aggressive towards copper in a corrosion pit and almost inert with respect to the general corrosion. Pitting is more likely to occur in waters with high sulphate concentrations.

- Calcium may have an indirect beneficial effect. For a water with a high sulphate concentration, pitting is less likely to occur if the calcium concentration is of the same magnitude or higher. Oxygen can also at low concentrations give potentials higher than the minimum pitting potential. The influence at the site of the pit of the direct oxidation of monovalent copper to divalent has a small influence on the minimum pitting potential.

- Corrosion pits where the transport of copper is dominated by monovalent copper may lead to precipitation of large amounts of porous cuprous oxide in and outside the cavity. Where the transport is dominated by divalent copper, precipitation, in the form of basic salts, occurs at higher pH values and outside the cavity.

- Precipitation in the cavity decreases the aqueous cross sectional area available for diffusion and migration to a higher extent than precipitation outside the cavity. Pits where the precipitation occurs mainly outside the cavity have higher growth rates.

- Factors favouring the type of pits dominated by monovalent copper are high chloride contents in the bulk water and high temperature. Factors favouring the type of pits dominated by divalent copper are a high sulphate concentration, low concentrations of other salts and a high potential.

- Pitting of copper has been observed in waters with a composition and temperature such that we find the minimum pitting potential in a range where cuprous oxide is not stable at the pH of the bulk water.

- Pitting of copper is possible in all waters we have studied. In some waters a corrosion pit will not propagate unless the cuprous oxide at external surfaces is stabilised or if there is electronic contact with a conducting more noble phase.

- Limits of the propagation rates for corrosion pits in copper can be given only as conditional of the corrosion potentials.

- In waters with chloride contents approaching that of seawater, pitting is possible with high propagation rates also at high pH values.

Table of contents

1 Introduction

Pitting corrosion of copper has been the subject of many theoretical and experimental studies. Since copper is extensively used in water plumbing, most of the experience of the pitting of copper comes from studies in tap water. In tap water systems pitting corrosion has been known to cause leaks in copper pipes short time after installation.

For an assessment of the integrity of a copper canister for spent nuclear waste against corrosion, the problem of pitting must therefore be addressed. The initial temperature in a deposit is estimated to be about 75°C which is similar to hot water systems but the environment will be soil rather than water. The canisters are to be deposited in compacted bentonite clay, which during uptake of water swells to form a dense mass around the canisters. The integrity of the copper canister against general corrosion has been judged more on grounds of the thermodynamic properties of copper than on experimentally determined corrosion rates. This fact together with the long time perspectives involved has made us take a thermodynamic approach also to the problem of pitting corrosion. Corrosion pits with a slow growth rate may develop and grow for many years under conditions not thought to cause pitting because the process is not identified as pitting.

Although the environment is soil rather than water we treat it as an aqueous system. An aqueous electrolyte is a prerequisite for the pitting of copper where many species diffuse and migrate between the site of a cathodic reaction and the anodic dissolution of copper at the base of a corrosion pit. A mathematical model for equilibria controlling the composition of the solution at various locations in and around a corrosion pit is coupled to the equations for mass transport in a solution without convection. The treatment of the environment as an aqueous system allows us to validate the model by comparing our results to experience and to results from laboratory experiments in water solutions.

Results from the calculations are not intended to form the sole basis for an assessment of the integrity of a copper canister against pitting corrosion. The intention is more to provide a common frame for interpretation of experimental data and for the various types of pitting reported in case studies.

2 Pitting processes

In this section we discuss the conditions that must prevail inside a corrosion pit for propagation to be possible. By a propagating corrosion pit we mean any concave copper surface that corrodes faster than a neighbouring flat copper surface. We establish that there is a maximum pH in a pit for continued growth. Sources of the acidic pH are reactions which reach a sufficient relative rate only above a certain potential which we define as the minimum pitting potential. The exact limits, with respect to pH and potential, are determined by the composition of the water outside the pit and by the temperature. One reaction that is necessary for pitting is the anodic dissolution of copper metal. The pit can not grow faster than the rate determined by the anodic dissolution. Also, the pit can not grow faster than the rate determined by the anodic current out from the pit. Furthermore, a large fraction of the oxidised copper must be transported out from the pit, through diffusion and migration. Otherwise, the pit volume would be completely filled by solid corrosion products. During stationary propagation, the pit grows with a rate determined by the slowest of these interlinked processes. We find experimental support from the literature that the electron transfer during the anodic dissolution of the copper metal is a relatively fast process. A comparison with a certain high pitting rate in section 5.5 shows that the rate is not significantly influenced by the kinetics of the anodic dissolution of the copper metal. The mass transport of aqueous reactants and corrosion products through porous solid corrosion products in the pit is the slow step in the chain; the rate determining step during propagation of a corrosion pit on copper. The anodic dissolution at the bottom of the pit behaves reversibly and can be treated as an equilibrium reaction. From the conditions prevailing at the bottom of the pit, a pH lower than the maximum pitting value and a potential high enough so that the reactions generating the low pH are possible, we calculate how the local equilibrium potential at the bottom of the pit would be observed as a corrosion potential measured between the copper metal and a reference electrode in the bulk outside the pit. The difference between the local equilibrium potential and the measured corrosion potential is the potential drop in the solution in the pit, caused by the passage of anodic current through the solution in the pit. By representing the points for the local condition in the pit and the measurable conditions outside the pit in a potential-pH diagram for copper we can draw some conclusions about the probable state of the unpitted copper surface outside the pit. The oxidation state of the copper surface outside the pit is vital for the pitting process. For a pitting process where the anodic processes in a pit are driven by a reduction at a large external cathodic area, cuprous oxide at an unpitted copper area is a likely site for the cathodic reduction of oxygen.

We find that, for oxygen reduction on electronically conducting cuprous oxide, the stability of the cuprous oxide imposes an upper potential limit. At potentials higher than a certain value the cuprous oxide can be oxidised to cupric oxide or to basic cupric salts. These reactions do not only consume oxygen, which otherwise may drive a pitting process, but also block the access of oxygen to the cuprous oxide by the presence of a non-conducting phase on top of the cuprous oxide. We find that, without introduction of other conductive phases such as carbon films, potentials much higher than the upper stability limit for cuprous oxide are unlikely to arise. If the minimum pitting potential is higher than the upper stability limit for cuprous oxide, pitting will not occur because copper metal in a conceivable corrosion pit would be galvanically protected, not from corrosion but from the

corrosion processes which cause the low pH necessary for propagation. In conclusion, for a water with a known composition, we calculate the minimum pitting potential and the maximum potential supported by cuprous oxide. The difference between the minimum pitting potential and the maximum supported potential is a measure of the margin against pitting. If the minimum pitting potential is lower than the maximum potential supported by cuprous oxide, pitting may occur and a reasonable estimate of the rate can be made.

The existence of corrosion pits driven by a small cathode at the site of the pit at a pH influenced by the anodic processes and lower than the bulk pH, is discussed in section 5.7.

2.1 Our interpretation of pitting

Pitting corrosion may be caused by an autocatalytic process such that the local dissolution rate is increased by processes associated with the local attack. We consider also the possibility that uneven corrosion may arise when large parts of a copper surface are, for some reason, unusually resistant against corrosion. For the latter case, no autocatalytic process is required and a local corrosion attack may occur because of locally lower resistance against corrosion. Our conclusions about the conditions at the site of the metal dissolution in a local corrosion attack are applicable for both cases.

2.2 An anodic condition for pitting

2.2.1 Incomplete coverage by cuprous oxide

Propagation of a pitting process is possible when further oxidation of copper metal at the bottom of the pit leads to an incomplete coverage of the metal by a protective oxide. Complete coverage of the metal by an adherent film of cuprous oxide would block not only the aqueous transport of corrosion products but also the access of water to the metal and thereby prevent further electrochemical oxidation of the underlying copper metal.

2.2.2 Low pH through formation of cuprous oxide

During pit propagation, copper metal at the bottom of the pit is oxidised to aqueous cupric species, to aqueous cuprous species, to cuprous oxide and at high potentials also to cuprous chloride. The oxidation to cuprous oxide, $Cu_2O(s)$, is coupled to a release of protons, which maintains a lower pH in the pit than outside in the bulk of the solution. Aqueous cupric species hydrolyse mainly at higher pH values and precipitate outside the pit and contribute to the low pH but the lowest pH values are to be found at the bottom of the pit and the source of this low pH is the protons released when $Cu_2O(s)$ is formed at the corroding metal.

2.2.3 Diffusion and migration out of the pit

Aqueous copper species and protons are driven out of the pit by diffusion and migration. The relative rates of transport for the species are determined by the concentration gradient and the diffusion coefficient. For the charged species the interaction between the ionic charge and the potential gradient in the solution may increase or decrease the rate of transport. The continuous oxidation and production of positive charge at the local anode at the bottom of the pit and the condition of electro-neutrality cause the potential gradient to have such a polarity that the transport rate of positive ions out of the pit is increased to higher values than diffusion alone would give. Protons, having positive charge and a high value of the diffusion coefficient, tend to have a high relative rate of transport in acid solution.

2.2.4 Balance between production and transport

The fraction of the oxidised copper, which may precipitate as cuprous oxide at the site of the oxidation, is determined by the solubility of the oxide. A low pH at the bottom of the pit leads to a high solubility of cuprous oxide. The fraction of the oxidised copper, which precipitates as cuprous oxide at the site of the oxidation, may therefore be relatively low. While, some cuprous oxide has to precipitate since that reaction seems to be the main source of protons. The oxide is the only hydrolysed form of monovalent copper and the hydrolysis of divalent copper seems to be too weak to sustain a low pH, at least at moderately high corrosion potentials. A low pH, constant in time, at the bottom of the pit requires a continuous production of protons to compensate the loss of acidity from the pit through diffusion and migration. Evidently a continuous propagation of a pitting process on copper requires a balance between the production of protons in the pit and the transport of protons out from the pit or of neutralising species into the pit.

2.2.5 A maximum pH in a corrosion pit

The incomplete coverage of the underlying copper metal by cuprous oxide, which a continuing pitting process requires, is possible only at slightly acid local pH values. The limiting pH is determined mainly by the chloride concentration but also by other factors, which affect the fraction of the oxidised copper, which is precipitated as cuprous oxide at the site of the oxidation. A pH value lower than pH 5 is often required at the bottom of the pit in order to have some free metal exposed. At higher local pH values, the oxidation of a certain volume of copper metal would precipitate as a larger volume of cuprous oxide at the metal surface.

2.2.6 A minimum potential for propagation

The oxidation of copper metal to cuprous oxide at the limiting local pH in the pit requires that the corrosion potential of the copper metal is higher than the equilibrium potential for $Cu(s)/Cu_2O(s)$ at the local pH. The implications of equilibrium considerations work in one direction only. A corrosion potential higher than the equilibrium potential is a necessary but not sufficient condition for precipitation of $Cu_2O(s)$. A corrosion potential higher than the equilibrium potential for $Cu(s)/Cu_2O(s)$ at a pH value lower than that at which the fraction of the oxidised copper which precipitates as cuprous oxide at the site of the oxidation barely covers the underlying metal, is thereby a necessary but not sufficient condition for propagation of a corrosion pit.

2.3 A cathodic condition for pitting

2.3.1 Cathodic reactions

One of the most common oxidising agents is dissolved oxygen. The electrochemical reduction of oxygen to water or to hydroxide is accompanied by a release of alkalinity or a consumption of acidity, depending on the pH at the site of the reaction. In both cases the reduction of oxygen causes a tendency to an increase in the pH locally. Other examples of oxidising agents are divalent copper, trivalent iron and hypochlorite. For both copper and iron the tendency to form hydroxide complexes are stronger for the higher oxidation state than for the lower. A reduction of the oxidation state of copper or of iron therefore has a tendency to increase the pH locally. A similar alkalisation would be expected if hypochlorite is present in the bulk water and reduced to chloride.

Although reductions from one solid oxide to another may not show this tendency, we find no likely oxidising agent for which the electrochemical reduction is coupled to a tendency to decrease the pH at the site of the reduction. We conclude that, whatever the oxidising agent, the pH at the site of the reduction is not likely to be lower than the bulk pH.

2.3.2 Conditions at the site of the cathode

In the potential-pH diagram in figure 2-1 the line *BA* represents a corrosion pit we have calculated. The measurable corrosion potential is about +285 mV, point *B*. The potential which the copper metal and the conductive cuprous oxide at the site of metal dissolution in the pit are subjected to is slightly lower, because of the potential drop in the solution, +269 mV, point *A*. The potential of cuprous oxide, in contact with the underlying copper metal but far from the site of the pit, is close to the measured corrosion potential since the potential drop in solution between the bulk and a surface under slow general corrosion, at a pH similar to that of the bulk, is low. The cathodic reactions necessary to drive the anodic reactions in the pit must take place at an electronically conductive surface. The effect of the cathodic reduction of oxygen on the pH, at a conductive surface, is that the local solution at the surface is slightly alkalised. Point *D* in figure 2-1 represents a point which would meet the specifications above for a cathodic site; the pH is slightly higher than the bulk pH which is pH 7.0, and the potential is such that the electronically conductive $Cu_2O(s)$ may have a stability compared to CuO(s). Basic sulphate and carbonate cupric salts may be more stable than $Cu_2O(s)$ at point *D*, but $Cu_2O(s)$ is not stable at higher potentials.

However, electric current in the electronically conductive phases passes only from positive to negative potentials so a cathode at point *D* can not drive an anode at point *A*. The stability of the cathode material, cuprous oxide, imposes an upper limit for the potential at which pitting of copper, with spatially separated anode and cathode, is possible. Above a certain potential value the copper metal in a conceivable corrosion pit is galvanically protected not only by cuprous oxide at sites where the cathodic reaction takes place, but by all cuprous oxide exposed to the bulk water. Below this potential there may still be corrosion of the cuprous oxide cathode but only in the form of anodic dissolution to aqueous cupric species and chemical dissolution to aqueous cuprous species. If the minimum pitting potential is lower than the upper stability limit for $Cu_2O(s)$, compared with solid cupric phases, the cathodic reduction of oxygen at cuprous oxide may drive an anodic corrosion pit as well as the general corrosion of the cuprous oxide.

The extent of the galvanic protection of copper metal in a pit by cuprous oxide at the pH of the bulk depends very much on the kinetic inertia of the cuprous oxide. The electrochemical corrosion of cuprous oxide to cupric oxide or to basic cupric salts is associated with a rate dependent activation over potential. The higher the rate of the oxygen reduction the higher the rate of the anodic reactions. The oxidation of cuprous oxide to cupric solid phases is forced to higher potentials and the potential may or may not reach a value at which copper metal at a pitting pH is not thermodynamically stable with respect to cuprous oxide. However, the protection by oxidation of cuprous oxide to solid cupric phases against pitting corrosion is twofold. Cathodic current is consumed by the oxidation and the access of oxygen from the bulk to cathodic sites on the cuprous oxide is blocked by the cupric oxide so that the overall rate of the oxygen reduction decreases. Furthermore, a particular cathodic site where the cuprous oxide exhibits a high degree of inertia against oxidation is becoming more alkaline by the oxygen

reduction giving a locally higher driving force for the oxidation. This illustrates the importance of avoiding conductive, non-corroding surfaces on copper. The detrimental effect of carbon films on copper with respect to pitting may be attributed as much to inertness against oxidation and dissolution as to superior catalytic effects for the oxygen reduction. Returning to figure 2-1, there may exist a small potential interval where cuprous oxide is stable relative to cupric oxide and where copper metal at a pitting pH is not thermodynamically stable. The rate of a pitting process, at such a relatively high pH at the bottom of the pit, is very low because the pit volume is almost completely filled by cuprous oxide with low porosity so that the resistance against aqueous current transport in the narrow channels in the pit is high. The pit depth as a function of time for such pits, assuming various pit geometries, is estimated from our model for the mass transport in and around the pit.

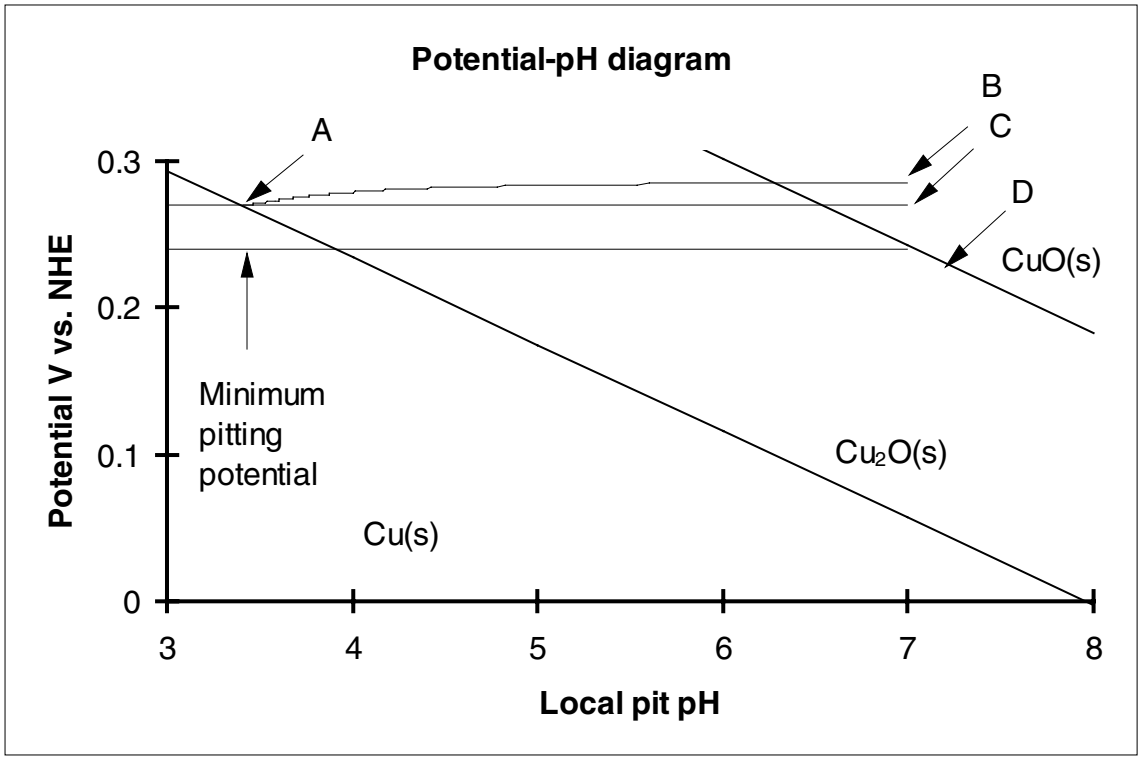

Figure 2-1. Potential pH diagram showing the relative stability regions for copper metal, cuprous oxide and cupric oxide at 25°C. See Text.

3 The model and the calculations

In this section we discuss the mathematical modelling of the mass transport and local equilibria in and around a corrosion pit. The geometric frame for the modelling of the mass transport is selected so that neither the exact shape nor the size of the corrosion pit has to be known. We achieve this by segmenting the site of the pit into volume elements such that a geometric factor is constant between the elements. This geometric factor describes the influence of the shape and size of the element on the rate of mass transport through the element. After the concentration profiles at the site of the pit have been calculated we can draw reasonable conclusions about the likely shape of a pit with this particular aqueous chemistry.

In the calculations of the concentration profiles, in and around a pit, we assume that there is local equilibrium within each volume element. The equilibrium concentrations for a large number of aqueous species, which are likely to be present in a corrosion pit, are calculated for each element. Solids may precipitate and dissolve to satisfy the equilibrium conditions. Cuprous oxide, which is commonly found in corrosion pits, may, because of its electronic conductivity, also provide sites for redox reactions. Given the geometric frame, the equilibrium conditions, a set of specified assumptions and approximations, we can calculate the concentration profile in and around a corrosion pit. Depending on the boundary conditions, the pit may or may not be able to propagate.

The boundary conditions include the bulk composition of the solution with which copper is in contact. The limits of the boundary conditions for which propagation of a corrosion pit is possible, result in a value for the minimum pitting potential of copper in a water with the specified composition. If we try to model a pitting process using boundary conditions which lead to a corrosion potential lower than the minimum pitting value, we find that this pit is not able to propagate. By calculating the concentration profile in a conceivable corrosion pit we determine the domains in which pitting is possible and the domains in which copper is immune to pitting.

The pitting domain is, in a water of a given composition, represented as a minimum pitting potential. For the free corrosion potential to attain a value higher than the minimum pitting potential, a cathodic process is required to take place at that potential. A site for this cathodic process is at the cuprous oxide surface outside the site of the pit. The likelihood that cuprous oxide is stable and accessible for aqueous oxygen decreases with increasing potential. We determine likely values for the maximum corrosion potentials at which cuprous oxide can act as a cathode. By matching the minimum potential at the anodic pit against the maximum potential at a cuprous oxide cathode we make a more precise and narrow estimate of the pitting domain than from the anodic condition alone. In the domain where pitting may occur we use the concentration profiles to estimate the pitting rate. Using a likely shape of the corrosion pit, an assigned value of the geometric factor for the volume elements corresponds to a certain depth of the pit. An assigned value of the geometric factor allows the growth rate to be calculated from the concentration profile. The development of the pit depth with time can be estimated from an integration of the growth rate. Our method for estimating the pitting rate is described in appendix 1.

3.1 A geometric model of the site of a corrosion pit

Figure 3-1 illustrates schematically how we imagine the site of a corrosion pit on copper. There is a cavity in the copper metal caused by a preferential anodic dissolution at the bottom of the cavity. Porous corrosion products fill up a large fraction of the cavity volume but extend also outside the cavity and outside the plane of the unpitted copper metal. Aqueous reactants and corrosion products diffuse and migrate between the bulk of the solution outside the pit and the site of the anodic dissolution at the bottom of the pit. Chemical transformations between aqueous species take place everywhere so that local equilibrium is always attained. Precipitation of solid corrosion products occurs whenever a local solution is saturated with respect to the solid.

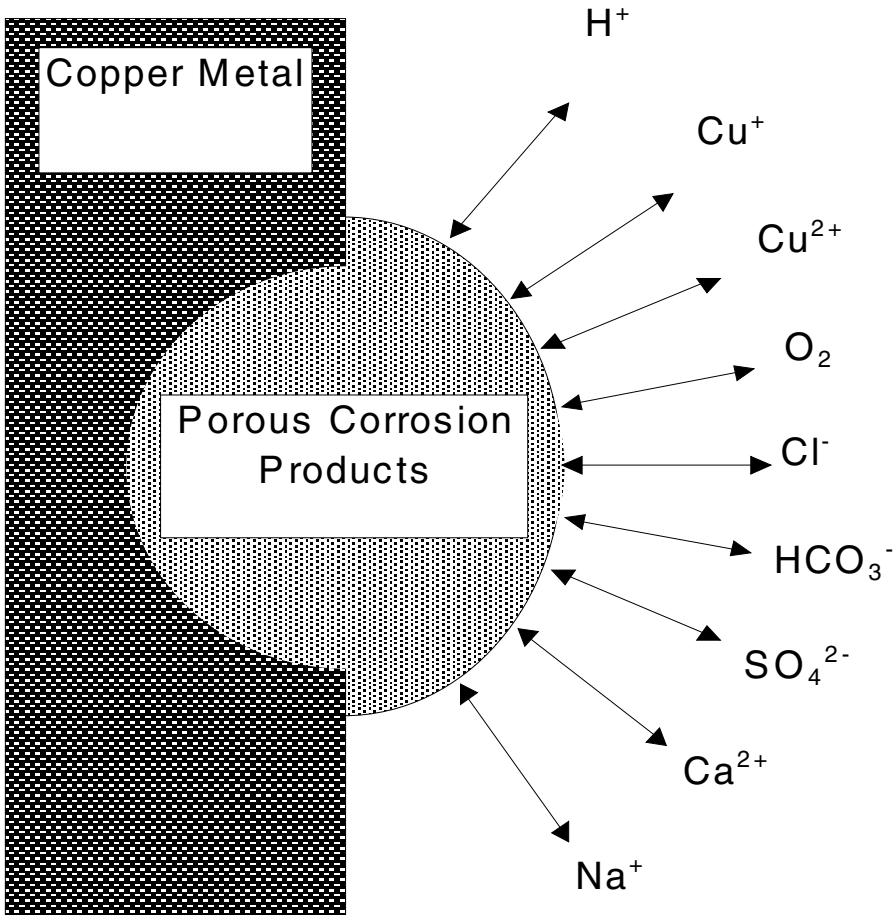

Figure 3-1. Schematic illustration of the site of a corrosion pit in copper with aqueous species diffusing and migrating between the bulk of the solution outside the crust of corrosion products and the site of metal oxidation at the bottom of the pit.

Figure 3-2 shows a schematic illustration of the description of the site of a corrosion pit as consisting of thin shells. The division is such that the ratio between the aqueous area and the thickness of the shell is constant between all shells. The mass transport through such shells is approximated as that through rectangular elements in one dimension. This approximation allows us to model the chemical behaviour of a corrosion pit without exact knowledge of the shape of the cavity or the shape of the crust of corrosion products outside the pit.

3.2 Equilibrium in a corroding system

By equilibrium we mean a local equilibrium in a small volume element. The site of the corrosion pit is considered as consisting of small volume elements, each in local internal equilibrium but not in equilibrium with neighbouring elements. The thin shells indicated in figure 3-2 are small only in one dimension, but since we treat the mass transport as unidirectional, the chemical composition of the solution is the same everywhere in the shell like element. The local equilibria attained are therefore also the same everywhere within an element.

Diffusion of an aqueous species between elements is a result of a difference in the activity of the species. The influx to a volume element is balanced by an outflux so that, during the stationary conditions we consider, there is no accumulation in a volume element. The effect of the flux through a volume element on the distribution of a component into various species containing that component is neglected. Local equilibrium is attained instantly so that, for example, the distribution of the total carbonate into hydrogen carbonate and carbonic acid is determined only by equilibrium at the local pH, in a volume element. The distribution is not influenced by the form in which carbonate enters or leaves the element through diffusion and migration.

3.3 The chemical system

3.3.1 The aqueous and solid compounds considered

Table 3-1 shows the aqueous species and the solid substances used to describe the chemical system in and around a corrosion pit on copper. Activities of species in the first column are calculated from activities of the components along the first row. As with most equilibrium calculations, the choice of components can be made with some degree of freedom. We use simple species that are mutually independent and have a high relative stability in the neutral to acid region, as components.

3.3.2 Thermodynamic data

The main part of the thermodynamic equilibrium constants in table 3-1 is taken directly from compilations made by Wallin /3-1/ and Lewis /3-2 /. Other sources have been Stability Constants /3-3, 3-4/ and Critical Stability Constants /3-5/. For some species not considered by Lewis, we have recalculated stability constants for 25°C to 75°C using the method of Criss and Cobble as described by Lewis /3-6/. For one of the basic sulphate salts of divalent copper and for an aqueous calcium carbonate complex we have not found background data required for such a recalculation. The basic sulphate salt antlerite is neglected at 75°C and the aqueous calcium carbonate is included with the same stability constant as at 25°C.

The activity of a species k in the left side column in table 3-1 is calculated from the activities of the components along the first row according to:

$$lg\ a_k = lg\ k_k + \sum_{n=1}^{N} M(k,n)\ lg\ a_n \qquad 3\text{-}1$$

M(k,n) is the stoichiometric content of component *n* in species *k*.

3.3.3 Activities and activity coefficients

The activities of the charged species are calculated from the concentrations, using Davies' approximation for the activity coefficients, g /3-7/.

$$\log\ \gamma = -Az^2\left(\frac{\sqrt{I}}{1+\sqrt{I}} - 0.2I\right) \qquad 3\text{-}2$$

where *I* is the local ionic strength and *A* is a temperature dependent constant calculated as:

$$A = 1.82x10^6(\varepsilon \cdot T)^{-3/2} \qquad 3\text{-}3$$

e is the dielectric constant for water. We use a value of 0.51 for *A* at 25°C and a value of 0.57 for *A* at 75°C. For neutral aqueous species we equate the activity with the concentration. Water is assumed to be present at unit activity.

3.3.4 Diffusion coefficients

Values for the diffusion coefficients in table 3-1 come from a variety of sources, handbooks, textbooks and journals. For some complex aqueous species no value for the diffusion constant has been found in the literature and a value has been estimated from the complexity of the species and a likely value of the ionic radius. The diffusion coefficients, *D*, for the higher temperature were calculated by use of the approximate relation /3-8/:

$$\frac{D\eta}{T} = constant \qquad 3\text{-}4$$

η is the viscosity of the solution. Using viscosity data for pure water /3-9/, an increase in the values of the diffusion coefficients by a factor of about 2.7 was obtained for a temperature increase from 25 °C to 75 °C.

3.3.5 Properties of the solid oxides and salts

All salts and oxides with the exception of cuprous oxide are considered to be insulators. $Cu_2O(s)$ is known to be a good semi-conductor and at the low current densities considered here, we assume that cuprous oxide behaves as a metallic conductor.

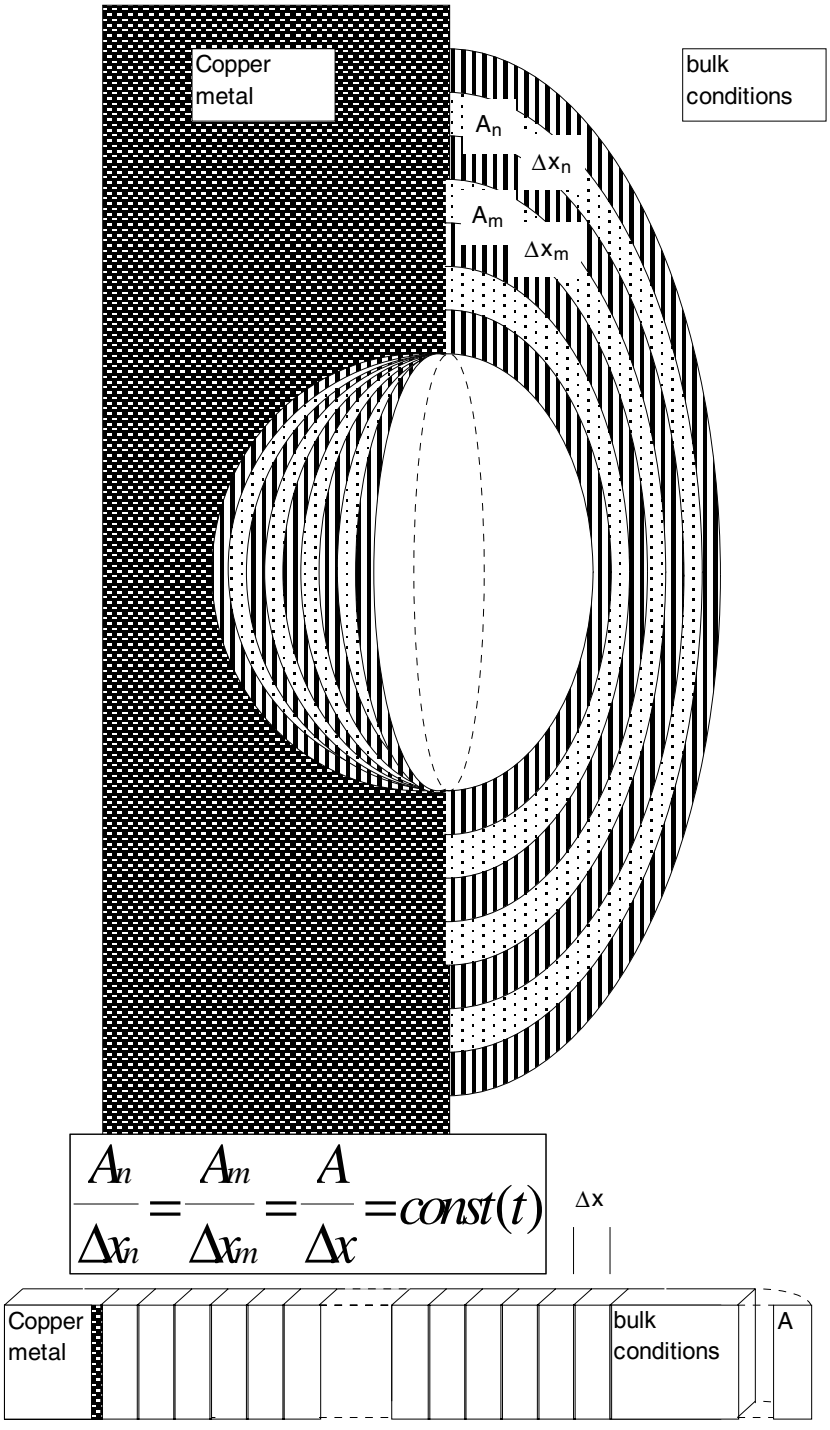

Figure 3-2. Schematic illustration of the description of the site of a corrosion pit as consisting of thin shells such that the ratio between the aqueous area of the shell surface and the thickness of the shell is constant. The mass transport through such shells is approximated as that through rectangular elements in one dimension.

Table 3-1. The chemical system considered. Diffusion coefficients for the aqueous species at 25°C and at 75°C. Equilibrium constants for the aqueous and solid species at 25°C and at 75°C. The charge of the aqueous species is shown and the stoichiometric contents of the components along the first row for all species is shown**.**

	$D \cdot 10^5$ (cm^2/s)		lg k		z	H^+	Cu^+	HCO_3^-	Cu^{2+}	SO_4^{2-}	Cl^-	Ca^{2+}	Na^+
	25°C	75°C	25°C	75°C									
H^+	9.31	25.83			1	1							
Cu^+	1.20	3.33			1		1						
HCO_3^-	1.18	3.27			-1			1					
Cu^{2+}	0.71	1.97			2				1				
SO_4^{2-}	1.06	2.94			-2					1			
Cl^-	2.03	5.64			-1						1		
Ca^{2+}	0.79	2.19			2							1	
Na^+	1.33	3.70			1								1
OH^-	5.27	14.61	-14.00	-12.70	-1	-1							
CuCl	1.20	3.33	2.70	2.71			1				1		
$CuCl_2^-$	1.20	3.33	5.50	5.60	-1		1				2		
$CuCl_3^{2-}$	1.20	3.33	5.70	4.96	-2		1				3		
$Cu_2Cl_4^{2-}$	0.90	2.50	13.10	9.50	-2		2				4		
CO_3^{2-}	0.92	2.55	-10.33	-10.17	-2	-1		1					
CO_2	1.92	5.32	6.352	6.05		1		1					
$Cu(OH)^+$	0.73	2.02	-8.00	-6.25	1	-1			1				
$Cu(OH)_2$	0.77	2.13	-15.06	-11.95		-2			1				
$Cu_2(OH)_2^{2+}$	0.50	1.38	-10.36	-8.80	2	-2			2				
$CuCl^+$	0.71	1.97	0.40	1.16	1				1		1		
$CuCO_3$	0.65	1.81	-3.60	-1.60		-1		1	1				
$Cu(CO_3)_2$	0.62	1.71	-10.83	-7.68	-2	-2		2	1				
$CuSO_4$	0.64	1.77	2.36	2.04					1	1			
$CaSO_4$	0.71	1.97	2.31	2.48						1		1	
$CaCO_3$	0.71	1.97	-	-6.53		-1		1				1	
$CaHCO_3^+$	0.71	1.97	1.00	1.00	1			1				1	
O_2(aq)	2.10	5.82	-	-		-4	-4		4				
Cu_2O(s)			0.80	0.00		-1	1						
CuCl(s)			6.73	6.30			1				1		
CuO(s)			-7.62	-6.00		-2			1				
$CuCO_3$(s)			-0.70	0.13		-1		1	1				
$Cu_2(OH)_2(CO_3)$(s)			-5.16	-3.37		-3		1	2				
$Cu_3(OH)_2(CO_3)_2$(s)			-2.70	-0.42		-4		2	3				
$Cu_4(OH)_6SO_4$(s)			-	-11.6		-6			4	1			
$Cu_3(OH)_4SO_4$(s)			-8.79			-4			3	1			
$Cu(OH)_2$(s)			-8.64	-7.18		-2			1				
$Cu_2(OH)_3Cl$(s)			-7.40	-5.90		-3			2		1		
$CaCO_3$(s)			-1.79	-1.08		-1		1				1	
$CaSO_4$(s)			5.04	5.55						1		1	
$peCu^+$			8.76	8.00			1						
$2peCu^{2+}$			11.44	11.00					1				
$peCu^{+1/+2}$			2.68	3.00			-1		1				

3.4 Assumptions made

A mathematical modelling of the behaviour of a corrosion pit in copper requires a number of assumptions and approximations. Some of these are explicitly stated in the text while others are more implicit. The validity of the assumptions is discussed in section 5. The calculations of the concentration profiles in and around a corrosion pit and the determination of the pitting potentials are based on the following assumptions and approximations:

- diffusion and migration are the only modes of transport
- the changes in the pit geometry caused by the pitting process are so slow that diffusion and migration of aqueous species can be regarded as occurring in a fixed geometry.
- the growth rate of the pit is so low that the solution and porous solids in any small volume element in the pit can be considered to be in local internal chemical equilibrium where the equilibrium constants are given in table 3-1.
- specific interaction between aqueous species can be neglected and activity coefficients for charged species can be calculated as a function of the local ionic strength according to equation 3-2.
- there is one axis in and outside the pit around which there is rotational symmetry. Perpendicular to this axis of symmetry there are surfaces along which no concentration changes. The flux of an aqueous species is always perpendicular to these surfaces.
- the flux of an aqueous species between two such surfaces separated by the distance Δx can be calculated by equation 3-5.
- if the two surfaces do not have the same centre of curvature, the distance separating them will not be constant but will vary with the distance from the axis of symmetry. For such surfaces there exists an average distance Δx_m such that equation 3-5 can be used.
- aqueous species diffuse and migrate through the pores in porous solid corrosion products and deposits without specific interaction with the solid.
- we do not allow a net dissolution of any solid phase from a volume element as that would not be consistent with stationary propagation. Metallic copper is the exception.

3.5 Mass transport and equilibrium problems

3.5.1 A mathematical formulation

We regard the site of the corrosion pit as segmented into volume elements. All elements have the same ratio between the aqueous cross sectional area and thickness, as indicated in figure 3-2. For simplicity, the equations are formulated for volume elements of unit dimensions, where appropriate.

3.5.2 Diffusion and migration

The equation used to calculate the flux, j, in moles per second of species n from element $i\text{-}1$ to element i is:

$$j_{n,i} = D_n \left[(C_{n,i} - C_{n,i-1}) + \frac{C_{n,i} - C_{n,i-1}}{\ln \frac{C_{n,i}}{C_{n,i-1}}} \left(\ln \frac{\gamma_{n,i}}{\gamma_{n,i-1}} + \frac{z_n F}{R\,T} (\Phi_i - \Phi_{i-1})\right)\right] \quad 3\text{-}5$$

where D is the diffusion coefficient, C is the concentration, g is the activity coefficient, z is the charge and F is the electrical potential. This expression for the flux is a result of the integration from x_0 to x_1 of the differential equation:

$$j_n = -D_n \left[\frac{\partial C_n}{\partial x} + C_n \left(\frac{\partial \ln \gamma_n}{\partial x} + \frac{z_n F}{R\,T} \frac{\delta \Phi}{\partial x}\right)\right] \quad 3\text{-}6$$

The integration was made with the approximation that the concentration gradient is constant between x_0 and x_1 . The differential equation was obtained by combining the equations:

$$j_n = -\frac{C_n D_n}{R\,T} \frac{\partial \mu_n}{\partial x} \quad 3\text{-}7$$

$$\mu_n = \mu_n^0 + RT \ln a_n + z_n F \Phi \quad 3\text{-}8$$

m_n is the chemical potential of species n, a_n is the activity and z_n is the charge. Since, in our system, the electrical potential may vary along the x-direction, the effects of the electrical potential on the chemical potential of charged species must be considered. The expression for the chemical potential contains a term for the change in the molar free energy caused by the electrical potential. The standard state is unit activity on the molar scale at potential zero. However, since we here are interested only in the potential gradient, the choice of potential reference is arbitrary.

3.6 Boundary conditions

The boundary conditions used to calculate the concentration profile in a corrosion pit and the mass transport rates contain the bulk concentrations or activities and a value for the flux of each component. All combinations of component fluxes are not consistent with the assumption of a stationary growth of a corrosion pit. We find that each combination of component fluxes that is consistent with these conditions corresponds to a unique value of the corrosion potential of the copper metal. By selecting a combination of component fluxes we implicitly select a corrosion potential for copper metal during pitting.

3.6.1 Constant component fluxes

The fluxes of components are constant under stationary conditions. E. g. in a region of a corrosion pit where chloride is not precipitated as a salt, the flux of chloride from element $i\text{-}1$ to i must equal the flux from element i to $i+1$. In our stationary model there is no accumulation of mass in an element unless precipitation occurs in that element. Chloride may in a pit occur not only as Cl^- but also as complex species e.g. CuCl and $CuCl_2^-$. The concentration of Cu^+ is not necessarily the same in the elements $i\text{-}1$, i, and

i+1, but there is in general a concentration gradient from the bottom of the pit to the bulk solution. The condition for stationary flux of chloride therefore has to include chloride in all species in which chloride occurs. The fraction of the flux of chloride as Cl^- from element *i-1* to *i* may be, and in general is, different from the flux of chloride as Cl^- from element *i* to *i+1*. The total flux of chloride atoms into an element is the same as the total flux of chloride atoms out of that element unless chloride is precipitated as a salt. If no chloride containing salt is precipitated in the pit then the total flux of chloride atoms is zero. If a chloride-containing solid is precipitated there is a flux directed towards the pit.

We find combinations of values for the fluxes of the components such that the fluxes are consistent with the precipitated solid phases. For each flux there has to be a matching source in or at the corrosion pit. For most components we can immediately say whether the flux is directed towards the pit or from the pit or if the flux is zero. Sodium is never precipitated in the corrosion pits we consider and since there is no source in the pit, the flux of sodium is zero. Solid cuprous chloride may or may not form so the flux of chloride is either directed towards the pit or equal to zero, respectively. We use an iterative method (trial and error) to determine values of the fluxes so that the calculated concentration profile is consistent with the stationary growth of a corrosion pit. By stationary growth we mean that a solid phase precipitates where that phase is already present and only there. In terms of the stoichiometric matrix, the stationary flux of the component *j*, which is constant between elements, can be written:

$$j_n = \sum_{k=1}^{N} M(k,n)\ j_k \qquad 3\text{-}9$$

M(k,n) denotes the stoichiometric contents of the component *n* in the species *k*.

3.6.2 Precipitation of oxides and salts

Precipitation of $Cu_2O(s)$ according to: $2\ Cu^+ + H_2O \Rightarrow Cu_2O(s) + 2\ H^+$ leads to changes in the component fluxes of Cu^+ and H^+ according to the stoichiometry of the oxide.

$$j_{Cu^+,i+1} = j_{Cu^+,i} + \Delta j \qquad 3\text{-}10$$

$$j_{H^+,i+1} = j_{H^+,i} - \Delta j$$

Δj is such that the equilibrium condition for $Cu_2O(s)$ is fulfilled. In general, precipitation of a metal ion as a solid salt or as an oxide leads to a change in the component flux of the metal, *Me*, to a change in the component flux of the ligand, *L*, and to a change in the component flux of protons according to the coefficients in the stoichiometric matrix, *M*, for the precipitated solid:

$$j_{Me,i+1} = j_{Me,i} + M_{solid,Me}\ \Delta j \qquad 3\text{-}11$$

$$j_{L,i+1} = j_{L,i} + M_{solid,L}\ \Delta j$$

$$j_{H^+,i+1} = j_{H^+,i} + M_{solid,H^+}\ \Delta j$$

Δj is such that the equilibrium condition for the solid is fulfilled. The correct value of the change in flux of the copper component, Δj, is found by a Newton-Raphson iteration with a numerically determined derivative.

3.6.3 Determination of the concentration profile

A large part of the numerical calculations consists of finding the concentrations and activities in the next element so that all component fluxes attain the desired values, respectively. For a given set of component fluxes we assume a set of component activities, assume an ionic strength, calculate the concentrations of all charged species, calculate the ionic strength and the activity coefficients and iterate until consistent. The concentrations of the neutral aqueous species are then calculated.

With the assumed set of component activities and consistent concentrations a potential difference is further assumed before the component fluxes are calculated. The deviation from neutrality and the deviations from the desired fluxes are used to estimate the change in potential difference and the changes in component activities required to make the solution charge equal to zero and to bring each component flux equal to the desired value, respectively. Since a change in one component activity may change several component fluxes, the influence of a change in each component activity on that component as well as on the fluxes of all other components is calculated. Taking the partial derivatives, this leads to a linear equation system, which is solved by conventional methods.

The new set of component activities is used to calculate a new ionic strength and a new set of concentrations. The whole procedure is iterated until the deviations in fluxes and neutrality are negligible.

3.6.4 The linearised equation system

Using a set of component activities and a potential difference, we calculate the net charge of the solution and the component fluxes. The deviation from the desired flux of component n and the net charge of the solution we term Dj_n and Dq, respectively. The equation system defining the changes in component activities and in potential difference required to bring all Dj_n and Dq equal to zero is non-linear. We use a form linearised around the last data set and iterate until all component fluxes have their desired vales and the solution is uncharged with negligible deviations.

For N components, there are N unknown component activities and one unknown potential difference. These are determined by the N known component fluxes and by the requirement of charge neutrality according to the matrix 3-12.

$$\Delta q = \frac{\partial q}{\partial \varepsilon}\Delta\varepsilon + \frac{\partial q}{\partial \ln a_1}\Delta \ln a_1 + \frac{\partial q}{\partial \ln a_2}\Delta \ln a_2 \quad \cdots \quad + \frac{\partial q}{\partial \ln a_N}\Delta \ln a_N$$

$$\Delta j_1 = \frac{\partial j_1}{\partial \varepsilon}\Delta\varepsilon + \frac{\partial j_1}{\partial \ln a_1}\Delta \ln a_1 + \frac{\partial j_1}{\partial \ln a_2}\Delta \ln a_2 \quad \cdots \quad + \frac{\partial j_1}{\partial \ln a_N}\Delta \ln a_N$$

$$\Delta j_2 = \frac{\partial j_2}{\partial \varepsilon}\Delta\varepsilon + \frac{\partial j_2}{\partial \ln a_1}\Delta \ln a_1 + \frac{\partial j_2}{\partial \ln a_2}\Delta \ln a_2 \quad \cdots \quad + \frac{\partial j_2}{\partial \ln a_N}\Delta \ln a_N$$

. 3-12

$$\Delta j_N = \frac{\partial j_N}{\partial \varepsilon}\Delta\varepsilon + \frac{\partial j_N}{\partial \ln a_1}\Delta \ln a_1 + \frac{\partial j_N}{\partial \ln a_2}\Delta \ln a_2 \quad \cdots \quad + \frac{\partial j_N}{\partial \ln a_N}\Delta \ln a_N$$

For a system of eight components there are 9x9 partial derivatives. It is convenient to take the derivative with respect to the natural logarithm of the component activity since this avoids the problems of negative activities which otherwise may occur during the iterations. We use $\varepsilon = \Delta\Phi F/RT$ in the iterations and calculate $\Delta\Phi$ only at convergence.

There are four types of derivatives in the equation system and each partial derivative is calculated through an explicit expression.

Derivative type 1

$$\frac{\partial q}{\partial \varepsilon} = 0 \qquad 3\text{-}11$$

The potential difference has no influence on the net charge in an element when all component concentrations are kept constant.

Derivative type 2

$$\frac{\partial q}{\partial \ln a_i} = \frac{\partial q}{\partial \ln C_i} = \sum M(n,i)\, z_n\, C_n \qquad 3\text{-}12$$

The effect on the charge of an increase in a component concentration is the sum of the increases in the species concentrations times the effect on the charge of the increase in the species concentration. The sum is taken over all aqueous species in which the component is a part. Since the derivative is taken with respect to the logarithm of the concentration instead of the concentration itself, the derivative is calculated as the charge of the species times the concentration.

Derivative type 3

$$\frac{\partial j_i}{\partial \varepsilon} = \sum_{n=1}^{N} M(n,i)\, D_n z_n \frac{C_{n,1} - C_{n,0}}{\ln \frac{C_{n,1}}{C_{n,0}}} \qquad 3\text{-}13$$

The influence of a change in potential difference on the flux of a component, *i*, is the sum of the effects on the flux of all species, *n*, in which that component is a part. Neutral species are not influenced by a change in potential. The effect on each species should be multiplied by the stoichiometric content of the component *M(n,i)*.

Derivative type 4

$$\frac{\partial j_k}{\partial \ln a_l} = \sum_{n=1}^{N} M(n,k)\, M(n,l)\, \frac{\partial j_n}{\partial \ln a_n} \qquad 3\text{-}14$$

The influence on the flux of component *k* of the activity of component *l* is equal to the sum of the influences on each species in which component *k* is a part and on which a change in the activity of component *l* has an influence. The strength of the influence on each species is determined by the influence on the activity of the species times the influence on flux of the species of the activity of the species. For each species the stoichiometric content of component *k* should be considered. The influence on the flux of a species of the activity of that species in the *i*:th element is calculated as:

$$\frac{\partial j_n}{\partial \ln a_n} = D_n \left(C_{n,i} + \frac{\ln\frac{\gamma_{n,i}}{\gamma_{n,i-1}} + z_n \varepsilon}{\ln\frac{C_{n,i}}{C_{n,i-1}}} \left(C_{n,i} - \frac{C_{n,i-1} - C_{n,i}}{\ln\frac{C_{n,i}}{C_{n,i-1}}}\right)\right) \qquad 3\text{-}15$$

3.7 Solution of the problem

3.7.1 About the computer program

A code to solve the mass transport-equilibrium problem has been developed in QuickBasic. The main part of the code is compiled for greater speed while the rest is in a form that can be edited also during execution so that vital parameter values can be changed for optimum performance under various circumstances. The program runs on a personal computer of ordinary capacity.

3.7.2 Input to the program

The definition of the chemical system, the number of aqueous and solid species, equilibrium constants, the stoichiometric matrix and the charge and diffusion coefficient for each aqueous species are read from a data file. Table 3-1 is a combination of such files for 25°C and 75°C, respectively. The bulk concentrations and the fluxes of the aqueous species, from the bulk towards the pit, are entered directly into the part of the code, which can be edited. The equation used to calculate activities from concentrations is built into the code.

3.7.3 Resolution and accuracy

Typically, about two hundred and fifty volume elements are used. The spacing of the elements is varied so that higher resolution is obtained when the complexity of the chemical system or the convergence of the iterative processes so demands. Charge neutrality is generally kept to a net charge below 10^{-15} M. The fluxes of components are generally, where a flux is to be kept constant, constant to a fraction below 10^{-12} of the corrosion rate. Precipitated solids have an activity equal to unity with deviations within 0.0005 logarithmic units. For aqueous species the equilibrium conditions are fulfilled within the double precision resolution of the computer. This accuracy is desirable since errors inevitably accumulate and an error in one element may be emphasised in the next. We also want to resolve effects of a small change in the composition of the bulk water on the pitting behaviour of copper, which might be obscured by a poor accuracy in the calculations.

3.7.4 Output from the program

The output from the program is a data file in a format compatible with Lotus 123 and Excel, maintaining the double precision from the calculations. A data file contains information for one particular pitting situation during steady state. The transport path from the bulk to the corroding copper metal at the bottom of the corrosion pit is

segmented into a number of elements. For the about 250 elements, the output file contains the calculated activities of all species considered. For the aqueous species, the free and the total concentrations are printed. The fluxes between elements as well as the potential difference between the elements are output.

A full printout to the data file is made so that we later can verify that equilibrium conditions are fulfilled and that the proper diffusion coefficients have been used, etc. This wealth of information contained in the output file is immediately condensed into a single page with eight graphs. Examples of such graphs are used in the section 4 to illustrate the chemical equilibria and the mass transport in and around a corrosion pit. The calculations necessary to estimate the maximum growth rate, for corrosion pits that can propagate, are performed within Excel.'

4 Results and interpretation

Calculations of corrosion pits on copper were made for three types of waters, *A*, *B* and *D*. The composition of the waters is shown in table 4-1. For waters *A* and *B* corrosion pits were calculated also for a large number of variations in the composition. The aqueous chemistry in and around propagating corrosion pits on copper is described for three different conditions. The results for water *A* and water *B* are compared for a temperature of 25°C. Results for water *B* at 75°C are compared with the results for waters *A* and *B* at 25°C. Detailed results are presented so that the role of the various water components in a particular water, in the pitting process can be clarified.

Estimated growth rates for corrosion pits in waters *A*, *B*, and *D* are shown for various potentials and variations in the composition of the waters. The minimum potentials for the propagation of a corrosion pit are compared with the likely values for the maximum potential at which reduction of an oxidising agent on cuprous oxide, outside the pit, can supply cathodic current to the anodic processes in the pit. If there is an overlap so that the minimum potential for pitting is lower than the maximum potential for the cathodic process we conclude that a pitting potential may be attained as a free corrosion potential. If there is no overlap we conclude that a corrosion pit is not likely to propagate unless the pitting potential is imposed on the copper through galvanic coupling to a phase with metallic properties which is more noble than cuprous oxide.

Table 4-1. Compositions of the waters for which calculations of the chemistry between the bulk water and the site of metal dissolution have been made. Total concentrations in millimoles/litre (mM) and in parts per million (ppm).

Bulk	**Water A**		**Water B**		**Water D**	
properties	mM	ppm	mM	ppm	mM	ppm
pH	7.5		7.0		7.5	
Chloride	10.00	354	4.00	142	540.00	19143
Carbonate	1.49	89	1.15	69	1.95	117
Sulphate	25.0	2402	4.00	384	27.10	2603
Calcium	1.90	76	0.54	21	8.71	349
Oxygen	0.02	0.6	0.010	0.3	0.020	0.6
Ionic Strength	85.20		17.00		624.57	

4.1 A corrosion pit in water *A* at 25°C

Stationary conditions for propagation of pitting of copper were calculated for various corrosion potentials in water *A* with the composition in table 4-1. We find that at potentials higher than about +215 mV (NHE) propagation of pitting is possible at 25°C. A detailed description of the results from a modelling of a corrosion pit for the potential 216 mV is given here. This potential could, in principle, be imposed on the copper either by a potentiostat, by a reduction of an oxidising agent at a conducting copper phase or at a more noble material with which there is galvanic contact. We will first discuss the implications of the imposed potential and then discuss some prerequisites for the attainment of this value through reduction of oxidising agents at a conducting copper phase, that is, as a corrosion potential.

The conditions described in this section refer to result for a few particular corrosion pits. Precipitated solids, pH limits and potentials etc. depend on the composition of the water and on the temperature. Although the numerical results are parts of a mathematical construction we present our interpretation of the results in terms of a real corrosion pit in copper.

4.1.1 pH domains for solids

Figure 4-1 shows the pH domains where solid corrosion products are formed. Cuprous oxide is present at the lower pH values in all the corrosion pits we have calculated. In this particular case a basic carbonate salt of divalent copper is the most stable cupric phase and is precipitated at higher pH values. The pH of the undisturbed bulk solution is 7.5 and the pH at the site of the metal dissolution at the bottom of the pit is about 4.3. Basic carbonate is precipitated between pH 6.9 and 6.4. Cuprous oxide is formed at pH values below 5.4. Thus, we find an occluded solution beneath a layer of porous corrosion products. The basic carbonate forms a crust shielding the occluded solution from the bulk solution. The occluded solution is not in direct contact with the underlying metal but is partly shielded by a layer of cuprous oxide. For propagation of a pitting process to be possible, there must be channels in the solid corrosion products through which the aqueous corrosion products can diffuse and migrate and through which the pit current can flow. We describe this as a porosity of the corrosion products.

The main source of the low pH value is the acidity released by the oxidation of metallic copper to cuprous oxide at the bottom of the pit. Precipitation of basic carbonate contributes to the acidity but only above pH 6.4. The hydrolysis of aqueous divalent copper is weak at low pH values and the monovalent copper does not form any aqueous hydrolysis complex.

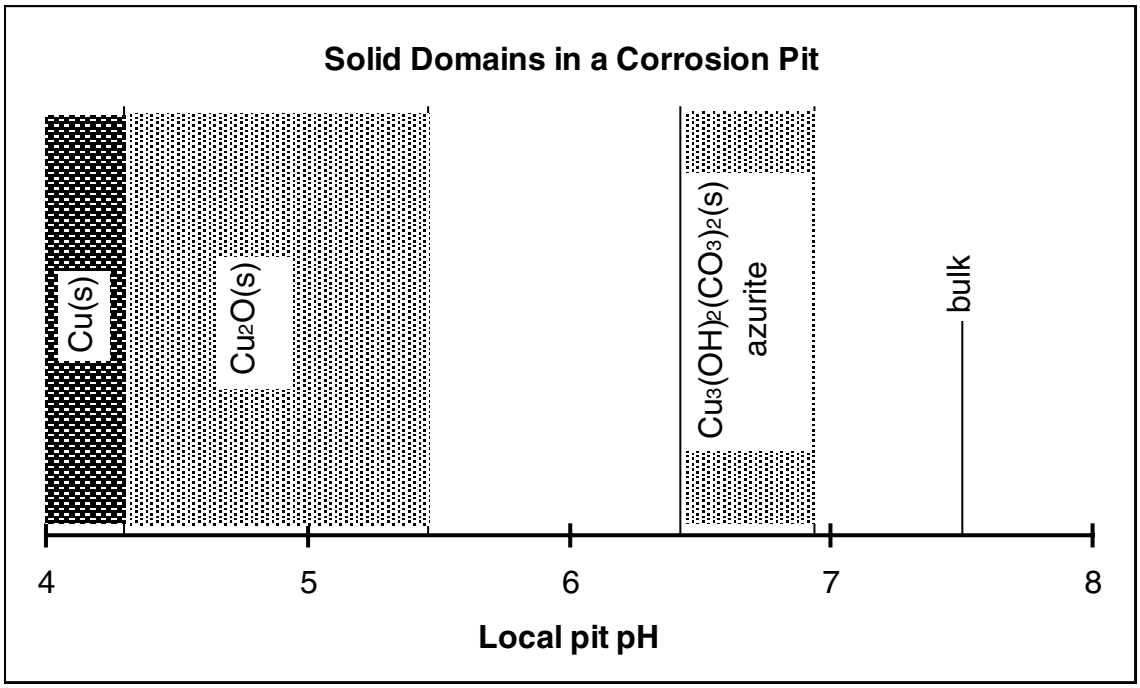

Figure 4-1. pH limits for precipitation of basic cupric salt and for cuprous oxide at a corrosion pit in copper. Water A, 25°C. 216 mV vs NHE.

4.1.2 Redox reactions

The redox conditions in and around the corrosion pit are shown in a potential-pH diagram in figure 4-2. The coexistence potentials for cuprous oxide with metallic copper and with cupric oxide are indicated by the thick lines in the diagram. The reversible potential for oxygen at 1.0 atmospheres is also shown. At the outer parts of the pit, at pH values higher than about 5.8, the redox conditions are controlled by aqueous oxygen. Dissolved oxygen from the bulk solution diffuses through the crust of basic carbonate and into the occluded solution. There, the oxygen meets a flux of monovalent copper species. The monovalent copper is oxidized to divalent copper, oxygen being reduced to water. In our model this homogenous oxidation of univalent copper by oxygen is assumed to take place instantaneously. The validity of this assumption is discussed in section 5.6.

The local production of divalent copper causes a peak in the concentration at the site of the reaction. The divalent copper species are transported partly towards the outer crust where precipitation to basic carbonate takes place, partly towards the cuprous oxide where reduction to univalent copper occurs.

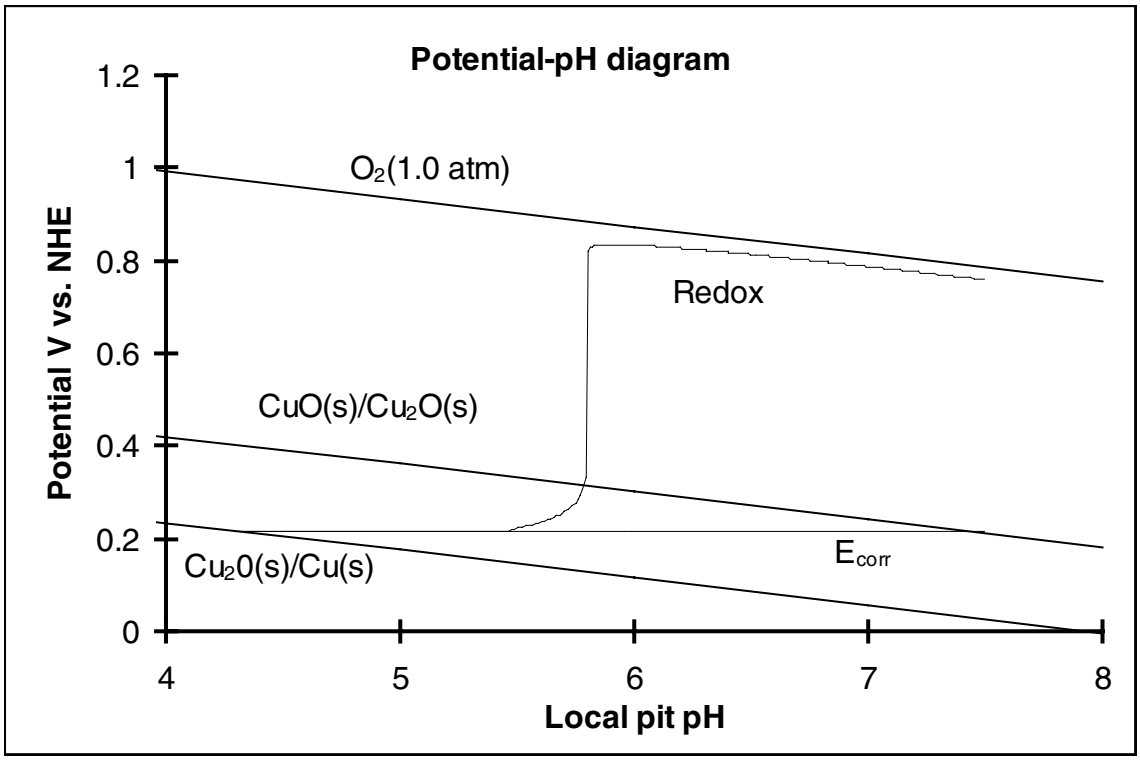

Figure 4-2. Potential pH diagram showing the redox potential at various locations in and around a corrosion pit as a function of the local pH. Water A, 25°C.

Figure 4-3 shows the fraction of the oxidised copper, which is transported as aqueous species, in the direction out of the pit, at various locations in and outside the pit as a function of the local pH. Copper is transported as monovalent species and as divalent species, the modes of transport being diffusion and migration. The fraction of the oxidised copper, which is transported as divalent copper, is also indicated in the diagram. Between pH 5.8 and pH 5.4 the transport of the divalent copper is negative. A fraction of the divalent copper produced through chemical oxidation of monovalent copper by oxygen is transported back towards the source of the aqueous copper, that is towards the site of the oxidation of copper metal. At pH 5.4 the divalent copper diffusing inwards encounters electronically conductive cuprous oxide. This electronically conductive cuprous oxide behaves like a metal where the divalent copper is reduced to monovalent copper. The cuprous oxide, although porous, is in contact with the underlying copper metal. The contact between the two conducting phases in the pit allows a local galvanic cell to establish. Both phases being conductors, the reduction of divalent copper at the outer surface of the cuprous oxide causes an oxidation of metallic copper at the bottom of the pit.

The oxidation current supplied by this local galvanic cell is however not enough to drive the pitting process. In this particular pit, and in all pits we have modelled, anodic current must be supplied from a cathodic process at an external site outside the pit.

4.1.3 Transport of copper

Seen from the site of the oxidation of the underlying copper metal at the base of the corrosion pit, the copper metal is oxidised to aqueous copper (47%) and to solid cuprous oxide (53%). This 53% of the oxidized copper which forms cuprous oxide at the copper surface does not fill the whole volume previously occupied by the metallic copper, so the cuprous oxide is porous. The aqueous copper is present in the solution in the pores as univalent copper and as divalent copper. The relatively high concentrations of the aqueous copper species give rise to a transport away from the site of the metal oxidation. The transport is driven mainly by diffusion but is influenced also by migration of ionic species in an electrical field. This electrical field is a combination of an iR-drop arising from the passage of current in a solution with limited conductivity and a diffusion potential arising from concentration gradients of ionic species with different diffusion coefficients.

As higher pH values are encountered, the solubility of cuprous oxide decreases. Precipitation of monovalent copper takes place. One effect of the electronic conductivity of the cuprous oxide is that the ratio between the concentrations of Cu^{+} and Cu^{2+} is approximately constant. Divalent copper is therefore reduced to monovalent copper continuously as long as cuprous oxide is present.

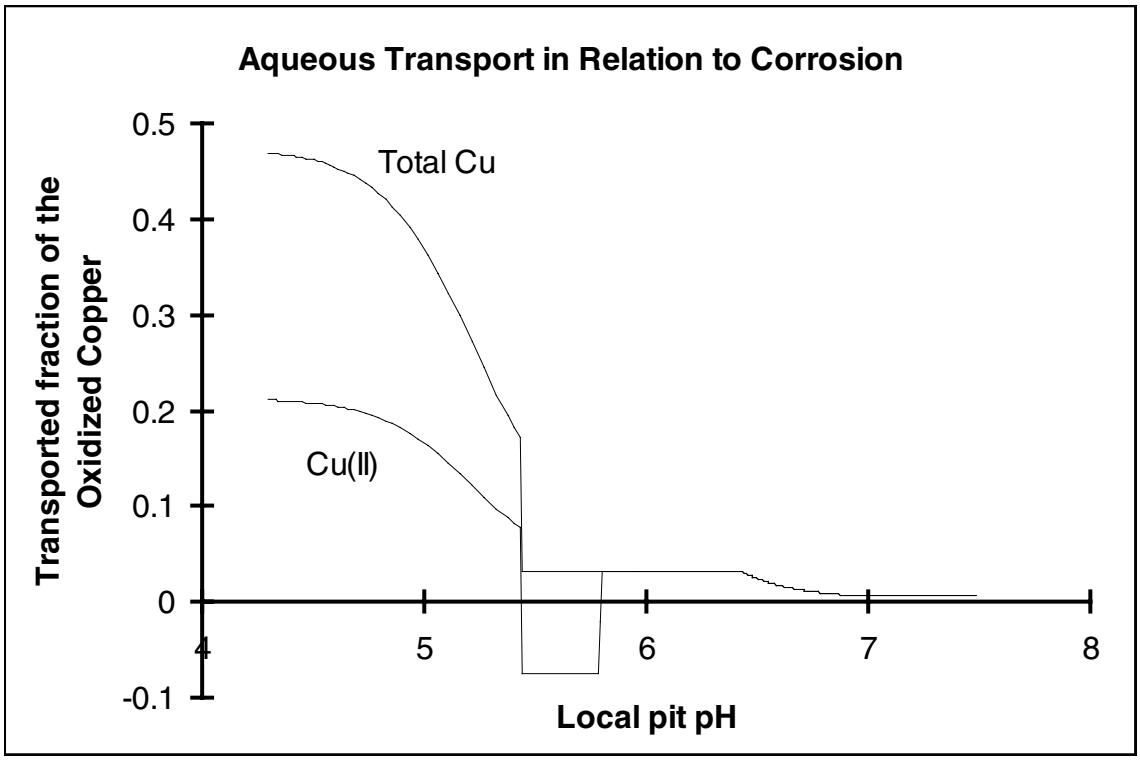

Figure 4-3. The fraction of the oxidised copper transported as aqueous species, in direction out of the pit, at various locations in and around a corrosion pit as a function of the local pH. Water A, 25°C.

4.1.4 Copper concentrations

Figure 4-4 shows the total concentrations of univalent and divalent copper at various locations in and around the pit as a function of the local pH. The linear ranges with slopes approximately equal to minus one at pH values lower than pH 5.4 is an effect of the presence of cuprous oxide. At a pH of about 5.8 there is a sharp drop in the concentration of monovalent copper marking the influence of the aqueous oxygen. The peak in the concentration of divalent copper at about pH 6 shows the site of the homogenous oxidation of monovalent to divalent copper by oxygen. Between pH 6.4 and pH 7.3 there is again an approximately linear range in the concentration of divalent copper. The slope is between pH 6.4 and pH 6.9 determined by the presence of and continuous precipitation of the basic carbonate, azurite, $Cu_3(OH)_2(CO_3)_2(s)$.

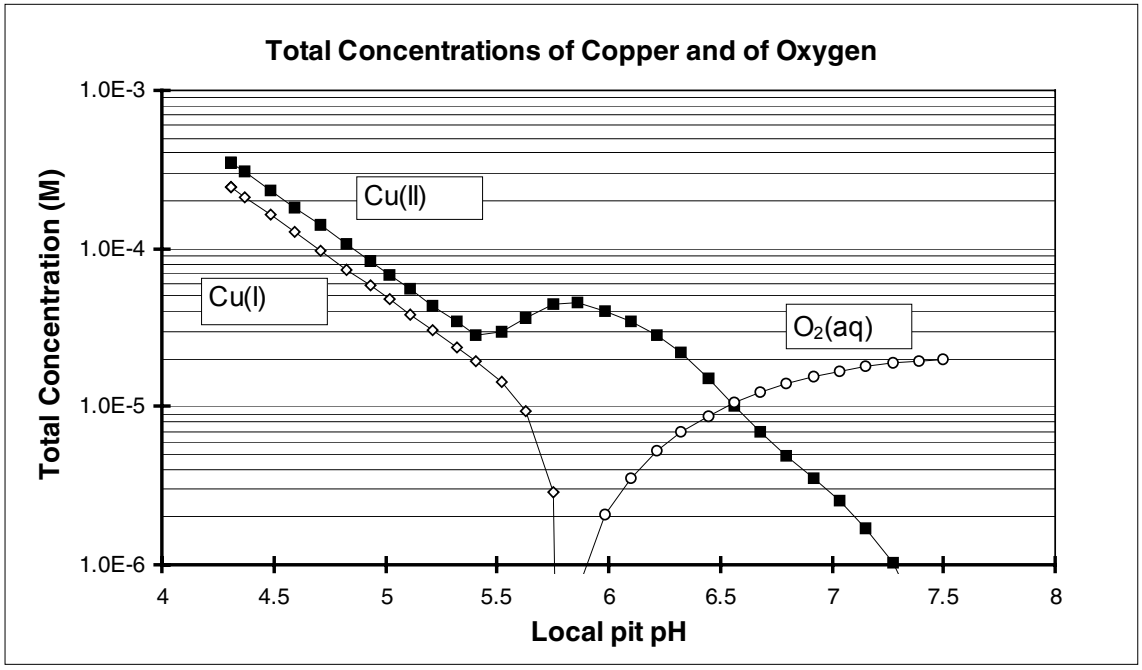

Figure 4-4. Total concentrations of copper(I), copper(II) and oxygen at various locations in and around a corrosion pit as a function of the local pH. Water A, 25°C.

4.1.5 Solids in the system

Figure 4-5 shows the activities of the copper containing solids considered at various locations in and around the pit as a function of the local pH. The solids have the logarithm of the activity equal to zero over the pH domains where they are present. For this pit, cuprous oxide is present at low pH and one of the basic carbonate salts, the carbonate rich azurite, is present over a range in the near neutral region. The other basic carbonate salt, the carbonate poor malachite, and the cupric oxide have maximum values close to zero indicating that at slightly different composition of the water one or both of these solids might precipitate. At low pH values the activity of the solid cuprous

chloride increases linearly with decreasing pH, indicating that at lower pH values, CuCl(s) would precipitate.

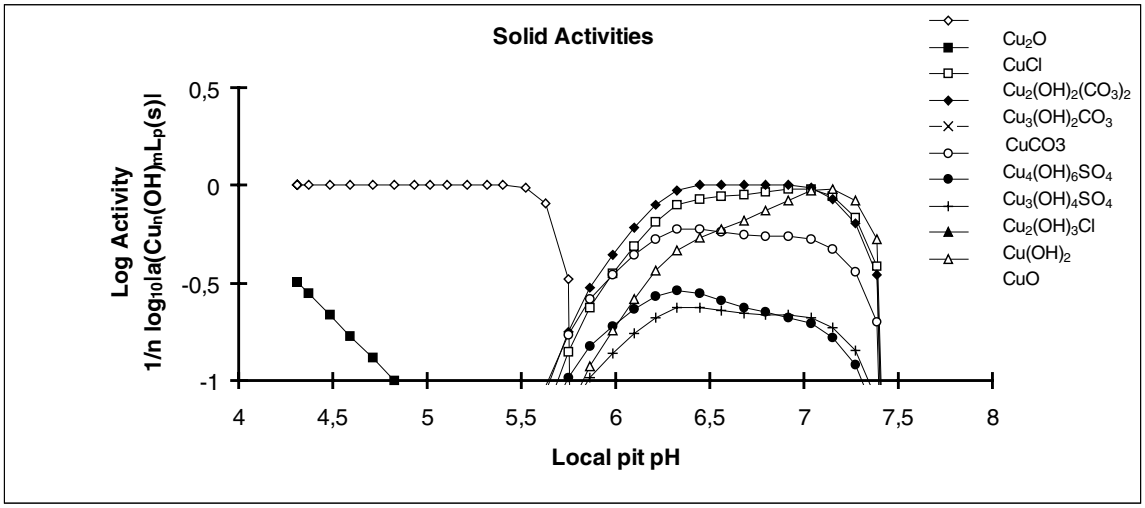

Figure 4-5. Activities of the solid copper species considered at various locations in and around a corrosion pit as a function of the local pH. Water A, 25°C.

4.1.6 Concentrations of water components

Figure 4-6 shows the total concentrations of some water components at various locations in and around the pit as a function of the local pH. Only the carbonate concentration shows a marked dependence on the location in the pit or on the local pH. There is a net transport of carbonate from the bulk solution towards the site of the pit where basic copper carbonate precipitates. This transport, which continues with successively decreasing rate until pH 6.4, which is the lower limit for precipitation in this pit, is driven mainly by diffusion. The necessary concentration gradient appears at pH values above pH 6.4. Below this pH value there is no net transport of carbonate and the changes in concentration are due to the difference in diffusion coefficients between HCO_3^- and CO_2 or H_2CO_3. Because of the pH gradient there are gradients also in the concentrations of the different carbonate species. The higher diffusivity of the neutral species results in a lower total concentration at pH values where the neutral form dominates.

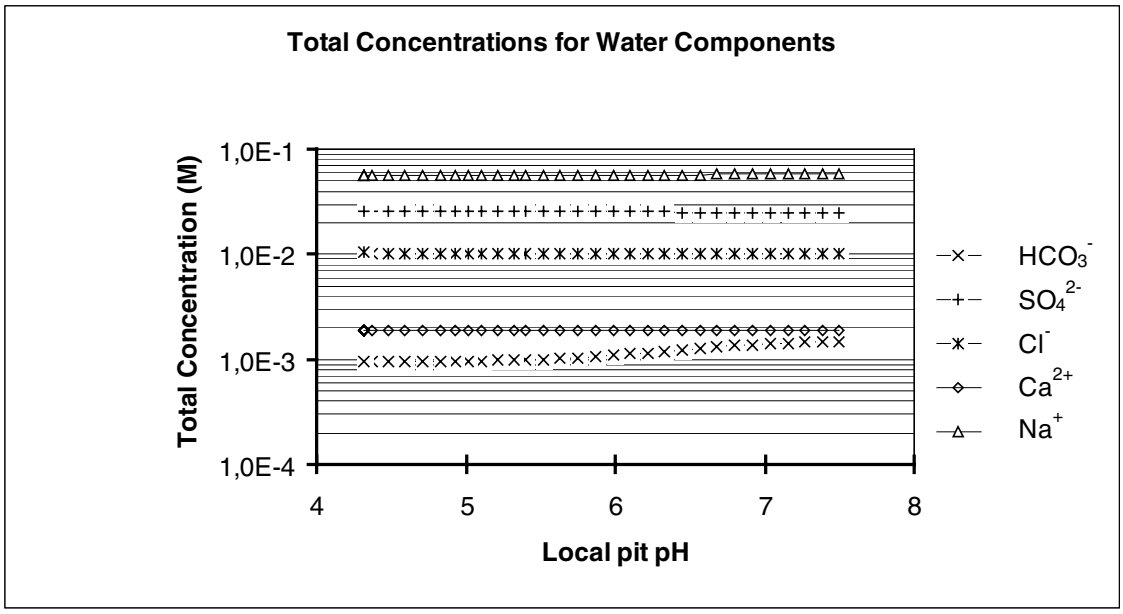

Figure 4-6. Total concentrations for water components at various locations in and around a corrosion pit as a function of the local pH. Water A, 25°C.

Although not evident in figure 4-6, there is an increase in the concentrations of sulphate and chloride towards lower pH values. The continuous production of positive charge at the site of the metal oxidation tends to create an excess of positive charge locally which must be balanced by negatively charged ions. This tendency towards imbalance in charge, is one cause of the electrical field in the solution. The polarity of the electrical field is such that the solution closer to the site of the oxidation is enriched in negative ions from the bulk solution and depleted in positive ions relative to the composition of the bulk. In this particular pit the potential drop in the solution, from the bulk to the site of the metal oxidation, is only about 0.3 mV so the enriching and depleting effects of the electrical field are small.

4.1.7 The ionic strength and activity coefficients

Figure 4-7 shows the local ionic strength and the activity coefficients for monovalent ions and for divalent ions at various locations in and around the pit as a function of the local pH. The calculation of the activity coefficients is an integral part of the modelling and the local value of the ionic strength is used to calculate the local activity coefficients. As figure 4-7 shows, the ionic strength is relatively constant from the bulk of the solution to the base of the pit at the lowest pH values. The activity coefficient for the monovalent ions is about 0.8 and for divalent ions about 0.4. The upper limit for applicability of the model for the dependence of activity coefficients on ionic strength is given to 0.5 M so the ionic strength found in this pit is well below the limit.

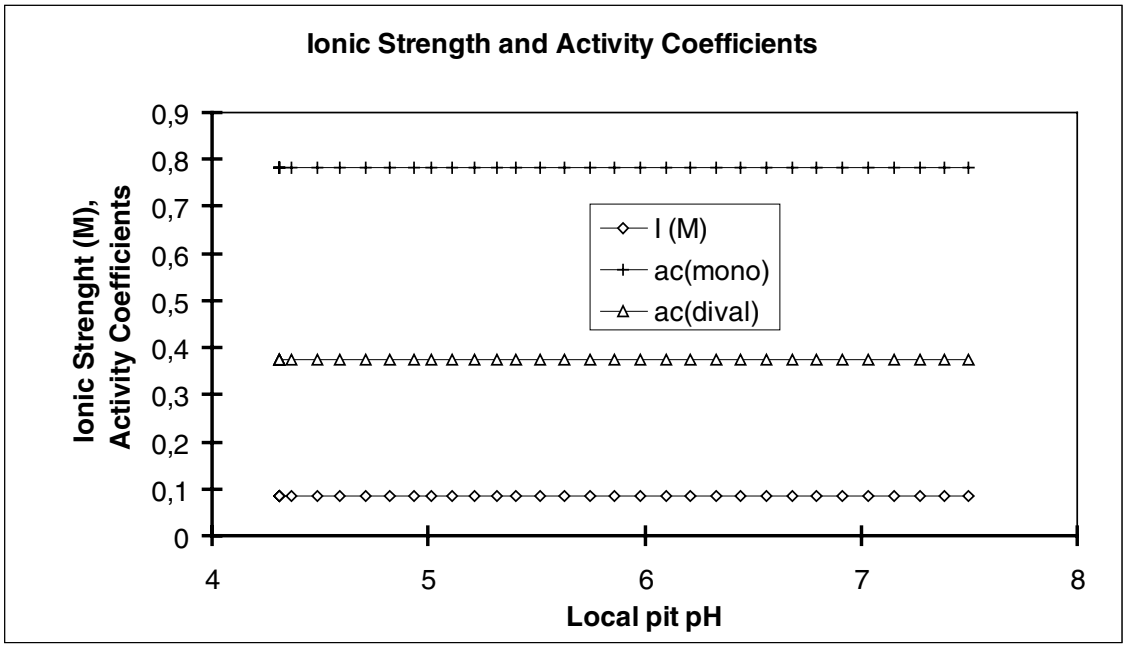

Figure 4-7. Ionic Strength and activity coefficients at various locations in and around a corrosion pit as a function of the local pH. Water A, 25°C.

4.1.8 Speciation of aqueous copper

Figure 4-8 shows the distribution of the local total concentration of monovalent copper into the various aqueous species considered, at various locations in and around the pit as a function of the local pH. The dominating species is the negatively charged dichloride complex $CuCl_2^-$. The neutral monochloride complex CuCl accounts for about 13% of the total concentration and the free cuprous ions Cu^+ accounts for about 4%. At pH values above 5.8 the speciation of monovalent copper is not important because redox conditions are controlled by aqueous oxygen and the total concentration of monovalent copper is very low.

Figure 4-9 shows the distribution of the local total concentration of divalent copper into the various aqueous species considered, at various locations in and around the pit as a function of the local pH. At pH values higher than pH 7.0, the neutral monocarbonate complex $CuCO_3$ dominates although there are several other species that appear at significant fractions. At low pH values the free cupric ion Cu^{2+} dominates but with a large contribution of the neutral sulphate complex $CuSO_4$.

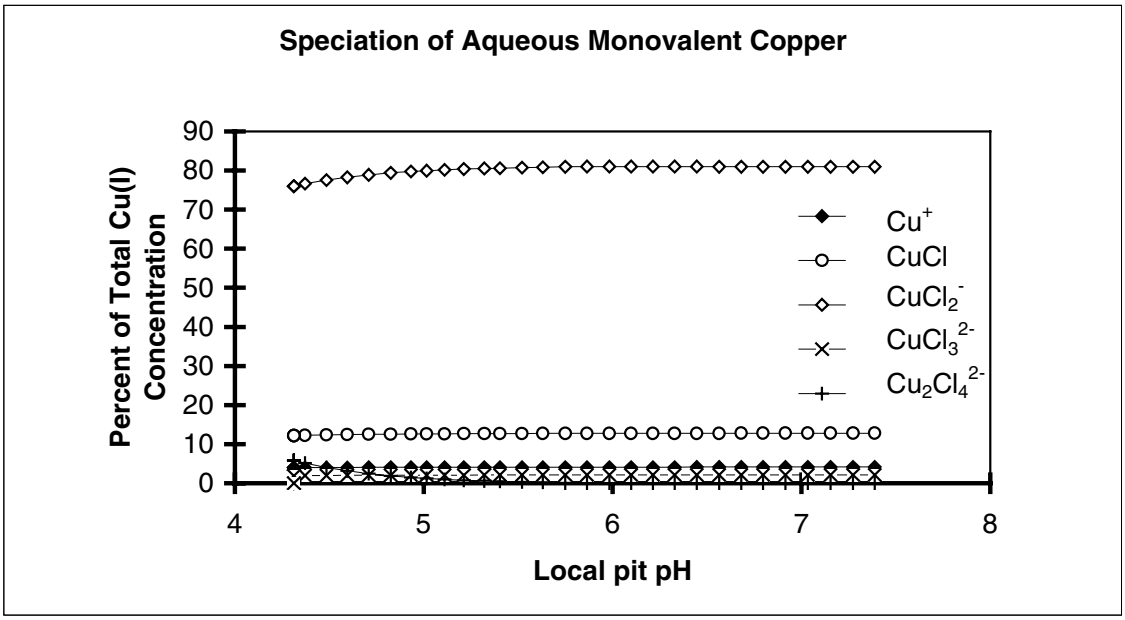

Figure 4-8. Speciation of monovalent copper at various locations in and around a corrosion pit as a function of the local pH. Water A, 25°C.

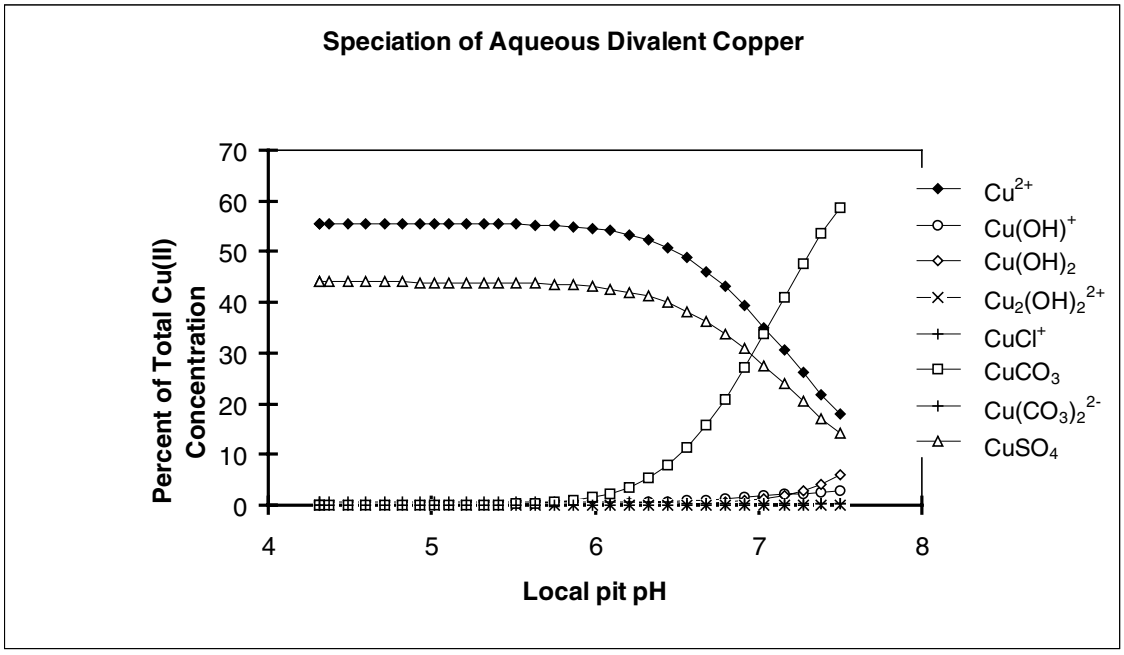

Figure 4-9. Speciation of divalent copper at various locations in and around a corrosion pit as a function of the local pH. Water A, 25°C.

4.1.9 Speciation of chloride, carbonate, sulphate and calcium

To make the picture of the aqueous chemistry in and around the pit complete we show also the speciation of the total concentrations of chloride, carbonate, sulphate and calcium. These distribution diagrams are shown in figures 4-10 to 4-13. Figure 4-10 shows that almost all of the aqueous chloride is present as the free chloride ion. The major complex species which is the dichloride complex with monovalent copper $CuCl_2^-$, reaches a maximum fraction of about 4% at the lowest pH at the site of the metal oxidation.

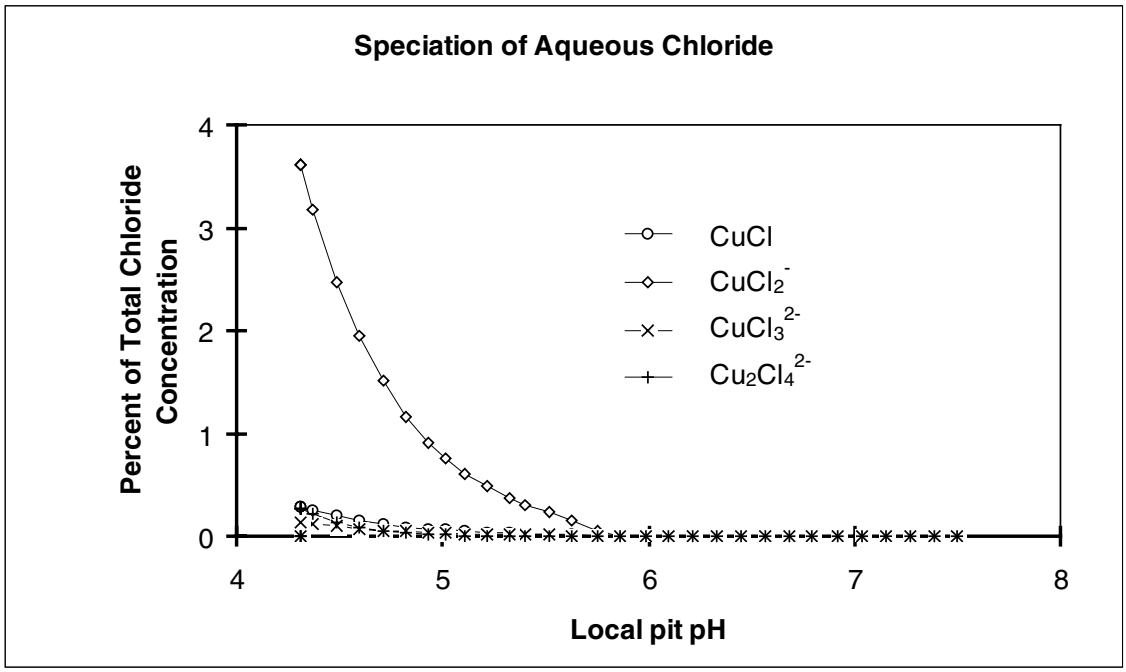

Figure 4-10. Speciation of aqueous chloride at various locations in and around a corrosion pit as a function of the local pH. Water A, 25°C.

Figure 4-11 shows that the carbonate is distributed between two major species. The carbonic acid or dissolved carbon dioxide dominates at low pH and the hydrogen carbonate at near neutral pH. The carbonate complexes with calcium and with divalent copper do not significantly contribute to the total carbonate concentration.

Figure 4-12 shows that almost all of the aqueous sulphate is present as the free sulphate ion. The major complex species is the aqueous calcium sulphate. The aqueous copper sulphate reaches a maximum fraction of about 0.6% at the lowest pH at the site of the metal oxidation.

The total calcium concentration is distributed between two major species. Figure 4-13 shows that the free calcium ion dominates over the whole pH region. The aqueous sulphate complex is present at a slightly lower fraction. The aqueous calcium carbonate species do not significantly contribute to the total calcium concentration.

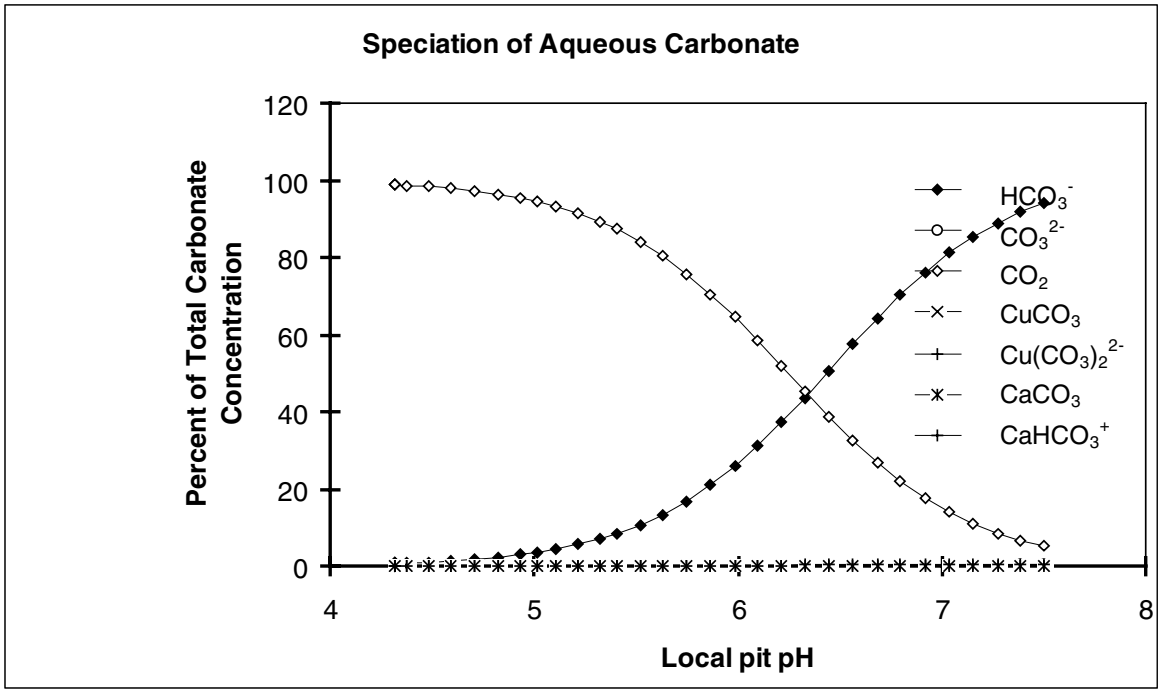

Figure 4-11. Speciation of aqueous carbonate at various locations in and around a corrosion pit as a function of the local pH. Water A, 25°C.

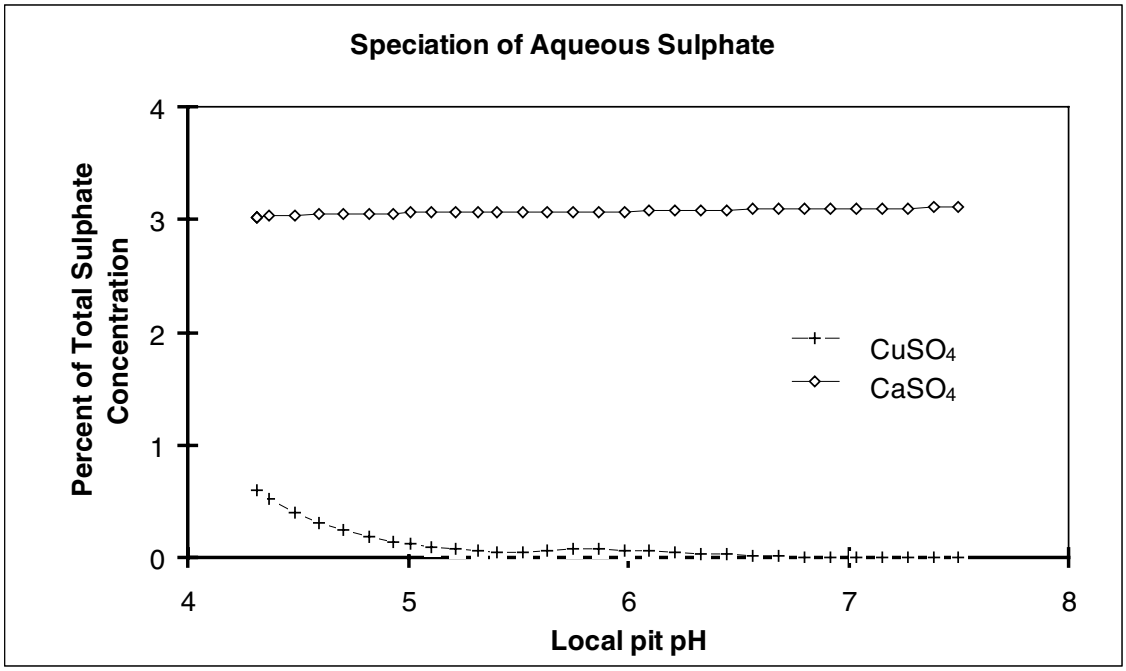

Figure 4-12. Speciation of aqueous sulphate at various locations in and around a corrosion pit as a function of the local pH. Water A, 25°C.

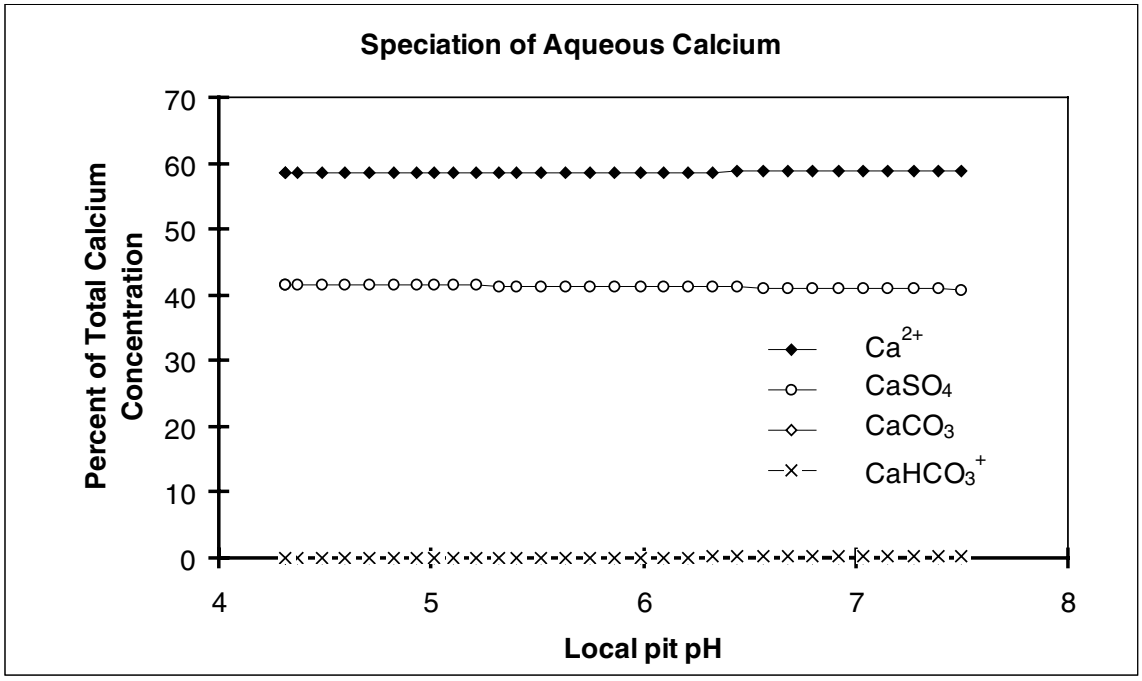

Figure 4-13. Speciation of aqueous calcium at various locations in and around a corrosion pit as a function of the local pH. Water A, 25°C.

4.1.10 Current transport

Figure 4-14 and 4-15 show the fraction of the total pit current transported by some species at various locations in and around the pit as a function of the local pH. Figure 4-14 shows the transport by species directly related to monovalent copper and to chloride. The transport by other major current transporting species is shown in figure 4-15. At pH values higher than about 5.8 the transport related to monovalent copper is insignificant because the redox conditions are dominated by dissolved oxygen. In the neutral region the hydrogen carbonate ion dominates the current transport with a small contribution from the carbonate ion (not shown in the figure) above pH 7. Below pH 5.8, no aqueous oxygen is present and species associated with the aqueous chemistry of monovalent copper become important for the current transport. At the lowest pH values, protons and chloride are the main current transporting species but the free cupric ion and sulphate contribute. The fraction of the current transported by the dichloride complex with monovalent copper, $CuCl_2^-$, has a negative sign i figure 4-14. This species diffuses away from the site of the metal oxidation against the potential gradient. Since, in this particular pit, no solid chloride salt is formed, the net transport of chloride is zero and the transport inwards of the free chloride ion is matched by a transport outwards by complexes formed with monovalent copper. Likewise, the transport of the sulphate ion inwards is matched, mainly by a transport of the complex with divalent copper outwards.

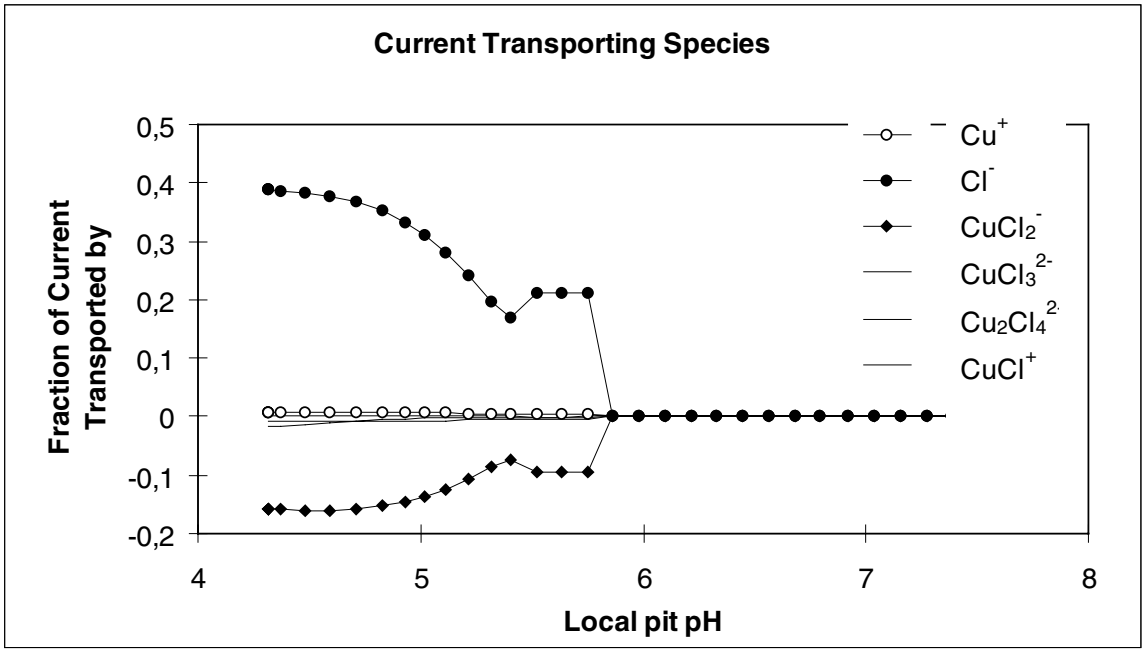

Figure 4-14. Current transport outwards by the cuprous and chloride containing species at various locations in and around a corrosion pit as a function of the local pH. Water A, 25°C.

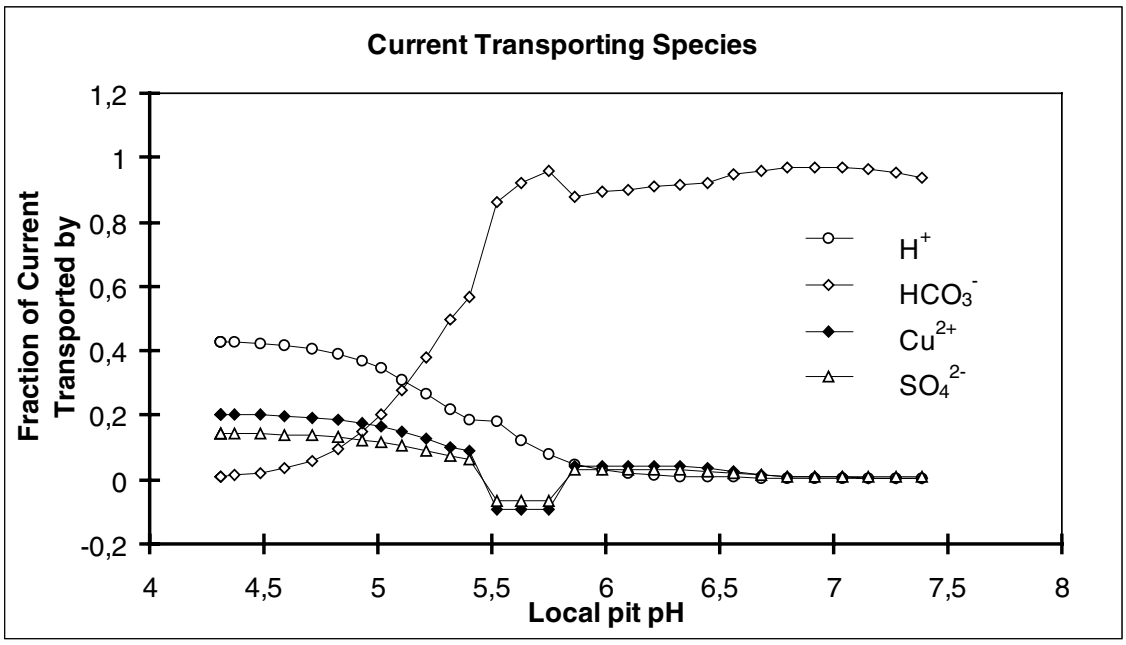

Figure 4-15. Current transport outwards by the major current transporting species at various locations in and around a corrosion pit as a function of the local pH. Water A, 25°C.

4.1.11 The growth of the corrosion pit

Figure 4-16 shows the estimated maximum pit depth for a corrosion pit in copper at a potential of + 216 mV (NHE) in water *A* as a function of time. A hemispherical pit shape which has the depth of 0.1 cm at time zero, is assumed. The pit grows with a rate inversely proportional to its depth so that the pit depth increases with the square root of time at this fixed potential. The calculated value for the time it would take to reach a depth of 0.5 centimetres is about 1500 years. The long time perspective is a result of our ambition to determine limits for where pitting processes can propagate. At potentials only slightly higher than the minimum pitting potential we find that, while propagation is possible, the process is very slow.

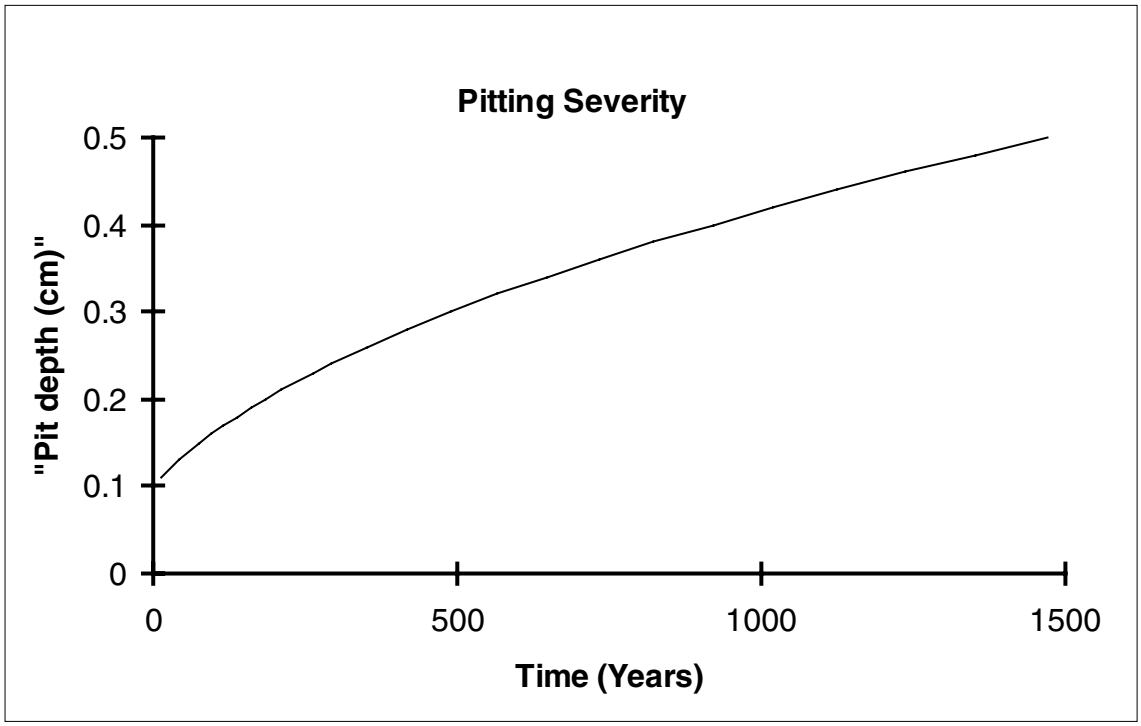

Figure 4-16. Estimated maximum growth rate for a corrosion pit on copper. Water A, 25°C. 216 mV vs NHE.

4.1.12 Conditions at the cathode.

We find that a corrosion pit in copper behaves as a net anode. Cathodic reactions such as the reduction of oxygen do take place in the pit but the extent is not enough to drive the pitting process. The site of the pit consumes positive charge from the metal and produces positive charge in the solution outside the pit. Charge transport always runs in closed loops so there has to be areas which behave as net cathodes, that is, sites at which an oxidising agent transfers negative charge from the metal to the solution.

For copper to attain a certain corrosion potential where propagation of an anodic corrosion pit is possible, there must exist an electronically conductive phase available at which the reduction can take place. If the reduction of the oxidising agent takes place at

solid cuprous oxide and this causes an oxidation of the cuprous oxide to cupric oxide or to basic cupric salts, these cupric phases would block the access of oxygen to the cuprous oxide. We conclude that for a corrosion potential on copper to be sustained so that a pitting process can propagate, the cuprous oxide must have a stability, relative to the cupric phases, at the pH of the bulk or higher.

Exceptions from this conclusion are when there is another noble electron conducting phase present. One such exception is when there is a film of elementary carbon at the inside of copper tubes.

Figure 4-17 shows the coexistence potentials for cuprous oxide with each of the cupric phases considered, at the pH of the bulk. At higher pH values, the coexistence potentials are lower. The straight line indicates the corrosion potential for a certain corrosion pit (+216 mV NHE). The corrosion potential is lower than the coexistence potentials for all cupric phases with cuprous oxide, except cupric oxide. Cupric oxide is the thermodynamically stable copper phase at +216 mV in water *A* at 25°C. Judging from this, one could say that cathodic reduction of an oxidising agent can not take place at cuprous oxide so that the corrosion pit considered can propagate. The surface of the cuprous oxide would be converted to cupric oxide, which would block the access of oxygen to the underlying cuprous oxide. Any cuprous oxide exposed through pores in a layer of cupric oxide would undergo the same oxidation.

The margin against stability of the cuprous oxide is however very small and well within the error limits for the equilibrium constants from which the coexistence potential was calculated. Furthermore, kinetic barriers against the formation of cupric oxide might prevent oxidation, especially when there is a small driving force for the process.

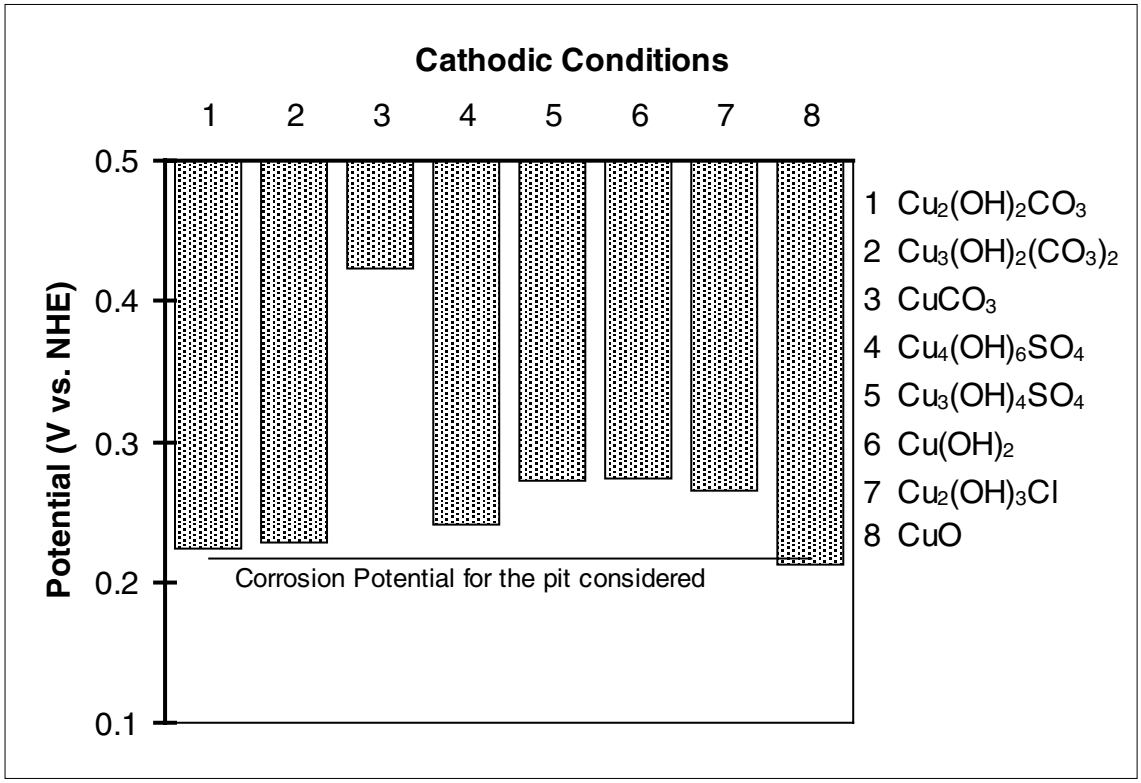

Figure 4-17. Coexistence potentials for $Cu_2O(s)$ with various cupric solids at bulk conditions. Water A, 25°C.

4.2 A corrosion pit in water *B* at 25°C

We give here a description of a corrosion pit in water *B* at 25°C in relation to a pit in water *A* at the same temperature. In water *B* with the composition given in table 4-1 we find that pitting is possible at potentials higher than about +240 mV (NHE). This is about 25 mV higher than the minimum pitting potential found for water *A*. Water *B* has a lower pH than water *A*, and lower concentrations of chloride, carbonate and sulphate. A detailed comparison between the results from a modelling of a corrosion pit in water *B* at 242 mV and the pit in water *A*, discussed in section 4.1, is given here. Both the pit in water *A* and the pit in water *B* are selected so that pitting is just barely possible. The corrosion potentials are in both cases only slightly higher than the minimum pitting potentials in the respective waters.

4.2.1 pH domains for solids

Figure 4-18 shows the domains where a basic carbonate salt of copper is precipitated and where cuprous oxide is formed. The same basic salt is formed as in water *A*. The pH of the undisturbed bulk solution of water *B* is 7.0 and the pH at the site of the metal dissolution is about 4.1. Basic carbonate is precipitated between pH 6.6 and pH 6.1. Cuprous oxide is formed at pH values below 5.1. Compared with the corrosion pit discussed for water *A*, the solid domains have been shifted towards lower pH values. The pH at the site of metal dissolution is also lower.

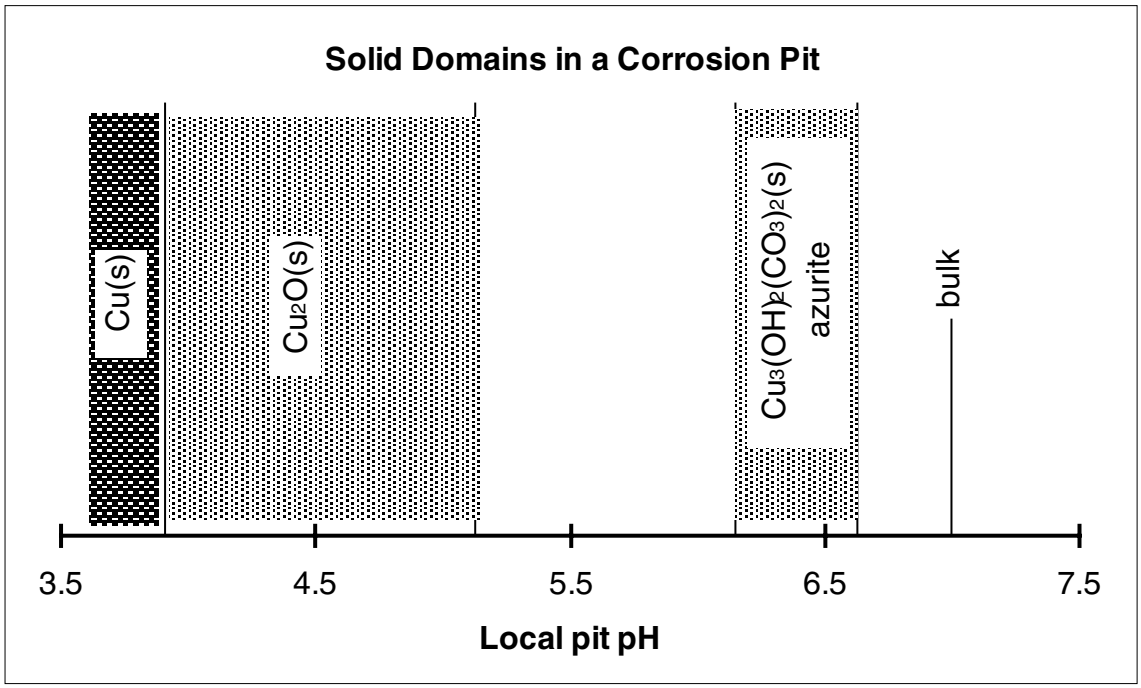

Figure 4-18. pH limits for precipitation of basic cupric salt and for cuprous oxide at a corrosion pit in copper. Water B, 25°C. 242 mV vs NHE.

4.2.2 Redox reactions

The redox conditions in and around the pit are illustrated in figure 4.19. The main difference between this diagram and the diagram for the pit in water *A* is that here, the sharp drop in redox potential occurs at a lower pH, about pH 5.5 for water B and about pH 5.8 for water *A*.

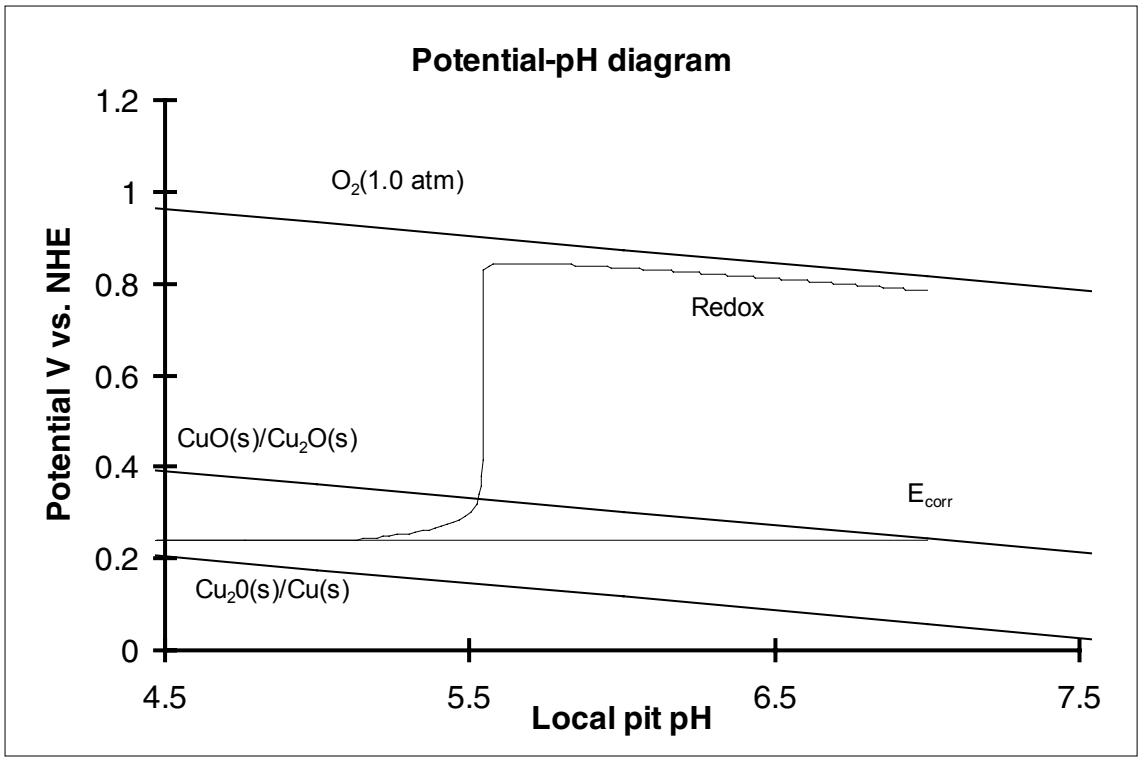

Figure 4-19. Potential pH diagram showing the redox potential at various locations in and around a corrosion pit as a function of the local pH. Water B, 25°C.

4.2.3 Transport of copper

Figure 4-20 shows the fraction of the oxidised copper, which is transported, away from the site of the metal oxidation at various location in and around the pit as a function of the local pH. At the base of the pit, about 41% of the oxidised copper form aqueous species and 59 % forms solid cuprous oxide. This 59% which forms solid oxide is higher than the 53% found for the pit in water *A*, but still does not completely fill the void previously occupied by the copper metal.

A further comparison shows that the fraction of the oxidised copper, which is transported as divalent copper is higher in the pit in water *B* than in the pit in water *A*. In water *B*, about 33% is transported as divalent copper, at the base of the pit, whereas only 20% is transported as divalent copper in water *A*, although the total fraction transported is higher in water *A*.

In water *A* there is a range where the transport of divalent copper is negative, that is, directed inwards. In water *B* there is no negative transport but a range where there is almost no net transport of divalent copper at all.

4.2.4 Copper concentrations

Figure 4-21 shows the total concentrations of monovalent and divalent copper at various locations in and around the pit as a function of the local pH. The plateau in the concentration of divalent copper between pH 5.1 and pH 5.5 marks the range where there is practically no net transport of divalent copper. A comparison with the copper concentrations found in the pit in water *A* shows that the total concentration of divalent copper is much higher in water *B* than in water *A* and that the total concentration of monovalent copper is slightly lower in water *B* than in water *A*. The pH at which the concentration of dissolved oxygen has decreased to 10^{-6} M is about pH 5.6 in water *B* while pH 5.9 was found for water *A*.

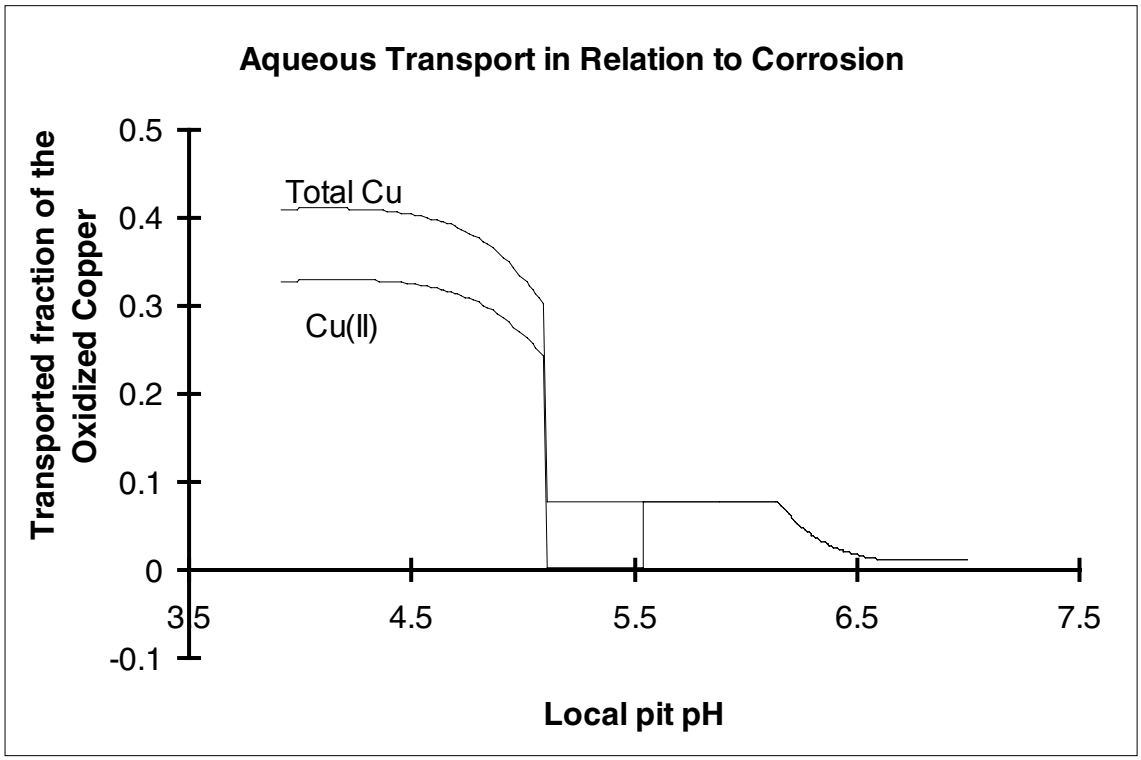

Figure 4-20. The fraction of the oxidised copper transported as aqueous species, in direction out of the pit, at various locations in and around a corrosion pit as a function of the local pH. Water B, 25°C.

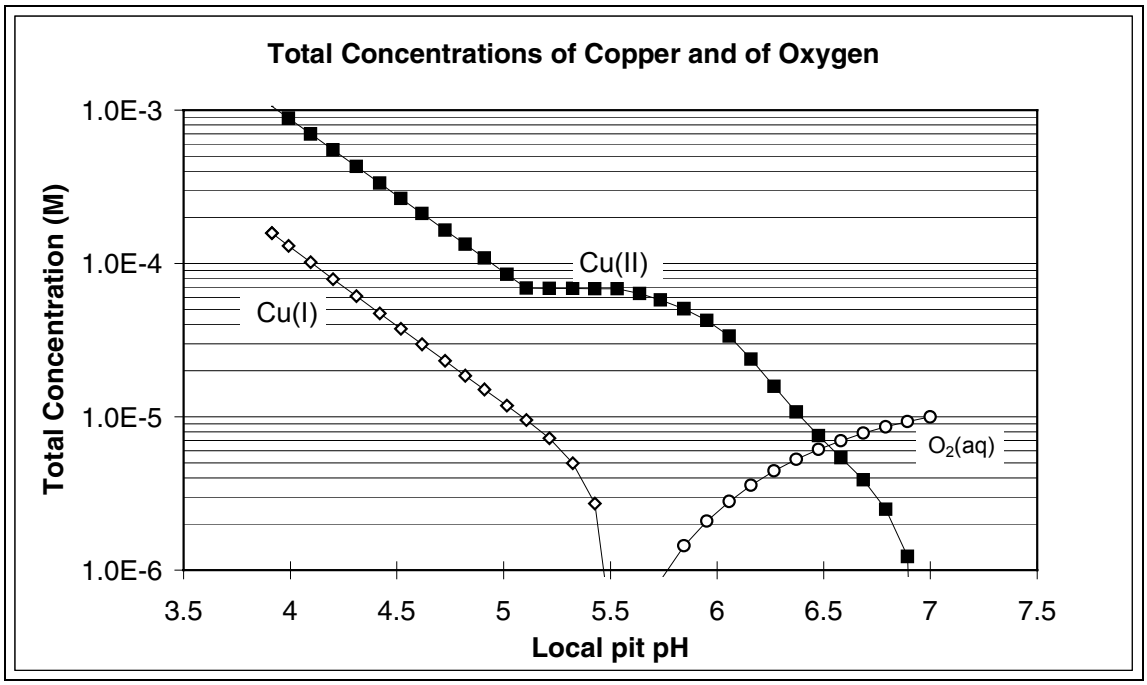

Figure 4-21. Total concentrations of copper(I), copper(II) and oxygen at various locations in and around a corrosion pit as a function of the local pH. Water B, 25°C.

4.2.5 Solids in the system

Figure 4-22 shows the activities of the copper containing solids considered at various locations in and around the pit as a function of the local pH. A comparison with the solid activities found in water *A* shows that the same solids reach saturation levels in both waters. The activity of the cupric oxide is not so close to saturation in water *B* as in water *A*. At low pH values, the cuprous chloride reaches about the same activity in water *B* as in water *A*.

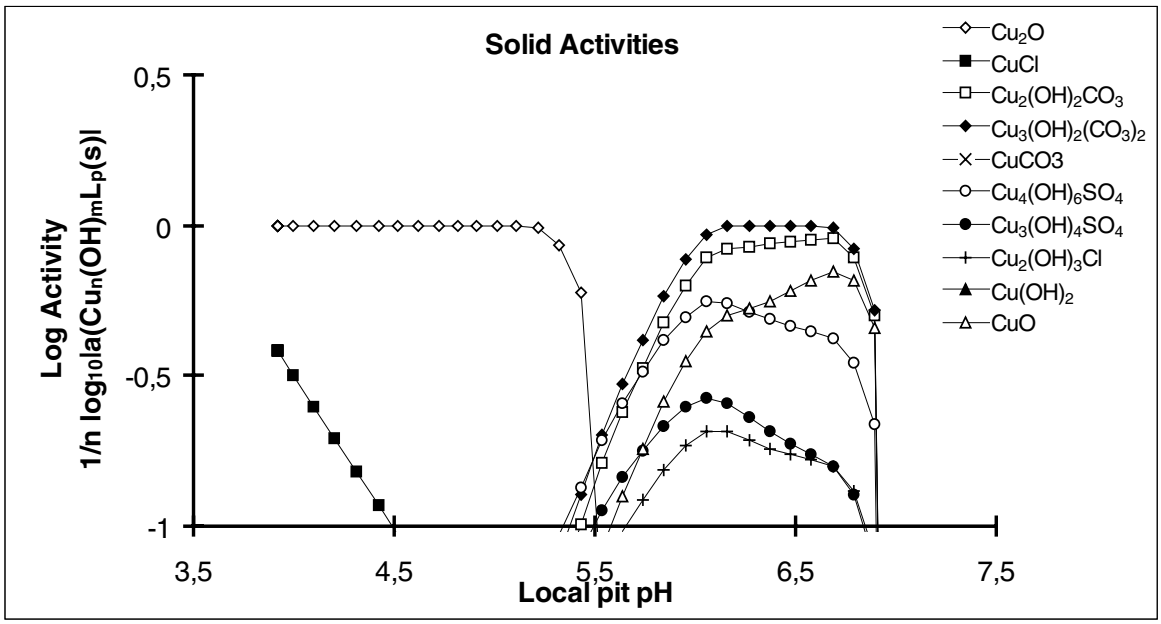

Figure 4-22. Activities of the solid copper species considered at various locations in and around a corrosion pit as a function of the local pH. Water B, 25°C.

4.2.6 Concentrations of water components

Figure 4-23 shows the total concentrations of some water components at various locations in and around the pit as a function of the local pH. A comparison with water *A* illustrates the lower ionic content of water *B*. The carbonate concentration shows a similar decrease towards lower pH values as in water *A*. The increase in the concentrations of components dominated by negatively charged species and the decrease in the concentrations of components dominated by positively charged species, which could barely be discerned for water *A* is clearly seen for water *B* in figure 4-23. The magnitude of the changes is larger for components dominated by highly charged species. The larger magnitude of the changes in concentration in water *B* than in water *A* reflects the higher potential drop in the solution. In water *B* this is about 2.2 mV to be compared with the 0.3 mV found for water *A*.

4.2.7 The ionic strength and activity coefficients

Figure 4-24 shows the local ionic strength and the activity coefficients for monovalent ions and for divalent ions at various locations in and around the pit as a function of the local pH. The lower ionic strength of water *B* results in higher activity coefficients than for water *A*. A small increase in the ionic strength is found at low pH values for water *B*. This is manifested as a decrease in the activity coefficients. The decrease in the activity coefficients for divalent ions is higher than for monovalent ions.

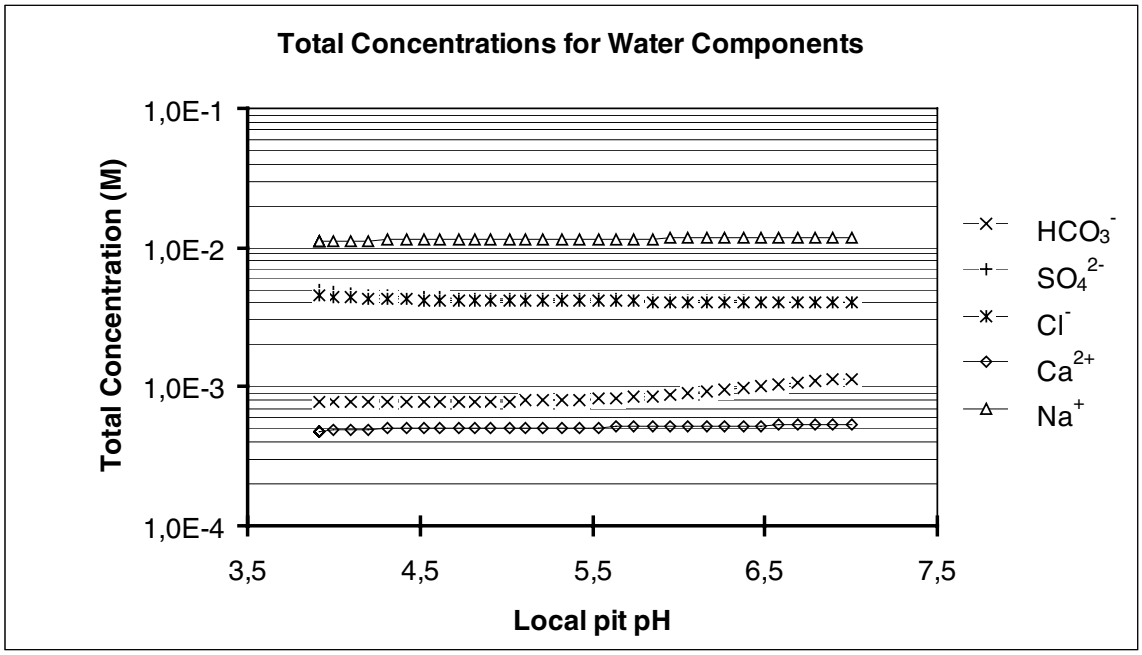

Figure 4-23. Total concentrations for water components at various locations in and around a corrosion pit as a function of the local pH. Water B, 25°C.

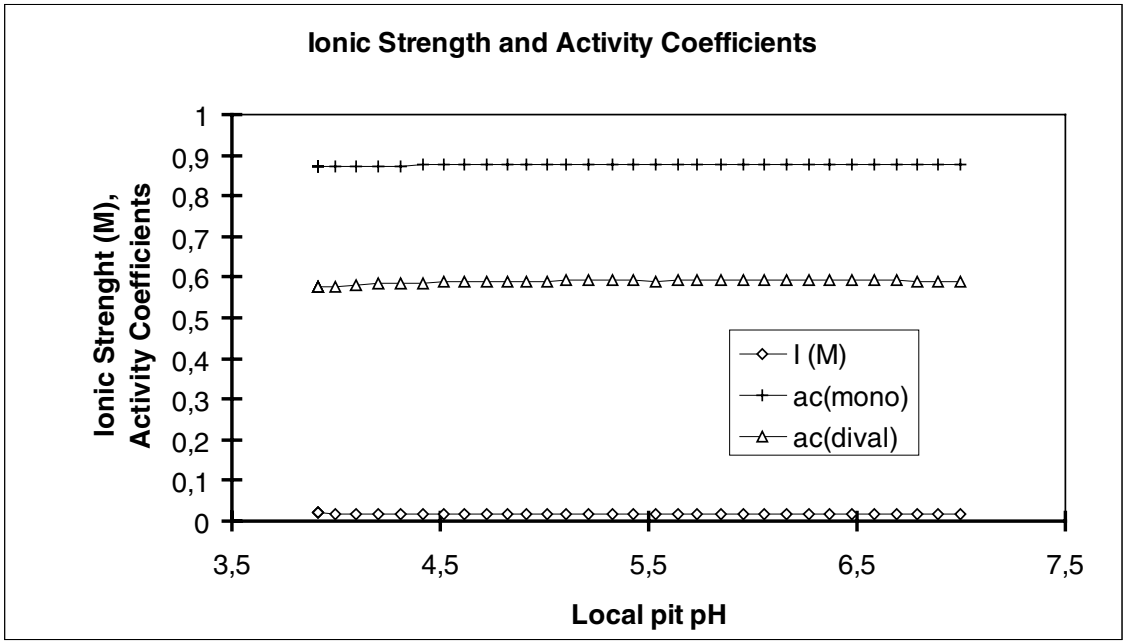

Figure 4-24. Ionic Strength and activity coefficients at various locations in and around a corrosion pit as a function of the local pH. Water B, 25°C.

4.2.8 Speciation of aqueous copper

Figure 4-25 shows the distribution of the local total concentration of monovalent copper into the various aqueous species considered, at various locations in and around the pit as a function of the local pH. A comparison with water *A* shows that the dichloride complex is less dominating in water *B* than in water *A*. The fractions of the neutral monochloride complex and the free cuprous ion are correspondingly higher.

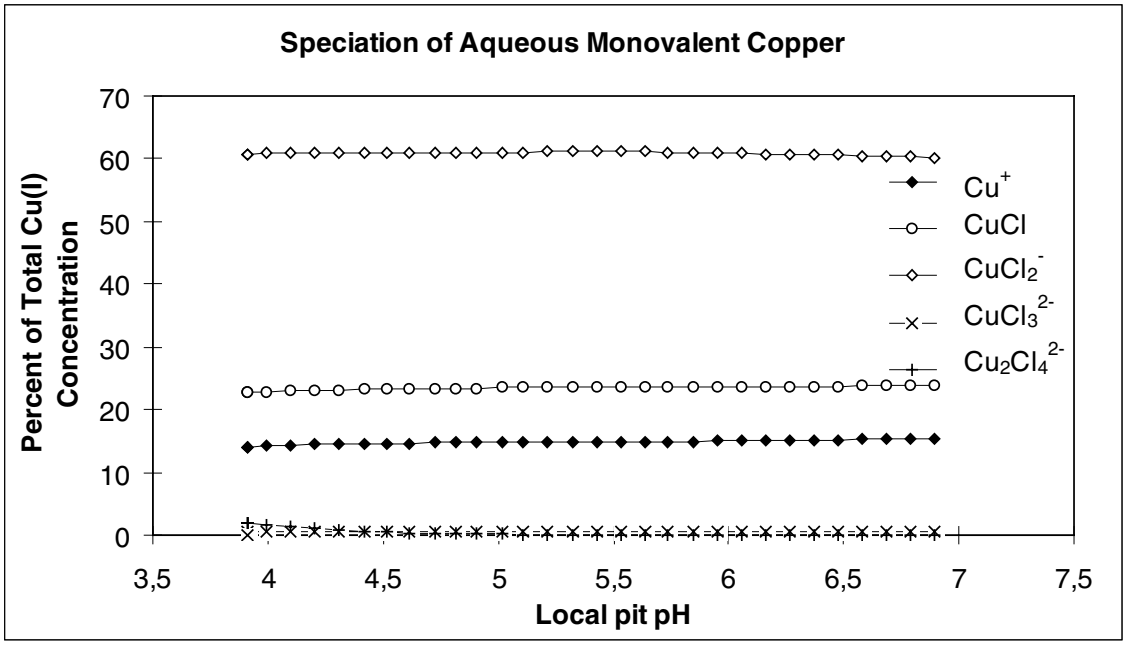

Figure 4-25. Speciation of monovalent copper at various locations in and around a corrosion pit as a function of the local pH. Water B, 25°C.

Figure 4-26 shows the distribution of the local total concentration of divalent copper into the various aqueous species considered, at various locations and around the pit as a function of the local pH. The dominating species are the same as in water *A* and over the same pH ranges. The main difference is that the neutral sulphate complex reaches a maximum fraction of about 25% in water *B* to be compared with the 40 % in water *A*.

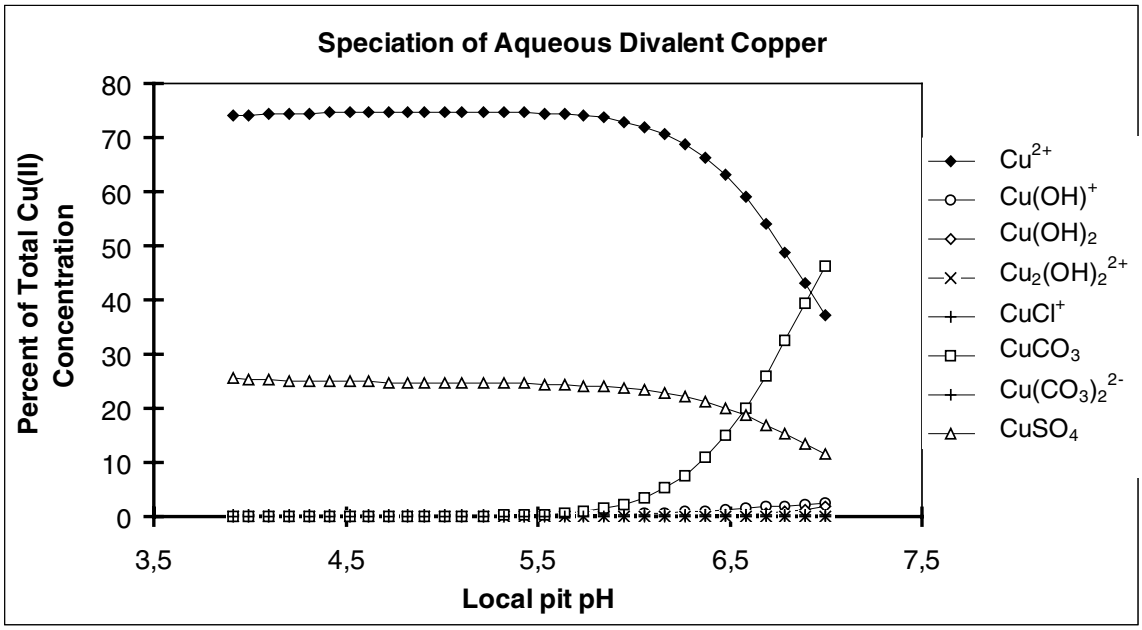

Figure 4-26. Speciation of divalent copper at various locations in and around a corrosion pit as a function of the local pH. Water B, 25°C.

4.2.9 Speciation of chloride, carbonate, sulphate and calcium

The differences in the speciation of chloride, carbonate, sulphate and calcium are small between water *A* and water *B*. Figure 4-27 shows that the dichloride complex with monovalent copper has a slightly higher maximum fraction of the total chloride concentration than in the pit in water *A*.

No effect on the speciation of carbonate can be seen from figure 4-28. The sulphate complex with divalent copper has increased from less than 1% in water *A* to more than 5% in figure 4-29 for water *B*. Calcium, in figure 4-30, shows a decreased influence of the sulphate complex with a corresponding increase in the fraction of the total concentration which is present as the free calcium ion.

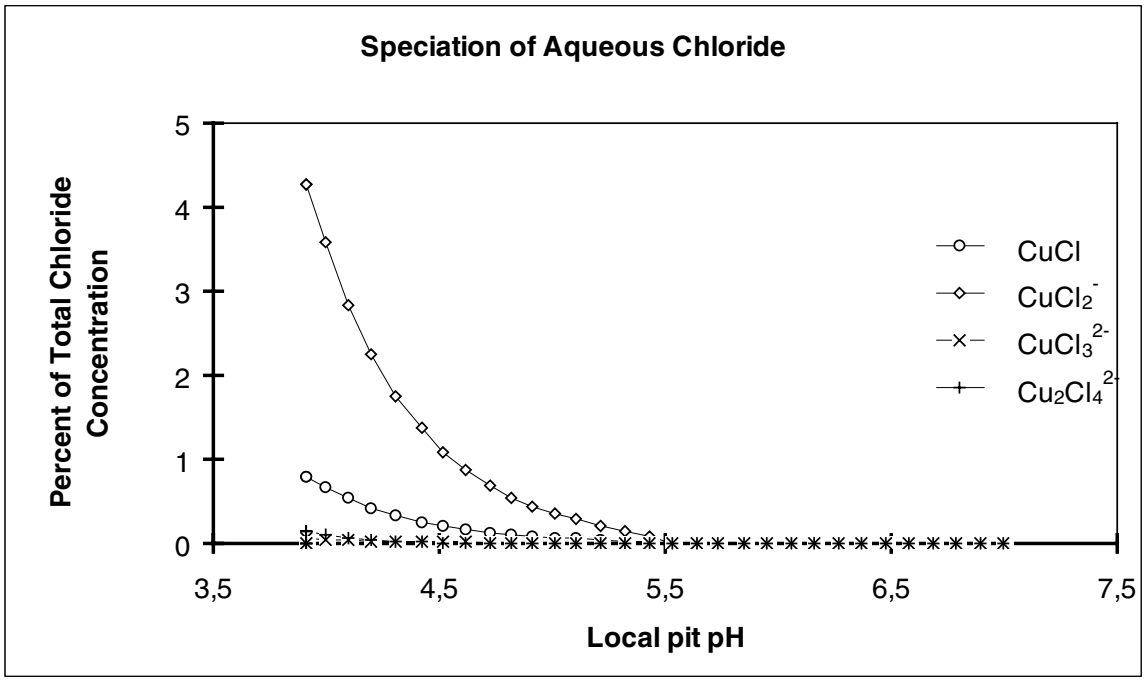

Figure 4-27. Speciation of aqueous chloride at various locations in and around a corrosion pit as a function of the local pH. Water B, 25°C.

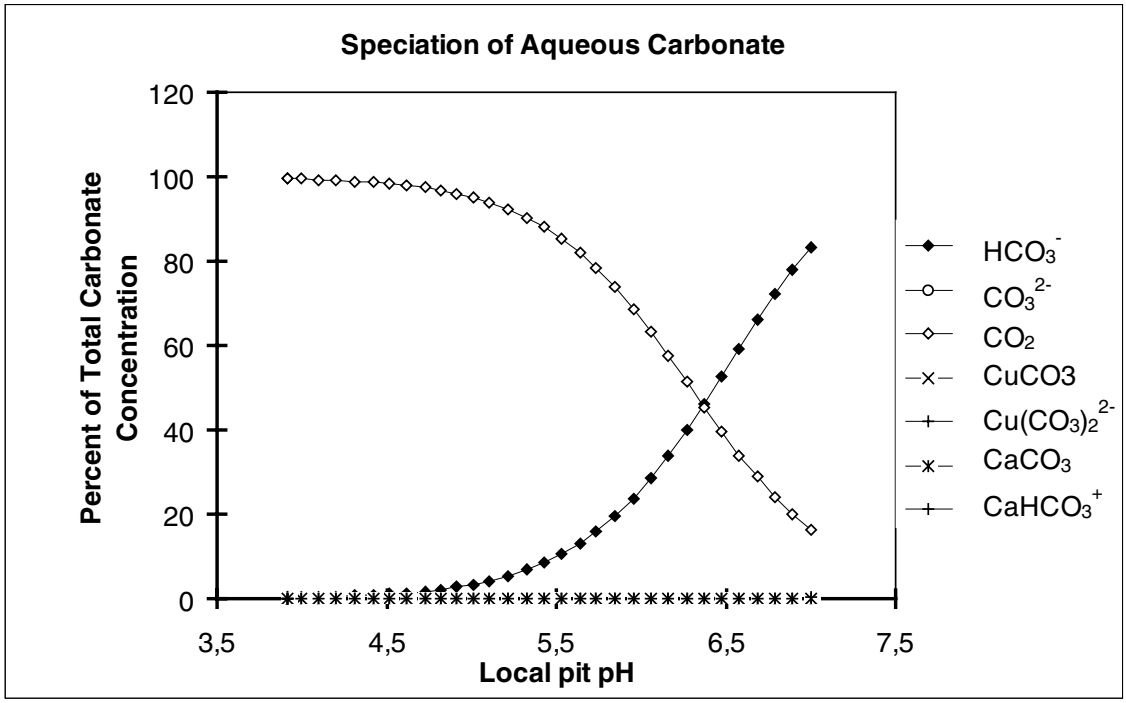

Figure 4-28. Speciation of aqueous carbonate at various locations in and around a corrosion pit as a function of the local pH. Water B, 25°C.

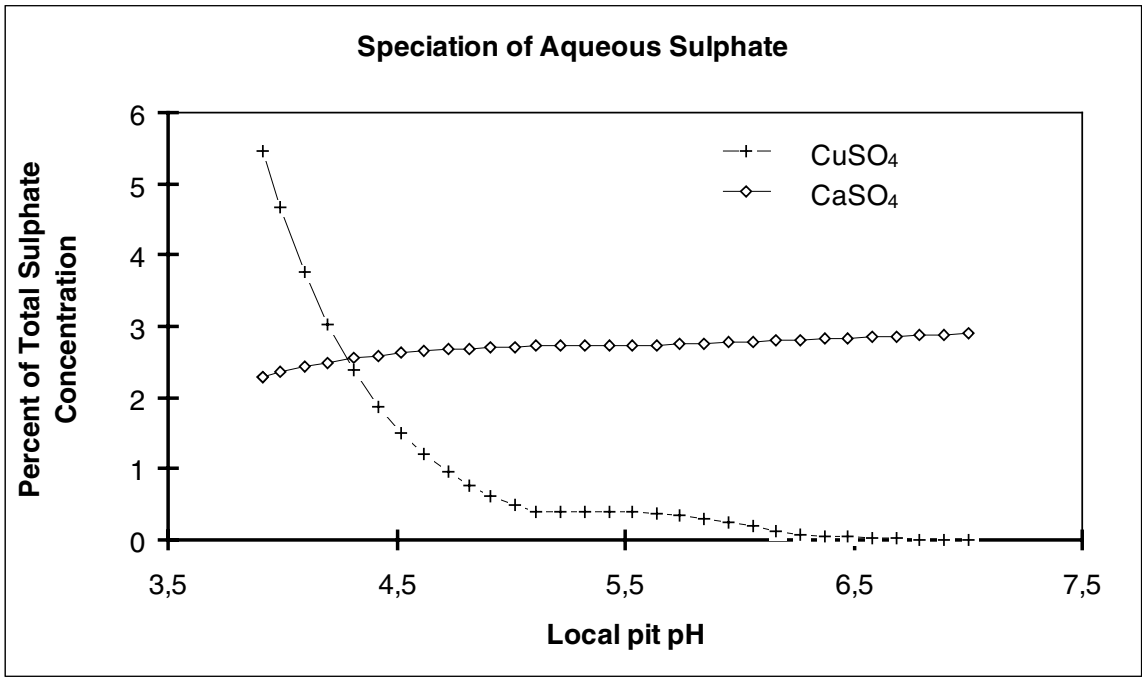

Figure 4-29. Speciation of aqueous sulphate at various locations in and around a corrosion pit as a function of the local pH. Water B, 25°C.

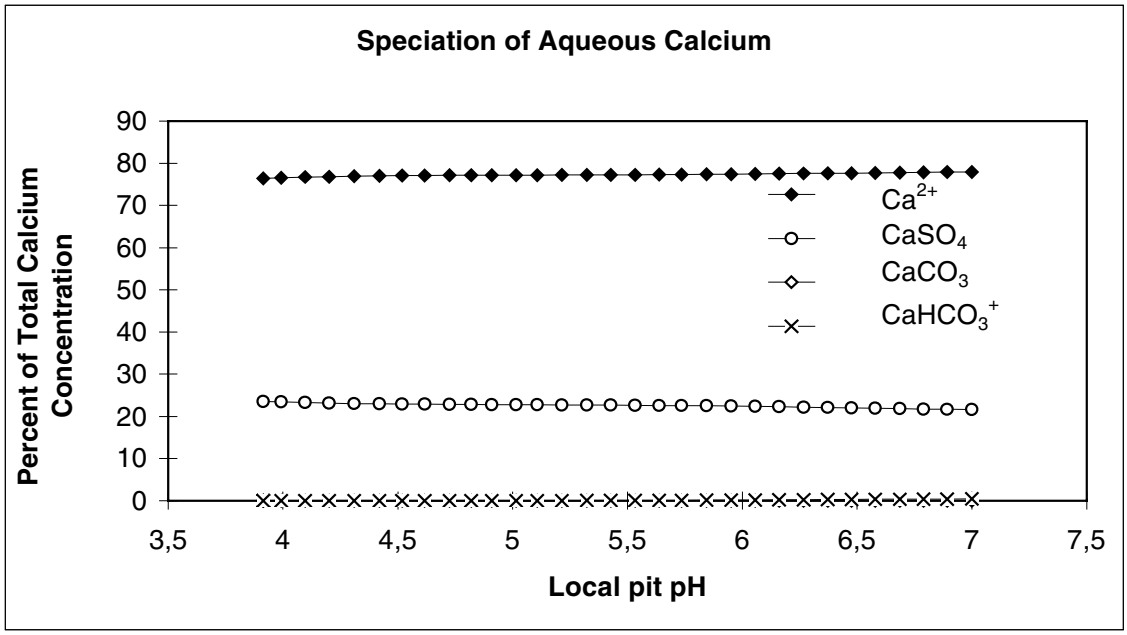

Figure 4-30. Speciation of aqueous calcium at various locations in and around a corrosion pit as a function of the local pH. Water B, 25°C.

4.2.10 Current transport

Figures 4-31 and 4-32 show the fraction of the total pit current transported by some species at various locations in and around the pit as a function of the local pH. In the near neutral range, the hydrogen carbonate dominates the aqueous charge transport just as in water *A*. At lower pH values, protons and divalent copper dominate. In contrast to the pit in water *A* the influence of chloride, which is related to monovalent copper, is low. The fraction of the current transported by the dichloride complex with monovalent copper is also much less negative than in water *A*.

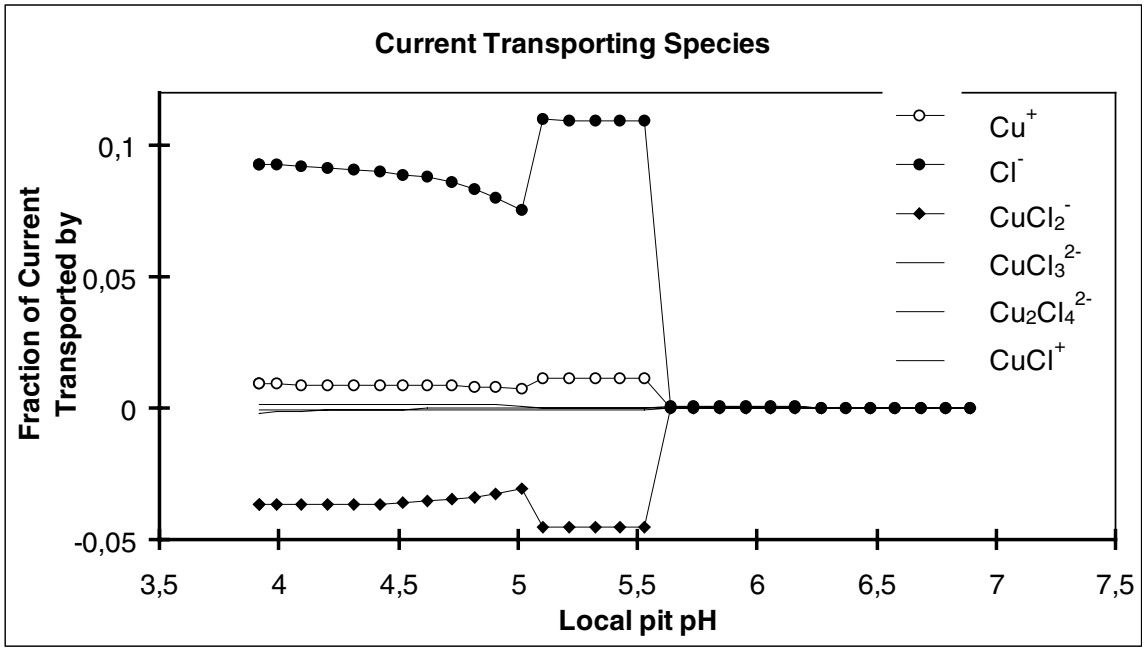

Figure 4-31. Current transport outwards by the cuprous and chloride containing species at various locations in and around a corrosion pit as a function of the local pH. Water B, 25°C.

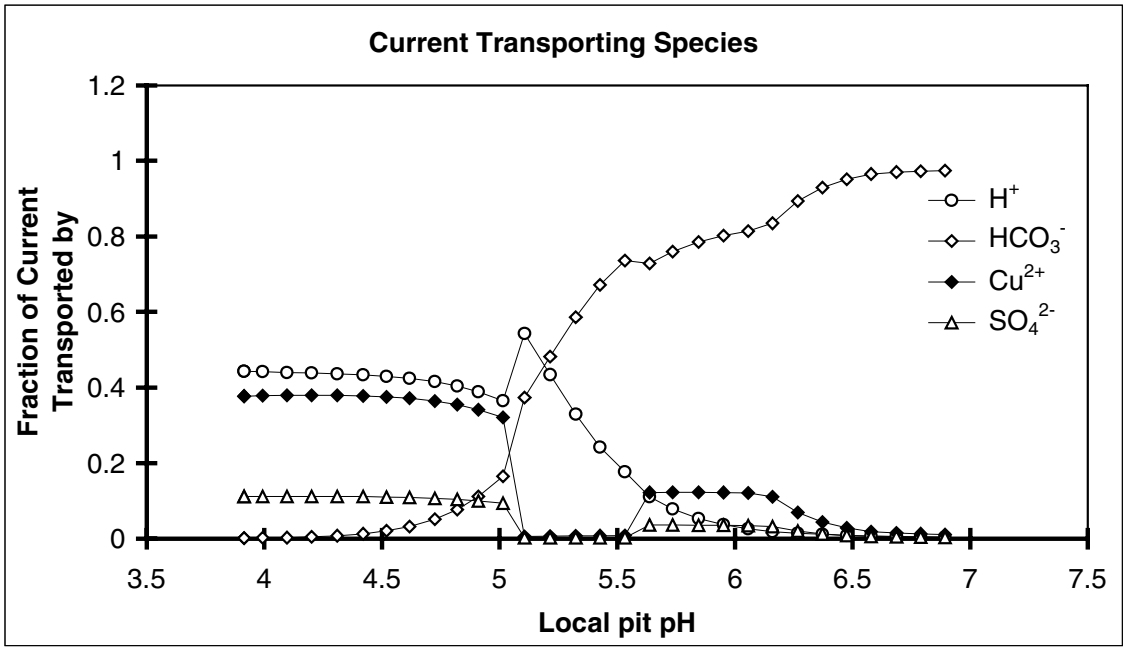

Figure 4-32. Current transport outwards by the major current transporting species at various locations in and around a corrosion pit as a function of the local pH. Water B, 25°C.

4.2.11 The growth of the corrosion pit

Figure 4-33 shows the estimated maximum pit depth for a corrosion pit in copper at a potential of + 242 mV (NHE) in water *B* as a function of time. The calculated value of the time to reach 0.5 cm pit depth is in this case about 4000 years to be compared with the 1500 years calculated for a corrosion potential of 216 mV in water *A*.

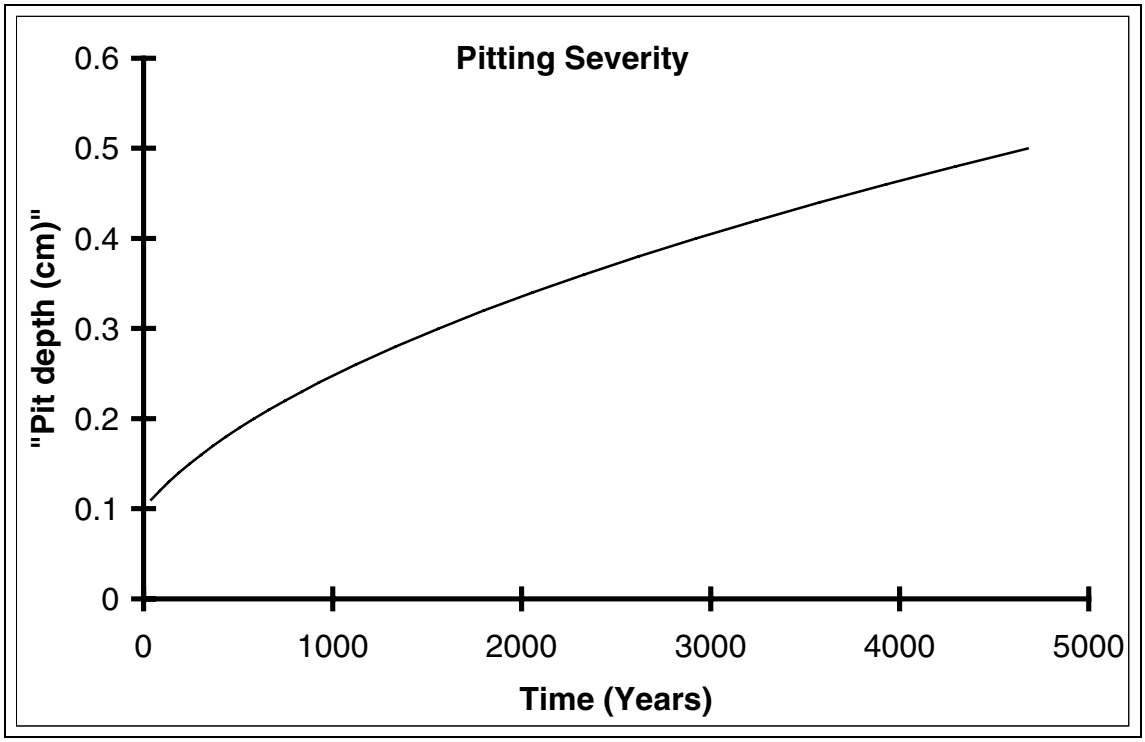

Figure 4-33. Estimated maximum growth rate for a corrosion pit on copper. Water B, 25°C. 242 mV vs NHE

4.2.12 Conditions at the cathode.

Figure 4-34 shows the coexistence potentials for cuprous oxide with each of the cupric phases considered, at the pH of the bulk. The straight line at +242 mV indicating the corrosion potential for the particular pit considered here is practically at the coexistence potential for cuprous oxide with three different cupric phases. Both basic carbonate salts and cupric oxide have the same thermodynamic stability as cuprous oxide at +242 mV in water *B* at 25°C. The margin against pitting, at the low rate determined by this potential, is zero and we find that propagation is possible.

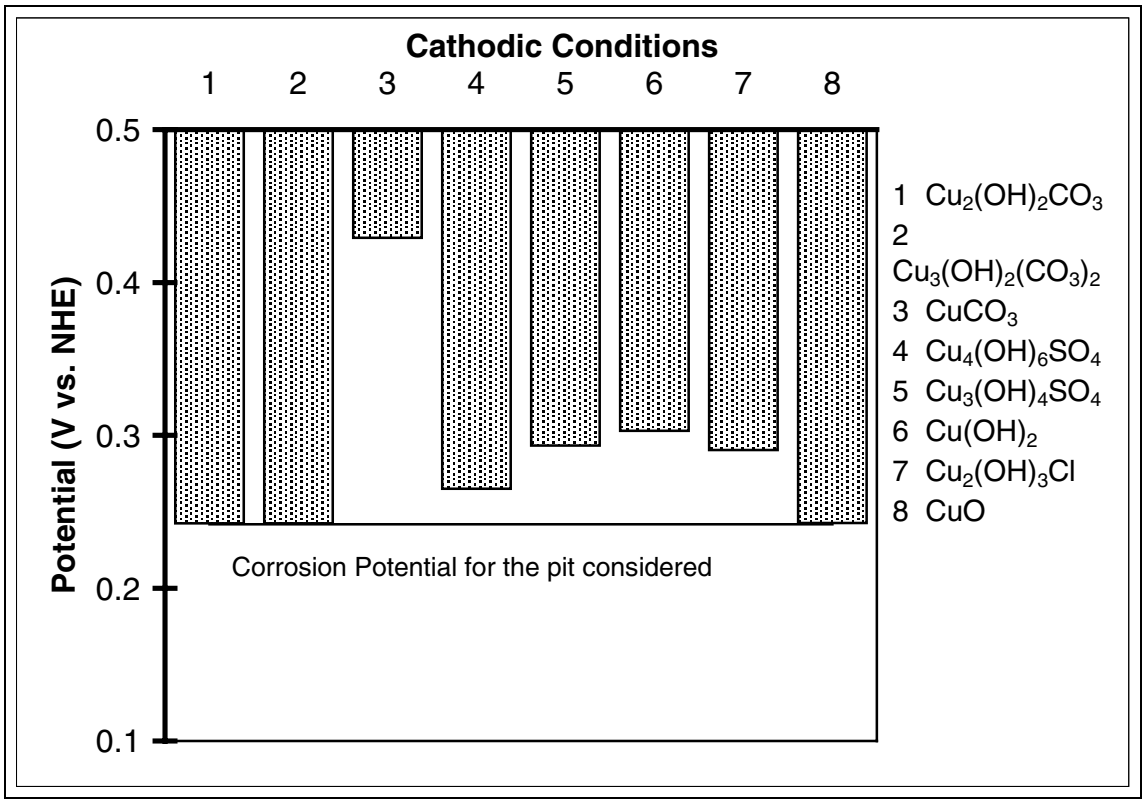

Figure 4-34. Coexistence potentials for Cu_2O(s) with various cupric solids at bulk conditions. Water B, 25°C.

4.3 A corrosion pit in water *B* at 75°C

A detailed description of a corrosion pit in water *B* at 75°C in relation to pits in waters *A* and *B* at 25°C is given here. In water *B* with the composition given in table 4-1 we find that at 75°C pitting is possible at potentials higher than about +215 mV. This is about the same value of the minimum pitting potential found as for water *A* at 25°C and lower than for water *B* at 25°C. A detailed comparison between the results from a modelling of a corrosion pit in water *B* at 75°C and 218 mV and the pits in waters *A* and *B* at 25°C, discussed in sections 4.1 and 4.2 respectively, is given here.

4.3.1 pH domains for solids

Figure 4-35 shows the domains where a basic carbonate salt of copper is precipitated and where cuprous oxide is formed. The carbonate poor malachite is precipitated here instead of the carbonate rich azurite which formed in waters *A* and *B* at 25°C. Compared with the pits at 25 °C, the precipitation limits are shifted towards higher pH values, the pH domain where basic carbonate precipitates is more narrow and the pH at the site of the metal oxidation is higher.

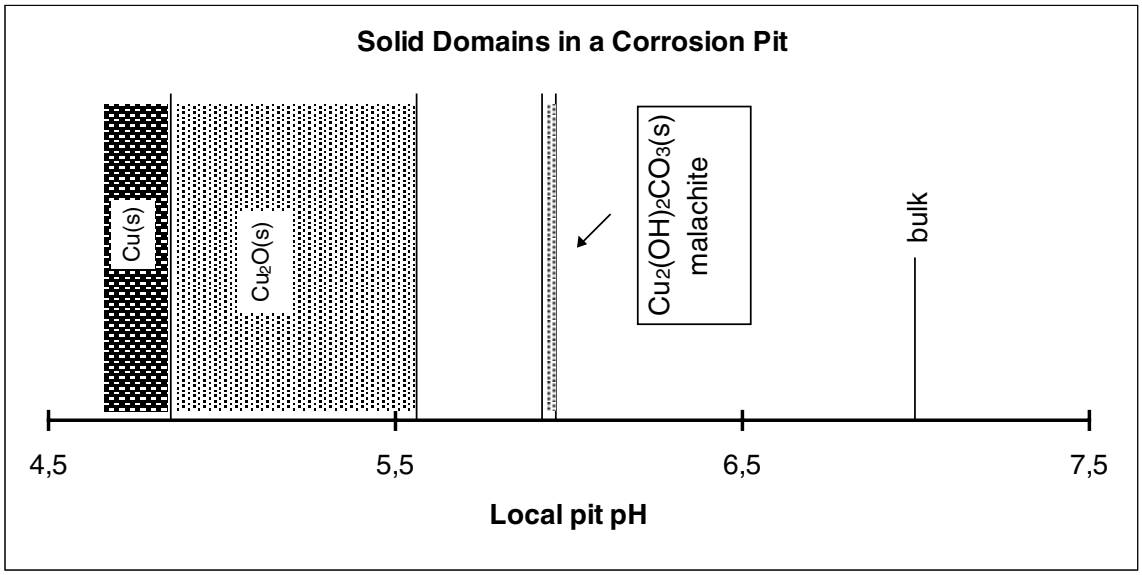

Figure 4-35. pH limits for precipitation of basic cupric and for cuprous oxide at a corrosion pit in copper. Water B, 75°C. 218 mV vs NHE.

4.3.2 Redox reactions

The redox conditions in and around the pit is shown in figure 4-36. The stability domain for cuprous oxide is smaller here than at 25°C. The sharp drop in redox potential occurs at about pH 5.8 which is similar to the values found for waters *A* and *B* at 25°C.

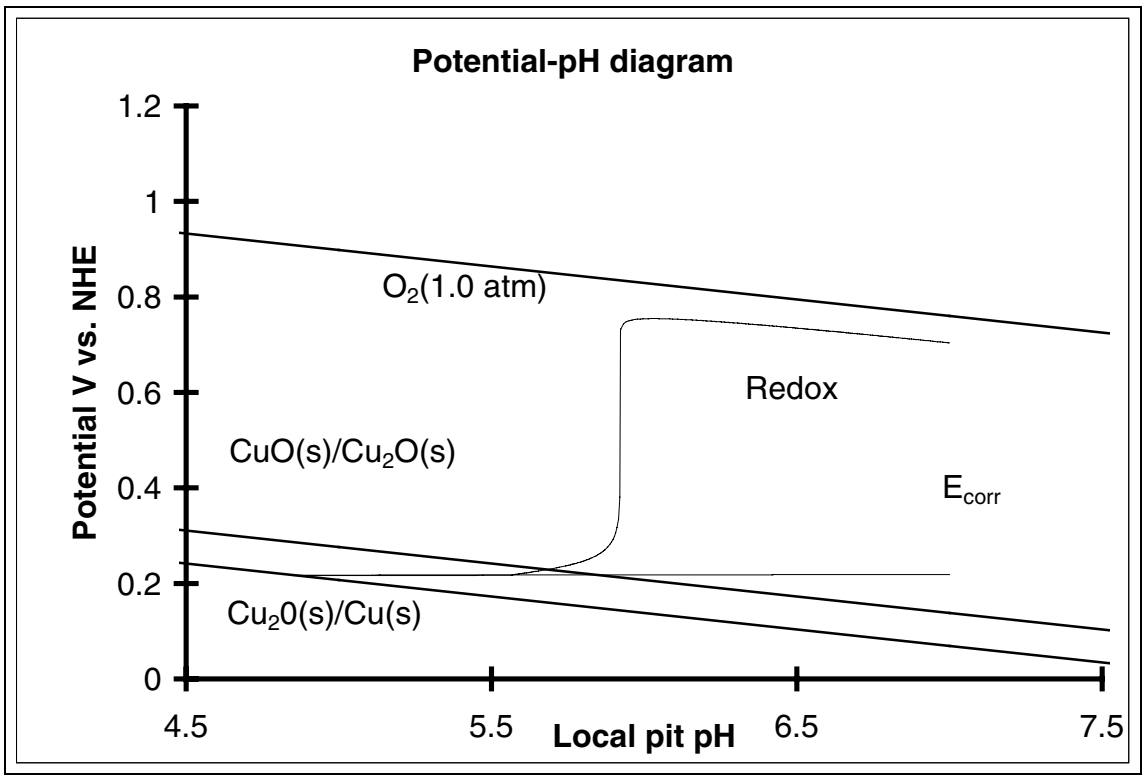

Figure 4-36. Potential pH diagram showing the redox potential at various locations in and around a corrosion pit as a function of the local pH. Water B, 75°C.

4.3.3 Transport of copper

Figure 4.37 shows the fraction of the oxidized copper, which is transported, away from the site of the metal oxidation at various location in the pit as a function of the local pH. A comparison with the pits found at 25°C shows that the copper transport in this pit is even more dominated by monovalent copper. The fraction of the oxidised copper transported as divalent copper is at most 8% to be compared with 33% for water *B* at 25°C and 20% for water *A* at 25°C. Figure 4.37 shows that there is a range where the transport of divalent copper is negative, that is, directed inwards. That was found also for water *A* at 25°C but not for water *B*.

4.3.4 Copper concentrations

Figure 4-38 shows the total concentrations of monovalent and divalent copper at various locations in the pit as a function of the local pH. In contrast to the pits at 25°C, at low pH values, the concentration of monovalent copper is higher than the concentration of the divalent copper.

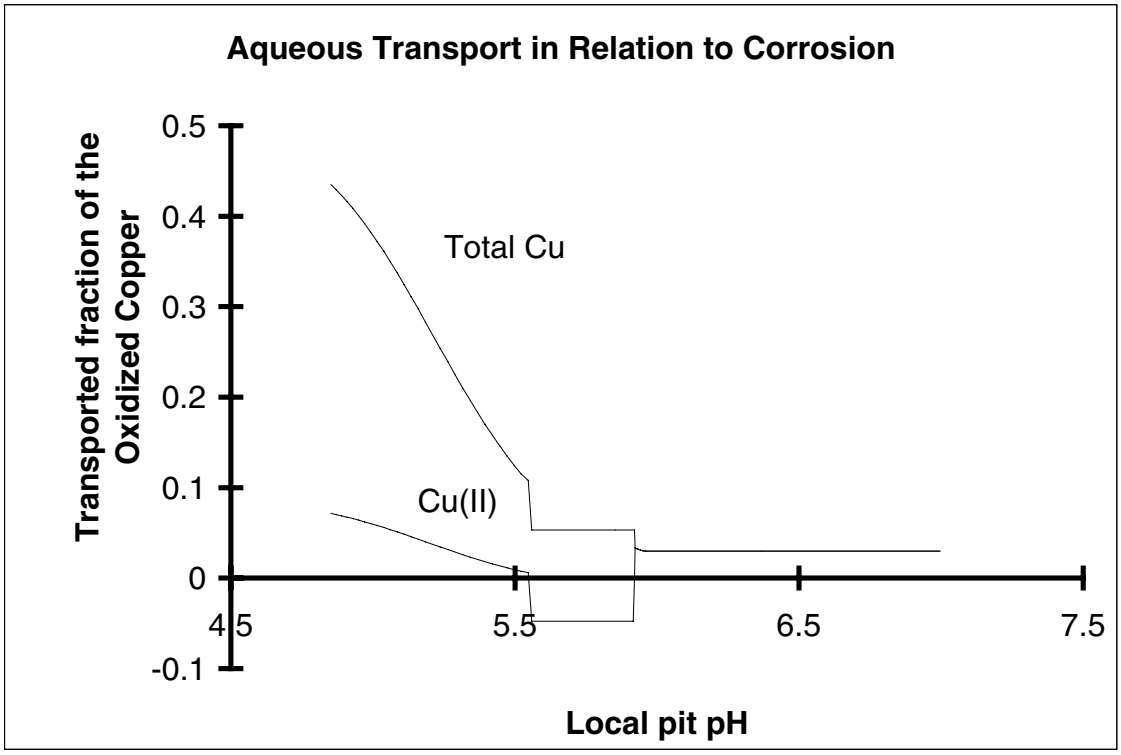

Figure 4-37. The fraction of the oxidised copper transported as aqueous species, in direction out of the pit, at various locations in and around a corrosion pit as a function of the local pH. Water B, 75°C.

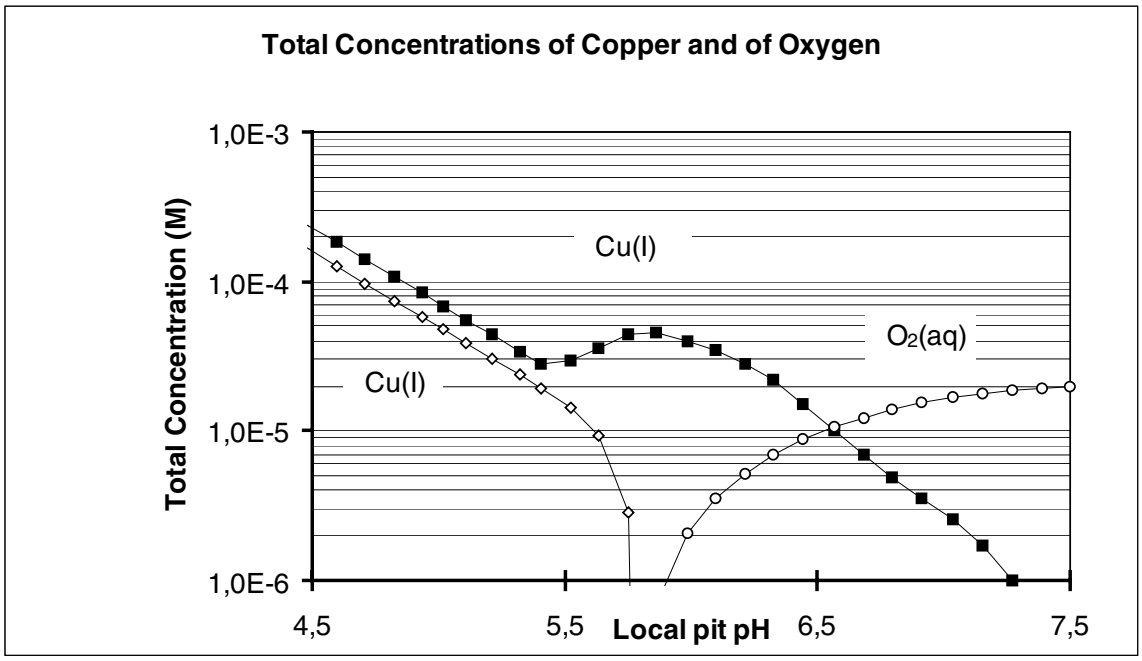

Figure 4-38. Total concentrations of copper(I), copper(II) and oxygen at various locations in and around a corrosion pit as a function of the local pH. Water B, 75°C.

4.3.5 Solids in the system

Figure 4-39 shows the activities of the copper containing solids considered at various locations in and around the pit as a function of the local pH. At about pH 6 the carbonate poor of the basic carbonate salts, malachite, reaches saturation. The activity of cupric oxide has over a wide pH range a value higher than unity. The solution is supersaturated with respect to this phase because we have suppressed the precipitation. The reason for doing this is that we find it likely that, unless already present, precipitation of this phase, CuO(s), does not occur until the solution is saturated with respect to cupric hydroxide, $Cu(OH)_2(s)$. This is discussed more fully in section 5-2. The activity of the monovalent copper chloride is lower at 75°C than at 25°C and is below the scale in figure 4-39.

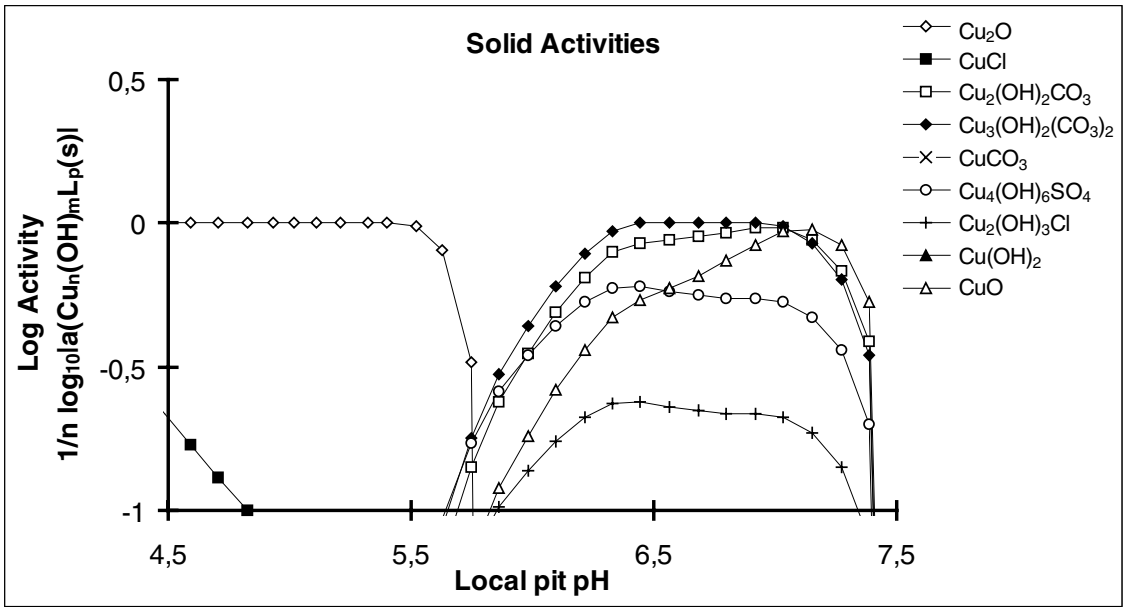

Figure 4-39. Activities of the solid copper species considered at various locations in and around a corrosion pit as a function of the local pH. Water B, 75°C.

4.3.6 Concentrations of water components

Figure 4-40 shows the total concentrations of some water components at various locations in and around the pit as a function of the local pH. The changes in the local concentrations with pH are even smaller here than at 25°C. Only the total concentration of carbonate shows a significant decrease towards lower pH values.

4.3.7 The ionic strength and activity coefficients

Figure 4-41 shows the local ionic strength and the activity coefficients for monovalent ions and for divalent ions at various locations in and around the pit as a function of the local pH. The ionic strength and the activity coefficients are very similar to those of water *B* at 25°C and practically constant over the whole pH range.

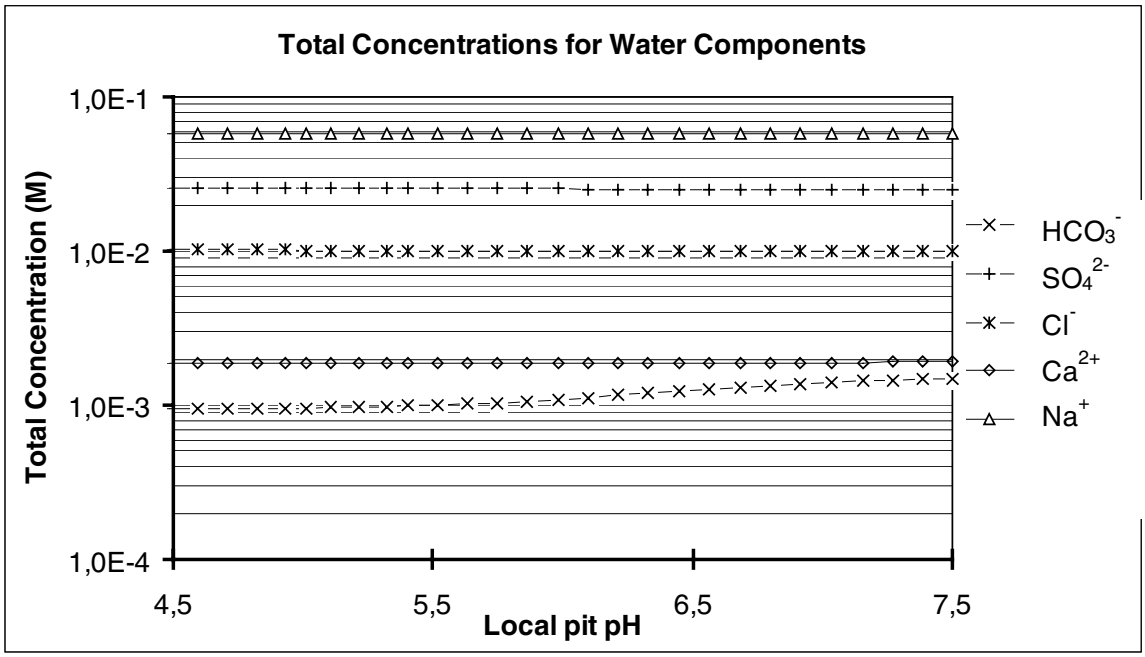

Figure 4-40. Total concentrations for water components at various locations in and around a corrosion pit as a function of the local pH. Water B, 75°C.

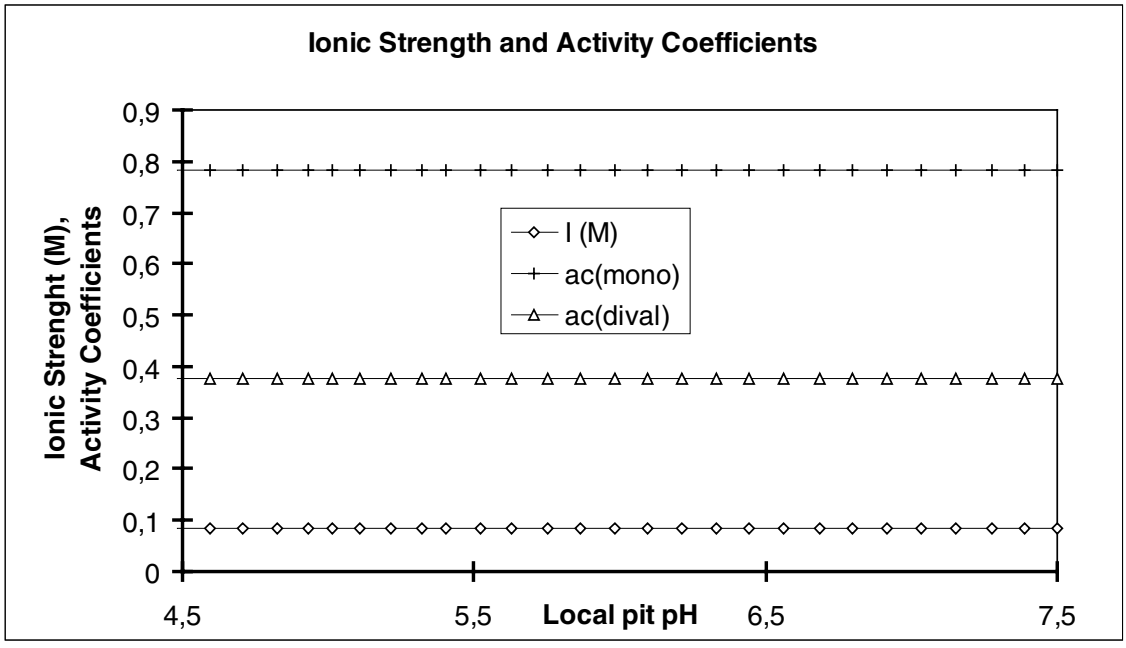

Figure 4-41. Ionic Strength and activity coefficients at various locations in and around a corrosion pit as a function of the local pH. Water B, 75°C.

4.3.8 Speciation of aqueous copper

Figure 4-42 shows the distribution of the local total concentration of monovalent copper into the various aqueous species considered, at various locations in and around the pit as a function of the local pit pH. The speciation is very similar to water *B* at 25°C.

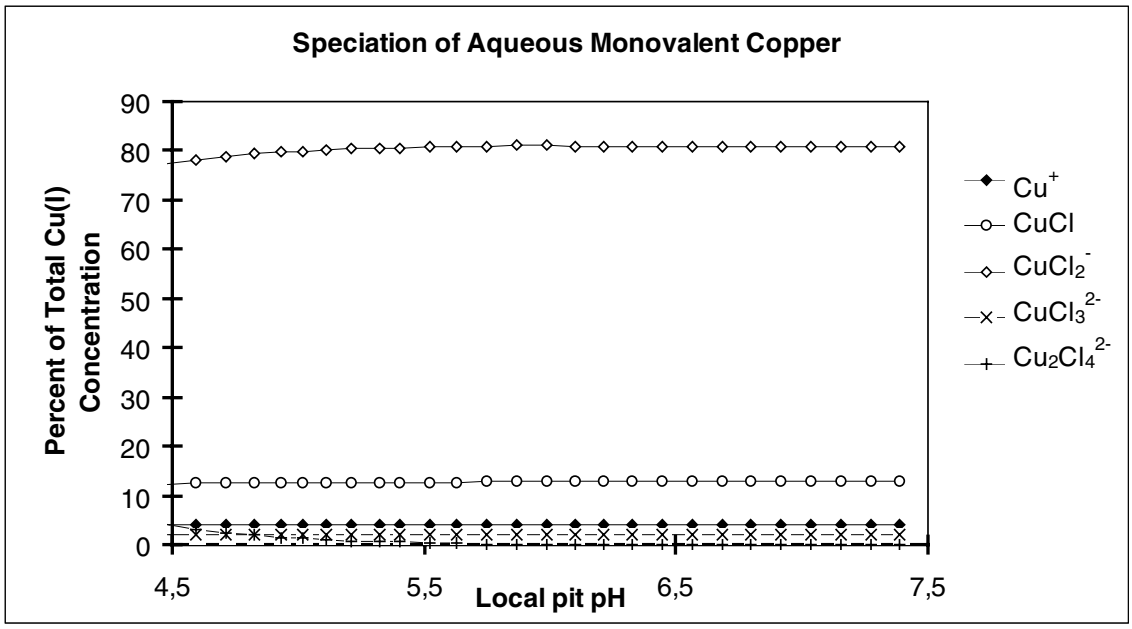

Figure 4-42. Speciation of monovalent copper at various locations in and around a corrosion pit as a function of the local pH. Water B, 75°C.

Figure 4-43 shows the distribution of the local total concentration of divalent copper into the various aqueous species considered, at various locations in and around the pit as a function of the local pit pH. Compared with the distribution in water *B* at 25°C, the carbonate complex and the dihydroxide complex have increased in stability. The sulphate complex has decreased in stability causing the free Cu^{2+} to be more dominating at low pH.

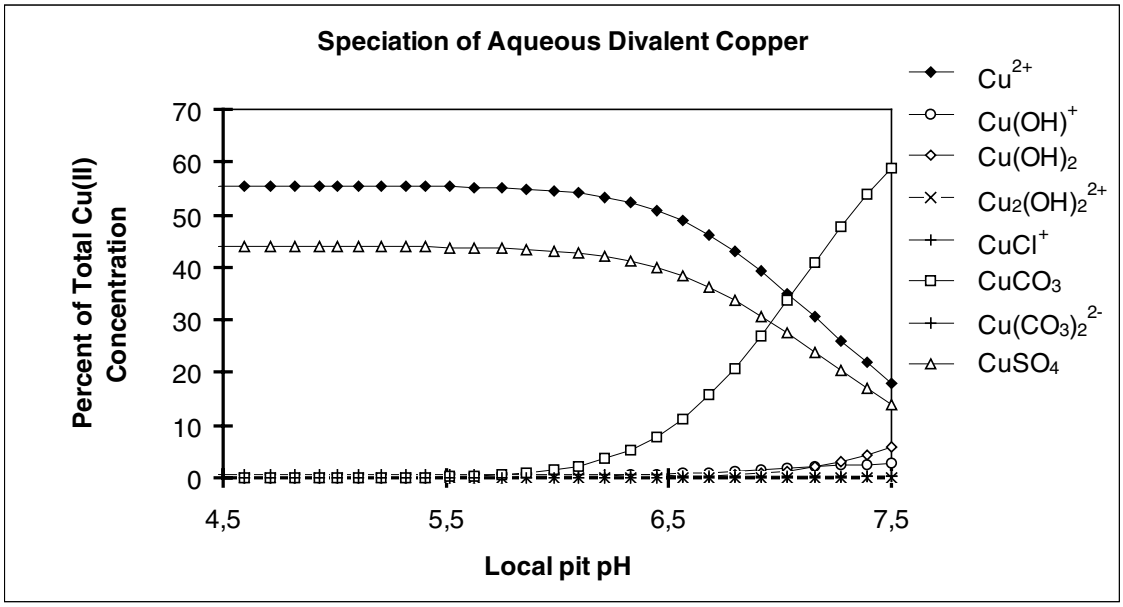

Figure 4-43. Speciation of divalent copper at various locations in and around a corrosion pit as a function of the local pH. Water B, 75°C.

4.3.9 Speciation of chloride, carbonate, sulphate and calcium

The differences in the speciation of chloride, carbonate, sulphate and calcium are small between water *B* at 75°C and the same water at 25°C. Figure 4-44 shows that the dichloride complex with monovalent copper has a slightly higher maximum fraction of the total chloride concentration than at 25 °C.

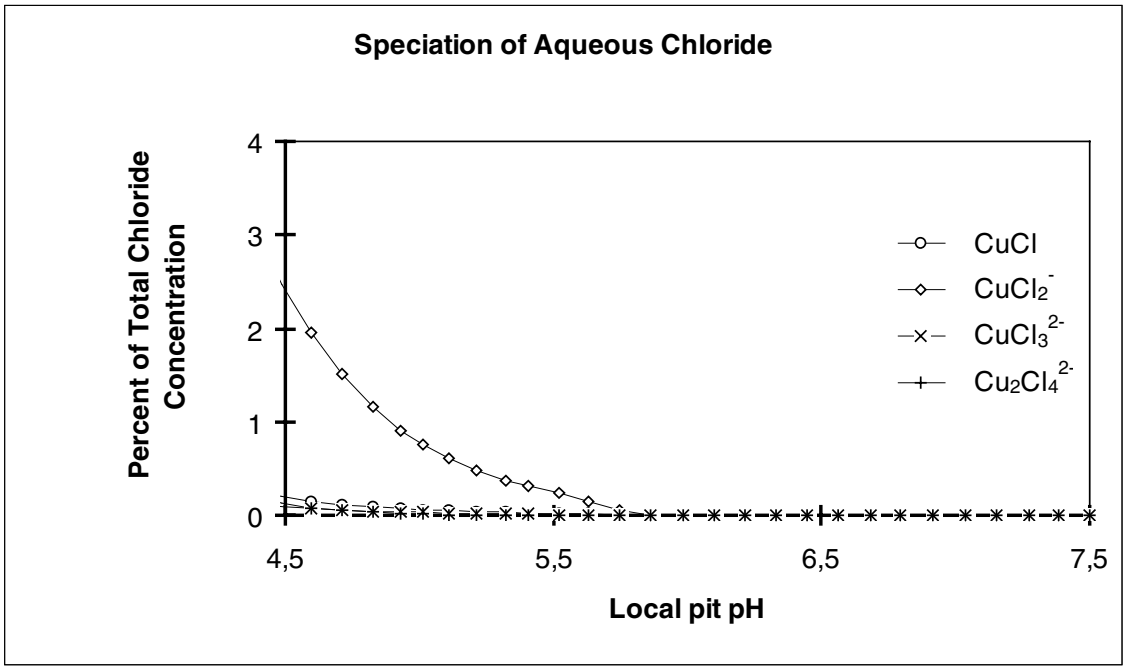

Figure 4-44. Speciation of aqueous chloride at various locations in and around a corrosion pit as a function of the local pH. Water B, 75°C.

Figure 4-45 showing the speciation of carbonate illustrates the shift in protolysis constant for carbonic acid from 6.3 at 25°C to 6.0 at 75°C. The aqueous copper carbonate reaches a maximum fraction of a few percent at pH 6.0.

The sulphate complex with divalent copper in figure 4-46 reaches only insignificant fractions of the total sulphate. This is more similar to the 1% found in water *A* at 25°C than the 5 % found in water *B* at 25°C.

The speciation of calcium, in figure 4-47, shows a distribution similar to the same water at 25°C with a relatively high fraction of the sulphate present as the aqueous sulphate complex.

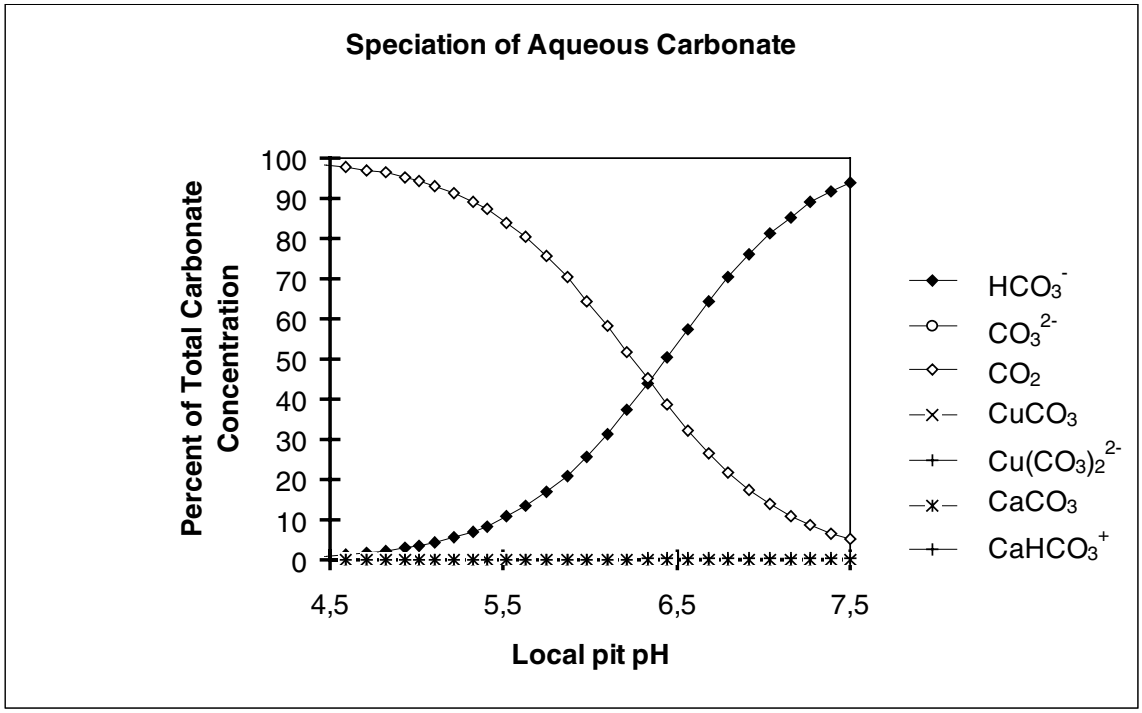

Figure 4-45. Speciation of aqueous carbonate at various locations in and around a corrosion pit as a function of the local pH. Water B, 75°C.

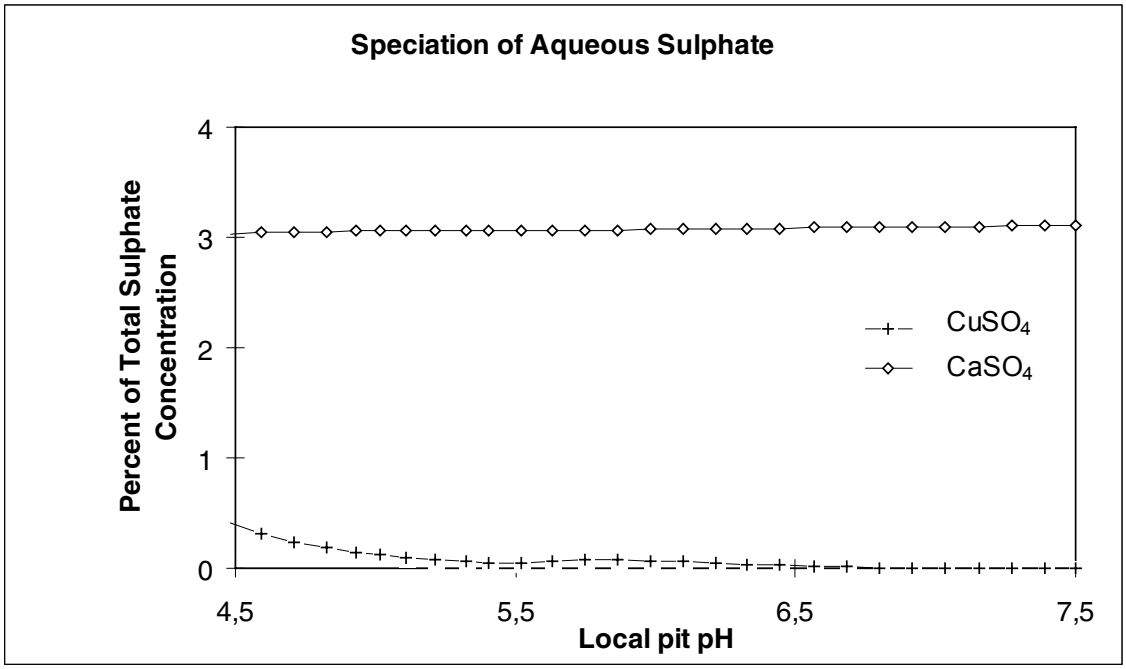

Figure 4-46. Speciation of aqueous sulphate at various locations in and around a corrosion pit as a function of the local pH. Water B, 75°C.

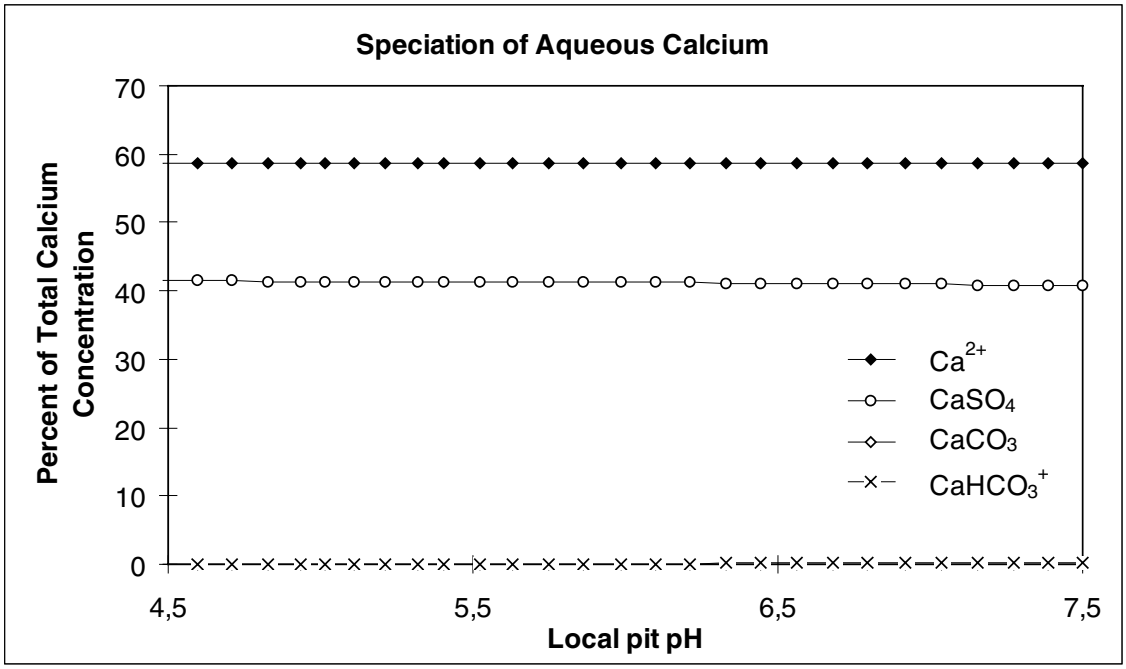

Figure 4-47. Speciation of aqueous calcium at various locations in and around a corrosion pit as a function of the local pH. Water B, 75°C.

4.3.10 Current transport

Figures 4-48 and 4-49 show the fraction of the total pit current transported by some species at various locations in and around the pit as a function of the local pH. At pH values higher than 5 the transport is dominated by hydrogen carbonate with contributions from chloride and from protons. Chloride ions and protons dominate the current transport at low pH. The cupric ion reaches a maximum fraction of about 10% at the lowest pH. Compared with the pits at 25 °C, the current transport in this pit in water *B* at 75°C is more similar to the results for water *A* than for water *B* where we found a maximum fraction for the cupric ion of about 40%.

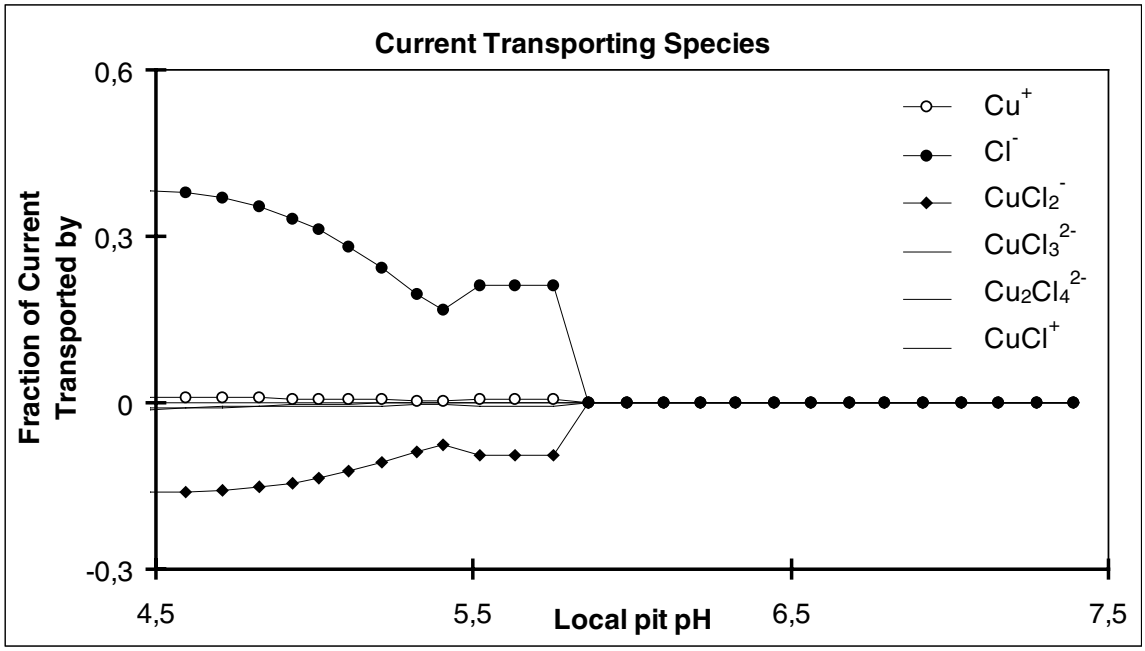

Figure 4-48. Current transport outwards by the cuprous and chloride containing species at various locations in and around a corrosion pit as a function of the local pH. Water B, 75°C.

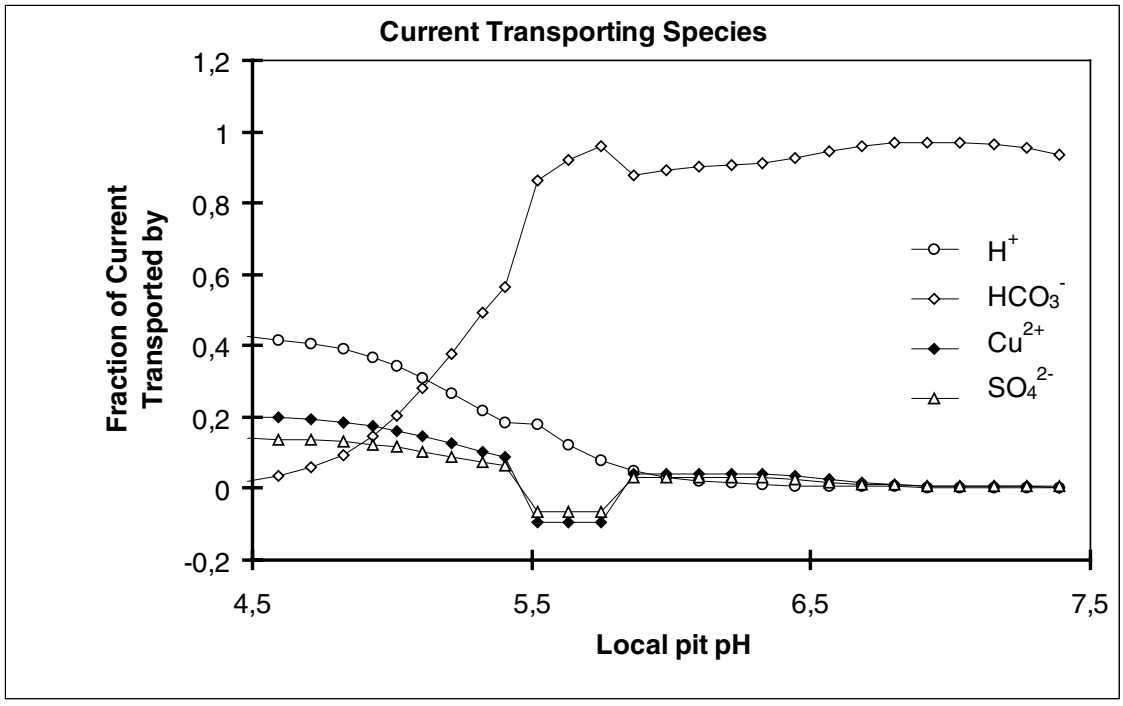

Figure 4-49. Current transport outwards by the major current transporting species at various locations in and around a corrosion pit as a function of the local pH. Water B, 75°C.

4.3.11 The growth of the corrosion pit

Figure 4-50 shows the estimated maximum pit depth for a corrosion pit in copper at a potential of + 218 mV (NHE) in water *B* as a function of time. The time scale here is such that, although a pitting process is possible, the growth rate is insignificant at this potential.

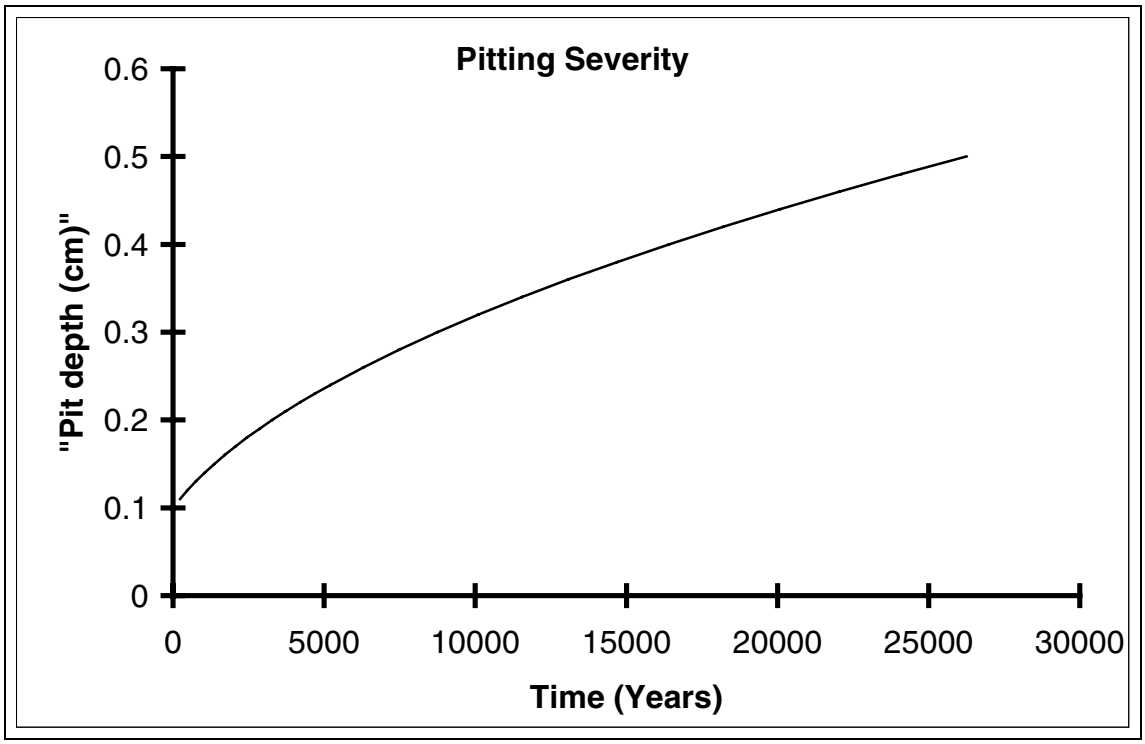

Figure 4-50. Estimated maximum growth rate for a corrosion pit on copper. Water B, 75°C. 218 mV vs NHE.

4.3.12 Conditions at the cathode.

Figure 4-51 shows the coexistence potentials for cuprous oxide with each of the cupric phases considered, at the pH of the bulk. The corrosion potential is in a domain where cuprous oxide is not stable, at the pH of the bulk. Several cupric phases have higher stabilities. From this we conclude that cuprous oxide is unlikely to behave as a net cathode and that the anodic current required to drive a pitting process can not be sustained by a reduction at cuprous oxide.

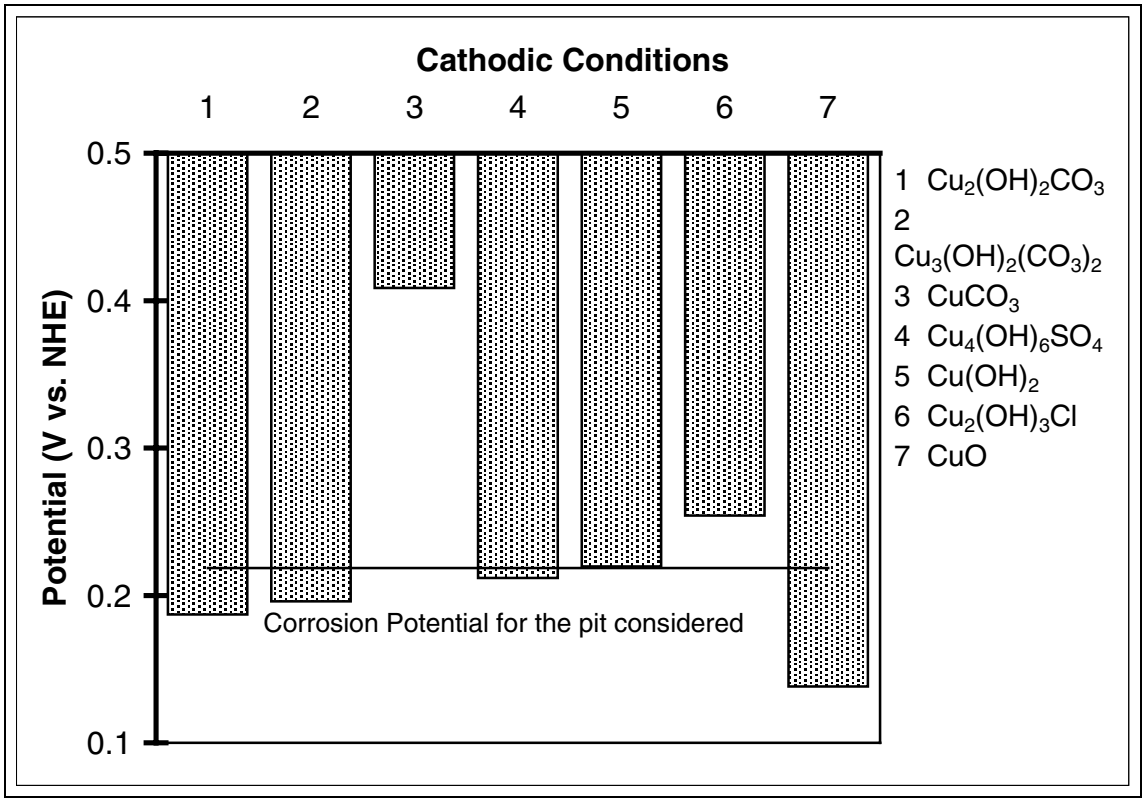

Figure 4-51. Coexistence potentials for Cu_2O(s) with various cupric solids at bulk conditions. Water B, 75°C.

4.4 Overview of the calculated corrosion pits

The chemistry between the bulk water and the solution at the site of dissolution of copper metal was calculated for various compositions of the bulk water. Two temperatures were considered 25°C and 75°C. In general, calculations were made for, at least, two corrosion potentials for each water composition and temperature. Interpolation or extrapolation of data for these corrosion potentials allows us to determine the minimum corrosion potential at which a corrosion pit can propagate.

Tables 4-2 to 4-8 show overviews of the environments for which we have calculated to chemistry between the bulk water and the site of metal dissolution in a corrosion pit. Table 4-2 shows an overview of the results for water *A* at 25°C. In order to study the influence of the various water components, the composition of the water was changed from that of water *A* one parameter at the time. For each water composition and

corrosion potential, the potential drop in the solution resulting from the corrosion current in the pit and the fraction of the oxidised copper which is transported away from the site of dissolution is listed in the table. The model geometry for which the calculations are made can be scaled down or up to, in principle, any size. The value of the corrosion current in the pit is a function of the size or depth of the corrosion pit. By attributing an initial depth of 0.1 cm, the minimum time for a particular pit to grow to 0.5 cm was estimated. Rounded values of the estimates of the minimum time to grow to 0.5 cm depth are listed for each calculated corrosion pit that can propagate.

4.4.1 Water *A* at 25°C

The calculated behaviour of a corrosion pit for water *A* at 25°C at a corrosion potential of 216 mV was described in section 4.1. Table 4-2 summarises results for five corrosion potentials in this water. About 500 years is the estimated time for the fastest growing pit we have calculated for water *A* at 25°C. The time required to reach a pit of 0.5 cm shows a strong dependence on the fraction of the oxidised copper that is transported away from the site of the metal dissolution and thereby on the corrosion potential. At a high transported fraction at the copper metal, the aqueous cross section available for aqueous mass transport of corrosion products is high and the growth rate is accordingly also high. The long time perspectives are consequences of the deep pits considered and of our ambition to study pitting at conditions where pitting is barely possible and to determine limits for the conditions under which a corrosion pit in copper can propagate. In water *A* as in all the variations in the compositions in table 4-2, a basic carbonate salt of divalent copper precipitates and forms what we interpret as a crust of corrosion products outside the pit. In water *A* with a total carbonate concentration reduced to 50%, the both basic carbonate salts precipitate in the crust. Cupric oxide also reaches saturation, but we have chosen to suppress the precipitation of this phase. Reasons for suppressing the formation of CuO(s) are discussed in section 5-4. The corrosion potentials required to obtain the pitting limit and the dependence on the water composition is discussed in sections 4.5 and 4.6. From table 4-2 it is evident that the iR-drop; the potential difference in the aqueous phase between the bulk of the solution and the solution at the site of the metal dissolution, is small. In a water with a conductivity as high as in water *A*, the iR-drop has no significantly effect on the value of the minimum pitting potential.

Table 4-3 shows an overview of the results for waters similar to water *A*, but where the total concentrations of chloride, carbonate and sulphate have been increased simultaneously. At 25°C the composition of the crust is the basic carbonate salt of divalent copper at all levels of increased concentrations in table 4-3. As the concentration in the bulk water increases, high values of the transported fraction of the oxidised copper are obtained also at moderately high corrosion potentials.

Table 4-2. Overview of environments for which calculations of the chemistry between the bulk water and the site of metal dissolution have been made. Water *A* with variations of one parameter at the time, 25°C.

Modifications to water *A*		Corrosion potential (mV)	iR drop (mV)	Crust com-position	Transported fraction of the oxidised copper at the site of metal dissolution	Time to grow to a pit depth of 5 mm (years)
none		199.4	0.24	1	0.40	-
none		202.5	0.25	1	0.41	>1000
none		216.2	0.31	1	0.47	>1000
none		221.4	0.35	1	0.49	800
none		223.8	0.37	1	0.51	500
pH decreased	0.3	207.4	0.25	1	0.43	>1000
pH decreased	0.3	214.4	0.29	1	0.46	>1000
$[Cl^-]$	50%	223.3	0.38	1	0.40	-
$[Cl^-]$	50%	225.7	0.41	1	0.42	>1000
$[HCO_3^-]$	50%	202.2	0.14	1,2,3	0.41	>1000
$[HCO_3^-]$	50%	208.1	0.16	1,2,3	0.44	>1000
$[SO_4^{2-}]$	50%	214.8	0.51	1	0.45	>1000
$[SO_4^{2-}]$	50%	223.2	0.60	1	0.48	700
$[O_2]$	50%	208.7	0.27	1	0.43	>1000
$[O_2]$	50%	218.9	0.33	1	0.48	1000
$[O_2]$	110%	223.9	0.38	1	0.51	500
$[O_2]$	400%	197.5	0.24	1	0.39	-
$[O_2]$	400%	204.8	0.26	1	0.42	>1000
$[O_2]$	400%	223.2	0.37	1	0.50	500

Crust composition:
1 $Cu_3(OH)_2(CO_3)_2$ azurite
2 $Cu_2(OH)_2CO_3$ malachite
3 CuO tenorite, precipitation suppressed

Table 4-3. Overview of environments for which calculations of the chemistry between the bulk water and the site of metal dissolution have been made. Water *A* with increasing salt concentrations. 25°C.

Modifications to water *A*		Corrosion potential (mV)	iR drop (mV)	Crust com-posi-tion	Transported fraction of the oxidised copper at the site of metal dissolution	Time to grow to a pit depth of 5 mm (years)
none		199.4	0.24	1	0.40	-
none		202.5	0.25	1	0.41	>1000
none		216.2	0.31	1	0.47	>1000
none		221.4	0.35	1	0.49	800
none		223.8	0.37	1	0.51	500
$[Cl^-],[HCO_3^-],[SO_4^{2-}]$	200%	176.2	0.22	1	0.49	>1000
$[Cl^-],[HCO_3^-],[SO_4^{2-}]$	200%	189.6	0.23	1	0.59	>1000
$[Cl^-],[HCO_3^-],[SO_4^{2-}]$	400%	140.0	0.19	1	0.20	-
$[Cl^-],[HCO_3^-],[SO_4^{2-}]$	400%	161.7	0.21	1	0.52	>1000
$[Cl^-],[HCO_3^-],[SO_4^{2-}]$	800%	129.0	0.17	1	0.23	-
$[Cl^-],[HCO_3^-],[SO_4^{2-}]$	800%	147.3	0.19	1	0.53	>1000
$[Cl^-]$	1600%	112.0	0.13	1	0.37	-
$[HCO_3^-],[SO_4^{2-}]$	800%					
$[Cl^-]$	1600%	128.3	0.15	1	0.64	250
$[HCO_3^-],[SO_4^{2-}]$	800%					
$[Cl^-]$	1600%	141.9	0.16	1	0.83	50
$[HCO_3^-],[SO_4^{2-}]$	800%					
$[Cl^-]$	3200%	97.9	0.08	1	0.65	120
$[HCO_3^-],[SO_4^{2-}]$	800%					

Crust composition 1 $Cu_3(OH)_2(CO_3)_2$ azurite

4.4.2 Water *A* at 75°C

Table 4-4 shows an overview of the results for water *A*, with variations, at 75°C. The composition of the crust is the basic carbonate malachite in water *A* without modifications. In a water where the chloride concentration has been decreased to 50%, high concentrations of divalent copper are required to obtain a sufficiently high fraction of the oxidised copper transported as aqueous species. Precipitation of both the basic carbonates occurs in the crust. When the total carbonate concentration in the bulk solution has been decreased to 50%, the basic sulphate, brochantite, forms the crust. In water *A* and in all variations in the composition in table 4-4, cupric oxide reaches saturation, but we have chosen to suppress precipitation of CuO(s).

Table 4-4. Overview of environments for which calculations of the chemistry between the bulk water and the site of metal dissolution have been made. Water *A* with variations of one parameter at the time, 75°C.

Modifications to water *A*		Corrosion potential (mV)	iR drop (mV)	Crust com-position	Transported fraction of the oxidised copper at the site of metal dissolution	Time to grow to a pit depth of 5 mm (years)
none		186.3	0.24	2,3	0.45	>1000
none		188.0	0.25	2,3	0.47	>1000
none		189.6	0.25	2,3	0.48	>1000
none		199.6	0.26	2,3	0.57	>1000
pH decreased	0.3	187.3	0.24	2,3	0.45	>1000
pH decreased	0.3	192.6	0.24	2,3	0.50	>1000
$[Cl^-]$	50%	211.9	0.29	1,2,3	0.43	>1000
$[Cl^-]$	50%	216.7	0.30	1,2,3	0.46	>1000
$[HCO_3^-]$	50%	176.7	0.13	3,4	0.47	>1000
$[HCO_3^-]$	50%	187.8	0.14	3,4	0.58	>1000
$[SO_4^{2-}]$	50%	183.9	0.43	2,3	0.43	>1000
$[SO_4^{2-}]$	50%	193.7	0.45	2,3	0.54	>1000
$[O_2]$	50%	192.5	0.25	2,3	0.51	>1000
$[O_2]$	50%	200.2	0.26	2,3	0.58	>1000

Crust composition	1	$Cu_3(OH)_2(CO_3)_2$	azurite
	2	$Cu_2(OH)_2\,CO_3$	malachite
	3	CuO	tenorite, precipitation suppressed
	4	$Cu_4(OH)_6SO_4$	brochantite

4.4.3 Water *B* at 25°C

Table 4-5 shows an overview of the results for water *B* with variations of one component at the time at 25°C. Results for three levels of decreased chloride concentration, two levels of decreased carbonate concentration, one increased and one decreased level of sulphate concentration and one level of decreased oxygen concentration are shown. The basic carbonate azurite precipitates and forms a crust of corrosion products in all waters in table 4-5. In the water where the total chloride concentration has been decreased to 50%, the basic sulphate also precipitates outside the pit. When the concentration of carbonate is decreased to 50%, the both basic carbonates and the basic sulphate brochantite, precipitate. Cupric oxide also reaches saturation, but we have chosen to suppress precipitation of CuO(s). For three calculated corrosion pits in water *B* with a chloride concentration decreased to 50%, no estimates of the time to grow to 0.5 cm pit depth are given. In these three pits cuprous chloride is precipitated at the site of the metal dissolution. Our method for estimating the maximum growth rate is not adapted to the presence of other solid corrosion products than cuprous oxide inside the plane of the unpitted copper surface and no estimate of the time to grow to 0.5 cm pit depth has been made.

Table 4-5. Overview of environments for which calculations of the chemistry between the bulk water and the site of metal dissolution have been made. Water *B* with variations of one parameter at the time, 25°C.

Modifications to water *B*		Corrosion potential (mV)	iR drop (mV)	Crust com-position	Transported fraction of the oxidised copper at the site of metal dissolution	Time to grow to a pit depth of 5 mm (years)
none		239.3	1.97	1	0.39	-
none		241.6	2.20	1	0.41	>1000
none		244.5	2.50	1	0.43	800
pH decreased	0.3	239.5	1.91	1	0.39	-
pH decreased	0.3	243.3	2.28	1	0.42	>1000
$[Cl^-]$	50%	277.6	12.23	1,4	0.66	12
$[Cl^-]$	50%	278.0	12.37	1,4	0.66	12
$[Cl^-]$	50%	278.4	12.58	1,4	0.66	12
$[Cl^-]$	50%	279.5	13.10	1,4	0.67	11
$[Cl^-]$	50%	286.1	16.45	1,4	0.70	no estimate
$[Cl^-]$	50%	285.5	16.11	1,4	0.70	no estimate
$[Cl^-]$	50%	285.8	16.26	1,4	0.70	no estimate
$[Cl^-]$	71%	225.7	1.30	1	0.28	-
$[Cl^-]$	71%	227.9	1.39	1	0.29	-
$[Cl^-]$	71%	229.8	1.47	1	0.30	-
$[Cl^-]$	71%	230.8	1.52	1	0.31	-
$[Cl^-]$	71%	231.8	1.57	1	0.32	-
$[Cl^-]$	71%	231.8	1.57	1	0.32	-
$[Cl^-]$	71%	231.9	1.57	1	0.32	-

$[Cl^-]$	71%	232.1	1.59	1	0.32	-
$[Cl^-]$	71%	232.1	1.58	1	0.32	-
$[Cl^-]$	71%	267.3	7.81	1	0.59	30
$[Cl^-]$	71%	267.3	7.81	1	0.59	30
$[Cl^-]$	71%	268.0	8.04	1	0.60	28
$[Cl^-]$	84%	242.0	2.29	1	0.40	-
$[Cl^-]$	84%	244.2	2.54	1	0.42	>1000
$[HCO_3^-]$	50%	262.8	5.97	1,2,3,4	0.57	40
$[HCO_3^-]$	50%	263.6	6.21	1,2,3,4	0.58	37
$[HCO_3^-]$	50%	264.5	6.49	1,2,3,4	0.58	35
$[HCO_3^-]$	71%	240.3	1.88	1	0.40	-
$[HCO_3^-]$	71%	241.2	1.96	1	0.41	>1000
$[HCO_3^-]$	200%	240.1	2.64	1	0.40	>1000
$[HCO_3^-]$	200%	242.6	2.88	1	0.42	>1000
$[SO_4^{2-}]$	50%	243.6	3.30	1	0.39	-
$[SO_4^{2-}]$	50%	244.9	3.50	1	0.40	-
$[SO_4^{2-}]$	200%	236.8	1.19	1	0.41	>1000
$[SO_4^{2-}]$	200%	240.2	1.39	1	0.44	700
$[SO_4^{2-}]$	200%	243.4	1.61	1	0.47	350
$[O_2]$	50%	239.5	2.00	1	0.39	-
$[O_2]$	50%	244.0	2.45	1	0.43	>1000
$[Ca^{2+}]$	1200%	239.9	1.96	1	0.39	>1000
$[Ca^{2+}]$	1200%	244.1	2.39	1	0.42	>1000

Crust composition	1	$Cu_3(OH)_2(CO_3)_2$	azurite
	2	$Cu_2(OH)_2CO_3$	malachite
	3	CuO	tenorite, precipitation suppressed
	4	$Cu_4(OH)_6SO_4$	brochantite

4.4.4 Water *B* at 75°C

Table 4-6 shows an overview of the results for water *B* with variations of one component at the time at 75°C. The composition of the crust is the basic carbonate malachite except for one pit for a water where the oxygen concentration has been decreased to 50%. Outside this pit there is no crust at all. Cupric oxide reaches saturation for all calculated pits in table 4-6, but we have chosen to suppress precipitation of CuO(s).

Table 4-6. Overview of environments for which calculations of the chemistry between the bulk water and the site of metal dissolution have been made. Water *B* with variations of one parameter at the time, 75°C.

Modifications to water B		Corrosion potential (mV)	iR drop (mV)	Crust com-position	Transported fraction of the oxidised copper at the site of metal dissolution	Time to grow to a pit depth of 5 mm (years)
none		211.7	0.99	2,3	0.40	>1000
none		213.2	1.00	2,3	0.41	>1000
none		217.7	1.03	2,3	0.43	>1000
none		221.3	1.05	2,3	0.45	>1000
none		236.3	1.23	2,3	0.52	800
pH decreased	0.3	213.1	0.92	2,3	0.40	-
pH decreased	0.3	213.9	0.92	2,3	0.41	-
$[Cl^-]$	50%	241.2	1.45	2,3	0.41	>1000
$[Cl^-]$	50%	243.1	1.50	2,3	0.42	>1000
$[HCO_3^-]$	50%	200.4	0.50	2,3	0.39	-
$[HCO_3^-]$	50%	204.0	0.52	2,3	0.41	>1000
$[SO_4^{2-}]$	50%	210.9	1.51	2,3	0.40	>1000
$[SO_4^{2-}]$	50%	216.0	1.56	2,3	0.43	>1000
$[SO_4^{2-}]$	50%	236.7	1.88	2,3	0.52	800
$[O_2]$	50%	215.4	1.01	3	0.42	>1000
$[O_2]$	50%	217.5	1.02	2,3	0.43	>1000

Crust composition	2	$Cu_2(OH)_2CO_3$	malachite
	3	CuO	tenorite, precipitation suppressed

4.4.5 Water *D* at 25°C

Table 4-7 shows an overview of the results for water *D* at 25°C. The composition of this water is selected to be similar to that of seawater and water *D* has an ionic strength which is higher than the recommended limit for our method of calculating activities from concentrations. Results for water *D* must therefore be considered to have a higher level of inaccuracy than results for the more dilute waters. The basic chloride salt of divalent copper forms a crust outside the pit in water *D*. As the pH of the bulk water is increased one unit from 7.5 to 8.5, both the basic chloride and cupric oxide precipitate. For water *D*, in contrast to the other water considered, we have chosen to precipitate CuO(s) rather than to suppress formation. The role of cupric oxide in the pitting of copper is discussed in section 5-4. As the pH of the bulk water is increased to higher values, the basic chloride no longer reaches saturation and cupric oxide alone constitutes the crust.

Table 4-7. Overview of environments for which calculations of the chemistry between the bulk water and the site of metal dissolution have been made. Water *D* with variations of one parameter at the time, 25°C.

Modifications to water *D*		Corrosion potential (mV)	iR drop (mV)	Crust com-position	Transported fraction of the oxidised copper at the site of metal dissolution	Time to grow to a pit depth of 5 mm (years)
none		69.7	0.00	5	0.94	12
none		75.6	0.00	5	0.95	9
pH increased	1.0	83.7	-0.02	5,6	1.00	6
pH increased	2.0	-24.1	0.00	6	0.88	600
pH increased	3.0	-39.3	0.01	6	0.71	>1000
pH increased	3.0	-27.5	0.01	6	0.85	>1000
pH increased	3.0	-19.4	0.01	6	0.92	>1000
pH increased	3.0	-8.4	0.01	6	0.96	600
$[O_2]$	50%	67.2	0.00	6	0.93	13
$[O_2]$	200%	76.2	0.00	5	0.95	9
$[O_2]$	13%	64.9	0.00	5	0.93	14

Crust composition	5	$Cu_2(OH)_3Cl$	atacamite
	6	CuO	tenorite

4.4.6 Water *D* at 75°C

Table 4-8 shows an overview of the results for water *D* at 75°C. The composition of the crust is cupric oxide in all cases considered in table 4-8. The corrosion pits we have calculated at the lowest pH, pH 7.5, have very high maximum growth rates. At higher pH values we find corrosion pits with more moderate growth rates.

Table 4-8. Overview of environments for which calculations of the chemistry between the bulk water and the site of metal dissolution have been made. Water *D* with variations of one parameter at the time, 75°C.

Modifications to water *D*		Corrosion potential (mV)	iR drop (mV)	Crust com-position	Transported fraction of the oxidised copper at the site of metal dissolution	Time to grow to a pit depth of 5 mm (years)
none		130.5	0.15	6	0.99	0.4
pH increased	1.0	1.3	0.00	6	0.89	25.0
pH increased	1.5	-26.8	0.01	6	0.55	>1000
pH increased	1.5	-18.4	0.01	6	0.68	500.0
pH increased	2.0	-33.2	0.02	6	0.45	>1000
$[O_2]$	10.%	86.4	0.04	6	0.99	1.5

Crust composition 6 CuO tenorite

4.5 Minimum potentials for pitting and maximum stability potentials for Cu_2O(s)

4.5.1 Water *A* at 25°C

Table 4-9 shows the estimated minimum potentials for propagation of a corrosion pit in water *A* with variations in one concentration at the time at 25°C. The minimum potentials were obtained through interpolation or extrapolation of the transported fraction of the oxidised copper at the site of metal dissolution as a function of corrosion potential to the limiting value of 0.4. Table 4-9 also shows that at the pH of the bulk solution, cupric oxide is the most stable solid cupric phase for all compositions of the bulk water. The potential at which cuprous oxide is stable in coexistence with cupric oxide is the same in all waters except where the pH of the bulk water has been decreased from pH 7.5 to pH 7.2. At potentials higher than the coexistence potential for cuprous oxide with the most stable cupric phase, reduction of an oxidising agent on Cu_2O(s) is not a stable situation. We find that if the minimum pitting potential is lower than the maximum potential for stability of Cu_2O(s) propagation of a corrosion pit supported by reduction of an oxidising agent from the bulk solution at Cu_2O(s) is possible. We express this as a negative value of the margin against pitting in the right column in table 4-9. For water *A* at 25°C we find that the difference between the minimum pitting potential and the maximum potential for stability of Cu_2O(s) is

negative for all variations in compositions in table 4-9 except where the chloride concentration has been decreased to 50% of that in water *A*.

Table 4-10 shows the same parameters as table 9 for water *A* with simultaneous increases in the concentrations of the chloride, the sulphate and the carbonate salts of sodium at 25°C. The values of the minimum pitting potentials show a steady decrease with increasing concentrations of the bulk water. Also when only the chloride concentration is changed from eight times that of water *A* to sixteen times that of water *A* the value of the minimum pitting potential decreases. The most stable cupric solid, at the bulk pH, shifts from cupric oxide to a basic carbonate salt as the concentration of carbonate increases. Although the increasing stability of the basic carbonate decreases the value of the coexistence potential with $Cu_2O(s)$, the margin against pitting shows increasingly negative values.

Table 4-9. Minimum potentials for pitting and maximum potentials for stability of cuprous oxide at conditions of the bulk solution. Water *A* with variations of one parameter at the time, 25°C.

Modifications to water *A*		Minimum pitting potential (mV)	Most stable Cu(II)solid at bulk pH	Coexistence potential for $Cu_2O(s)$ with most stable Cu(II)solid (mV)	Margin against pitting (mV)
none		200	CuO	213	-13
pH decreased	0.3	201	CuO	231	-30
$[Cl^-]$	50%	223	CuO	213	10
$[HCO_3^-]$	50%	198	CuO	213	-15
$[SO_4^{2-}]$	50%	202	CuO	213	-10
$[O_2]$	50%	201	CuO	213	-12
$[O_2]$	400%	200	CuO	213	-13

Table 4-10. Minimum potentials for pitting and maximum potentials for stability of cuprous oxide at conditions of the bulk solution. Water *A* with increasing salt concentrations, 25°C.

Modifications to water *A*		Minimum pitting potential (mV)	Most stable Cu(II)solid at bulk pH	Coexistence potential for Cu_2O(s) with most stable Cu(II)solid (mV)	Margin against pitting (mV)
none		200	CuO	213	-13
$[Cl^-]$,$[HCO_3^-]$,$[SO_4^{2-}]$	200%	164	CuO	213	-49
$[Cl^-]$,$[HCO_3^-]$,$[SO_4^{2-}]$	400%	153	$Cu_3(OH)_2(CO_3)_2$	206	-53
$[Cl^-]$,$[HCO_3^-]$,$[SO_4^{2-}]$	800%	139	$Cu_3(OH)_2(CO_3)_2$	194	-55
$[Cl^-]$	1600%	113	$Cu_3(OH)_2(CO_3)_2$	194	-81

4.6 Water *A* at 75°C

Table 4-11 shows the same parameters for water *A* with variations in one parameter at the time for 75°C. The value of the minimum pitting potential is practically unchanged when the pH of the bulk water is decreased from 7.5 to 7.2 but the margin against pitting decreases because of the increasing stability of cuprous oxide relative to cupric oxide. The most stable cupric solid is CuO in all variations of the water composition considered. The stability of the cupric oxide is such that the coexistence potential with cuprous oxide is much lower than the minimum pitting potentials. The values of the margin against pitting show relatively large positive values.

Table 4-11. Minimum potentials for pitting and maximum potentials for stability of cuprous oxide at conditions of the bulk solution. Water *A* with variations of one parameter at the time, 75°C.

Modifications to water *A*		Minimum pitting potential (mV)	Most stable Cu(II)solid at bulk pH	Coexistence potential for Cu_2O(s) with most stable Cu(II)solid (mV)	Margin against pitting (mV)
none		181	CuO	104	77
pH decreased	0.3	182	CuO	124	58
$[Cl^-]$	50%	208	CuO	104	104
$[HCO_3^-]$	50%	170	CuO	104	66
$[SO_4^{2-}]$	50%	181	CuO	104	77
$[O_2]$	50%	179	CuO	104	76

4.6.1 Water *B* at 25°C

Table 4-12 shows the same parameters for water *B* with variations in one parameter at the time for 25°C. The basic carbonate azurite is the most stable cupric solid at the pH of the bulk water in all variations except where the carbonate concentration has been decreased, where the sulphate concentration has been changed or where the calcium concentration has been increased. Several cupric solids have similar stabilities and small changes in the environment may decide which of them is the most stable. The dependence of the minimum pitting potential on a change of one concentration is small and the margin against pitting is relatively close to zero in all water compositions in table 4-12.

Table 4-12. Minimum potentials for pitting and maximum potentials for stability of cuprous oxide at conditions of the bulk solution. Water *B* with variations of one parameter at the time, 25°C.

Modifications to water *B*		Minimum pitting potential (mV)	Most stable Cu(II)solid at bulk pH	Coexistence potential for Cu_2O(s) with most stable Cu(II)solid (mV)	Margin against pitting (mV)
none		240	$Cu_3(OH)_2(CO_3)_2$	242	-2
pH decreased	0.30	240	$Cu_3(OH)_2(CO_3)_2$	251	-11
$[Cl^-]$	50%	233	$Cu_3(OH)_2(CO_3)_2$	242	-9
$[Cl^-]$	71%	242	$Cu_3(OH)_2(CO_3)_2$	242	0
$[Cl^-]$	84%	242	$Cu_3(OH)_2(CO_3)_2$	242	-1
$[HCO_3^-]$	50%	240	CuO	243	-3
$[HCO_3^-]$	71%	240	CuO	243	-2
$[HCO_3^-]$	200%	240	$Cu_3(OH)_2(CO_3)_2$	231	10
$[SO_4^{2-}]$	50%	245	CuO	242	2
$[SO_4^{2-}]$	200%	235	CuO	243	-8
$[O_2]$	50%	240	$Cu_3(OH)_2(CO_3)_2$	242	-2
$[Ca^{2+}]$	1200%	242	CuO	243	-1

4.6.2 Water *B* at 75°C

Table 4-13 shows the same parameters for water *B* with variations in one parameter at the time for 75°C. As in water *A* at the same temperature, the stability of cupric oxide is such that the coexistence potential with cuprous oxide is much lower than the minimum pitting potentials. The margin against pitting shows relatively large positive values for all water compositions in table 4-13.

Table 4-13. Minimum potentials for pitting and maximum potentials for stability of cuprous oxide at conditions of the bulk solution. Water *B* with variations of one parameter at the time, 75°C.

Modifications to water *B*		Minimum pitting potential (mV)	Most stable Cu(II)solid at bulk pH	Coexistence potential for Cu_2O(s) with most stable Cu(II)solid (mV)	Margin against pitting (mV)
none		211	CuO	138	73
pH decreased	0.3	213	CuO	159	54
$[Cl^-]$	50%	239	CuO	138	80
$[HCO_3^-]$	50%	202	CuO	138	83
$[SO_4^{2-}]$	50%	210	CuO	138	75
$[O_2]$	50%	213	CuO	138	76

4.6.3 Water *D* at 25°C

For water *D* at 25°C we have not determined any value of the minimum pitting potential. Table 4-14 shows results for corrosion pits calculated for pH values from 7.5 up to 10.5 in the bulk water. At bulk conditions, cupric oxide is the most stable cupric solid in all cases. The coexistence potential for CuO with Cu_2O is in all cases we have calculated corrosion pits for, higher than the corrosion potentials. The margin against pitting shows large negative values.

Table 4-14. Pitting potentials and maximum potentials for stability of cuprous oxide at conditions of the bulk solution. Water *D* with increasing pH at 25°C.

Modifications to water D		Propagating corrosion pit calculated for potential (mV)	Most stable Cu(II)solid at bulk pH	Coexistence potential for Cu_2O(s) with most stable Cu(II)solid (mV)	Margin against pitting (mV)
none		70	CuO	213	<-100
pH increased	1.0	84	CuO	154	<-100
pH increased	2.0	-24	CuO	95	<-100
pH increased	3.0	-39	CuO	35	~ -100

4.6.4 Water *D* at 75°C

For water *D* at 75°C with increases in the pH up to pH 9.5, as shown in table 4-15, we have also calculated propagating corrosion pits at potentials lower than the potential for coexistence between CuO(s) and Cu_2O(s).

Table 4-15. Pitting potentials and maximum potentials for stability of cuprous oxide at conditions of the bulk solution. Water *D* with increasing pH at 75°C.

Modifications to water *D*		Propagating corrosion pit calculated for potential (mV)	Most stable Cu(II)solid at bulk pH	Coexistence potential for Cu_2O(s) with most stable u(II) solid (mV)	Margin against pitting (mV)
none		131	CuO	104	< 0
pH increased	1.0	1	CuO	35	< 0
pH increased	1.5	-27	CuO	0	< 0
pH increased	2.0	-33	CuO	-35	< 0
$[O_2]$	10%	86	CuO	104	< 0

4.7 The dependence of the minimum pitting potential on the composition of the water

The dependence of the minimum pitting potential on the composition of the water was studied by varying the concentration of the sodium salts of chloride, carbonate and sulphate in the water. The influence of pH and of the oxygen concentration was also investigated. For each of the water compositions we calculated the chemistry in and around a corrosion pit at various corrosion potentials.

Figure 4–52 shows the calculated fractions of the oxidised copper, which is transported, away from the site of the metal oxidation, at the bottom of a corrosion pit, for various corrosion potentials. This is shown for water *A* at 25° with variations in the composition of the bulk water. Each corrosion potential is calculated as the minimum potential at which copper metal can be oxidised to give certain local concentrations of copper ions plus the potential drop in the solution between the site of the metal oxidation and the bulk of the solution outside the corrosion pit. The minimum potential at the site of the metal dissolution is the equilibrium potential between copper metal and dissolved cuprous and cupric ions. The iR-drop is a result of the current associated with the diffusion and migration of the charged species out from the pit.

Figure 4–52 shows that there is an almost linear relation between the fraction of the oxidised copper, which is transported away from the site of the metal oxidation and the corrosion potential. At a value of the transported fraction of 0.4, the volume of the cuprous oxide formed at the site of the metal oxidation is equal to the volume of the corroded copper metal, leaving no aqueous volume for formation and mass transport of aqueous corrosion products. Propagation of the corrosion process is possible only when

the volume of the cuprous oxide formed is smaller than the volume previously occupied by the metallic copper. For a corrosion pit to propagate we find that 40% of the corrosion products must form aqueous species diffusing and migrating away from the site of the metal oxidation. The minimum pitting potential for water *A* is estimated as the interpolated value of the corrosion potential at which the transported fraction is 0.4.

4.7.1 Water *A* at 25°C

Figure 4–52 shows the calculated fractions of the oxidised copper, which is transported, away from the site of the metal oxidation, at the bottom of a corrosion pit, for various corrosion potentials. For water *A* at 25° we find that the minimum pitting potential is insensitive to a decrease in the bulk pH and insensitive also to an increase in the concentration of the dissolved oxygen. However, when the chloride concentration is reduced to 50%, a corrosion potential about 20 mV higher is required to obtain a transported fraction of 0.4.

The effect of a decrease in the sulphate contents is smaller but in the same direction. The effect when the sulphate concentration is reduced to 50% is that the pitting potential is increased by about 2 mV. When the concentration of hydrogen carbonate is reduced to 50%, the effect is small but a slightly lower corrosion potential is sufficient to obtain the pitting limit of a transported fraction of 0.4.

4.7.2 Water *A* at 75°C

Figure 4–53 shows that the pitting potential in water *A* at 75°C is sensitive mostly to changes in the concentrations of chloride, hydrogen carbonate and sulphate. A decrease of the pH of water *A* from 7.5 to 7.2 demands slightly higher corrosion potentials to obtain the same transported fraction. Oxygen shows a negligible influence. A decreased concentration of chloride shifts the minimum pitting potential to higher values whereas decreased concentrations of hydrogen carbonate or sulphate shift the minimum pitting potentials to lower values.

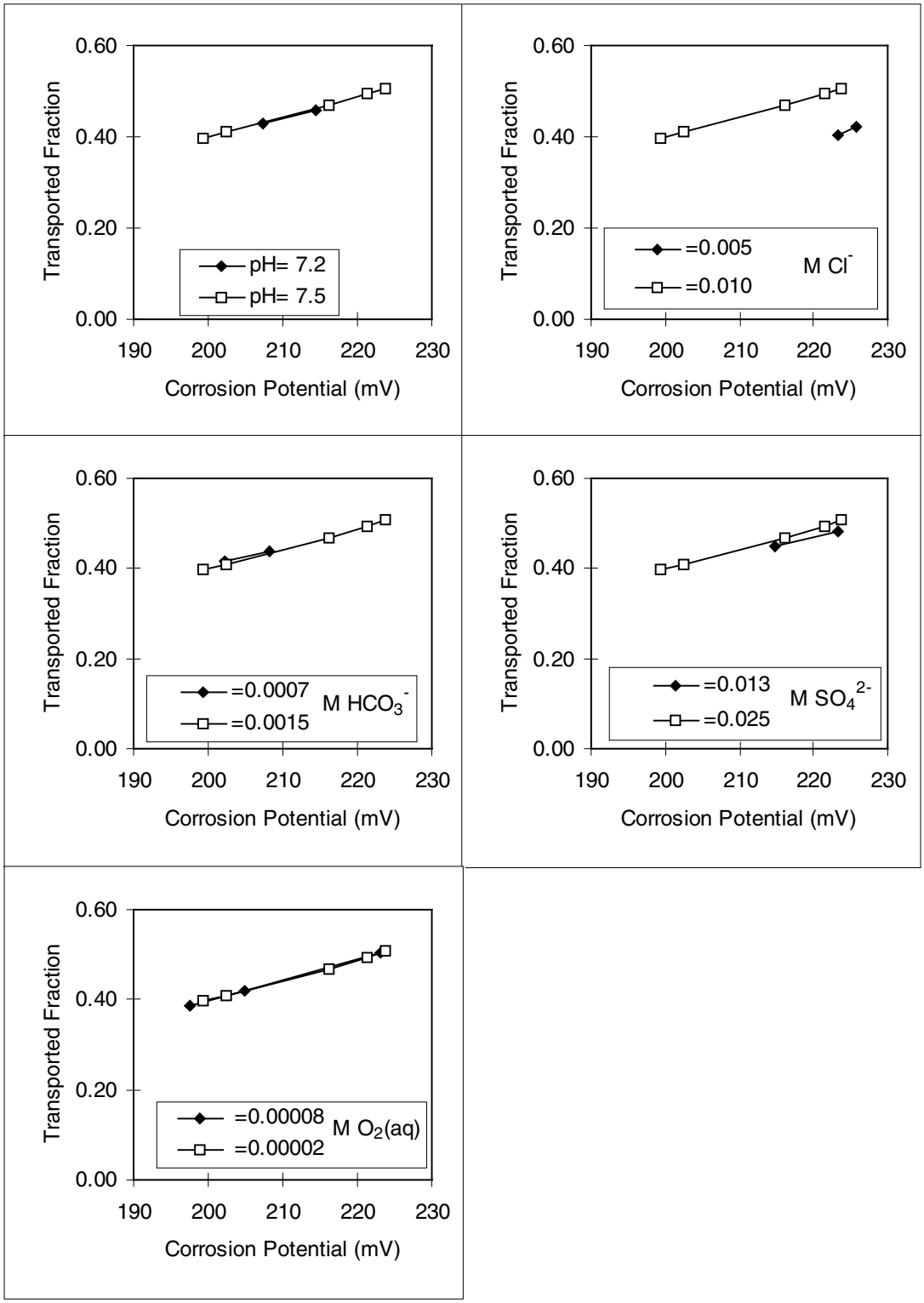

Figure 4-52. Transported fraction of the oxidised copper at the site of the metal dissolution as a function of the corrosion potential. Water A (open symbols) at 25°C with variations in one parameter at the time (filled symbols). Total concentrations in moles/litre.

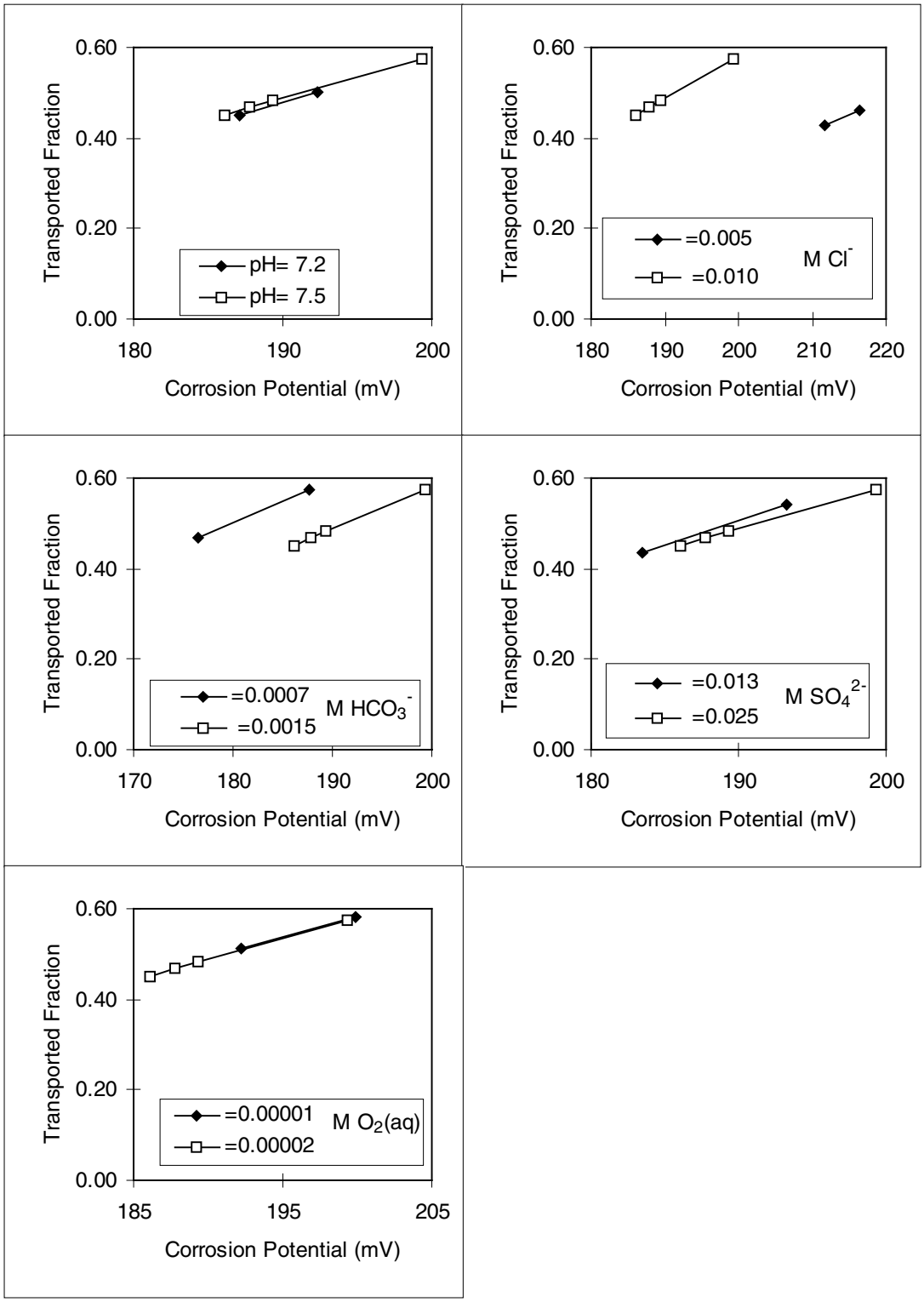

Figure 4-53. Transported fraction of the oxidised copper at the site of the metal dissolution as a function of the corrosion potential. Water A (open symbols) at 75°C with variations in one parameter at the time (filled symbols). Total concentrations in moles/litre

4.7.3 Water *B* at 25°C

Figure 4–54 shows that a decrease of the pH of water *B* from 7.0 to 6.7 has little influence on the distribution between solid and aqueous corrosion products at the site of the metal oxidation. The same corrosion potentials are required to obtain a transported fraction of 0.4. The influence of a decrease in the concentration of dissolved oxygen is also negligible. For the chloride concentrations 2.8 mM and 2.0 mM we have not found solutions to the mass transport and equilibrium problem which are in agreement with the assumptions in the range around the pitting limit. However, the interpolated values for 2.8 mM chloride indicate that slightly higher corrosion potentials are required to obtain a transported fraction higher than 0.4 when the chloride concentration is decreased from 4.0 mM. The effect when the sulphate concentration is decreased to 50% and increased to 200%, respectively, is that the pitting potential decreases with increasing sulphate concentration. There is practically no effect of the carbonate concentration between 0.8 mM and 2.3 mM. As with the low chloride concentration we have not been successful in the modelling of the chemistry and mass transport for a corrosion pit around the pitting limit at low carbonate concentrations (<0.8 mM). When almost all sodium in water *B* has been exchanged for calcium slightly higher corrosion potentials are required to obtain the pitting limit.

4.7.4 Water *B* at 75°C

Figure 4–55 shows that the pitting potential in water *B* at 75°C is sensitive mostly to changes in the concentrations of chloride and hydrogen carbonate. The effect of a decrease in the concentration of sulphate is in the same direction as for water *A* at 75°C but smaller. A decreased pH demands slightly higher corrosion potentials to obtain the pitting limit and a decrease in the concentration of oxygen shows little or no effect.

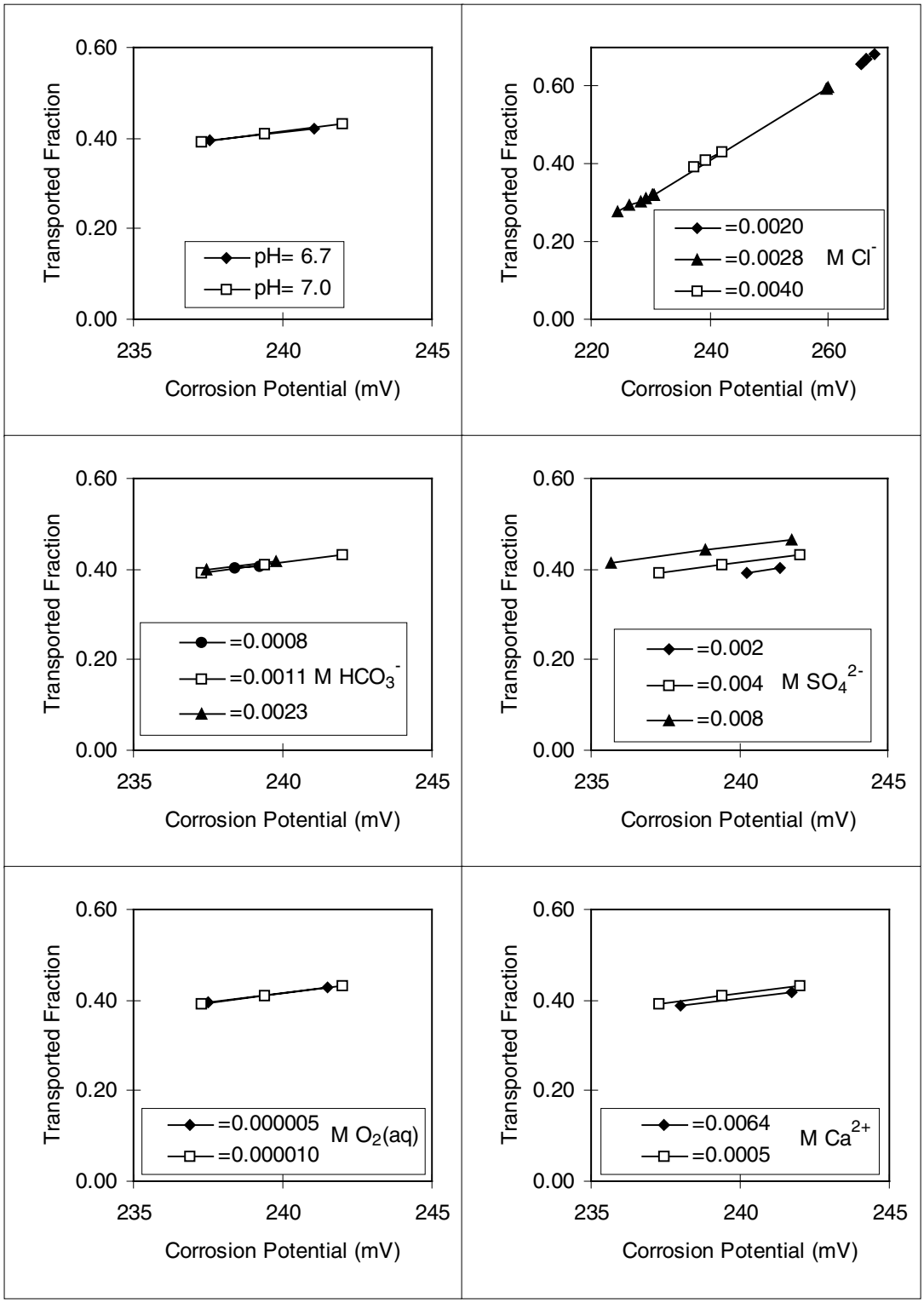

Figure 4-54. Transported fraction of the oxidised copper at the site of the metal dissolution as a function of the corrosion potential. Water B (open symbols) at 25°C with variations in one parameter at the time (filled symbols). Total concentrations in moles/litre

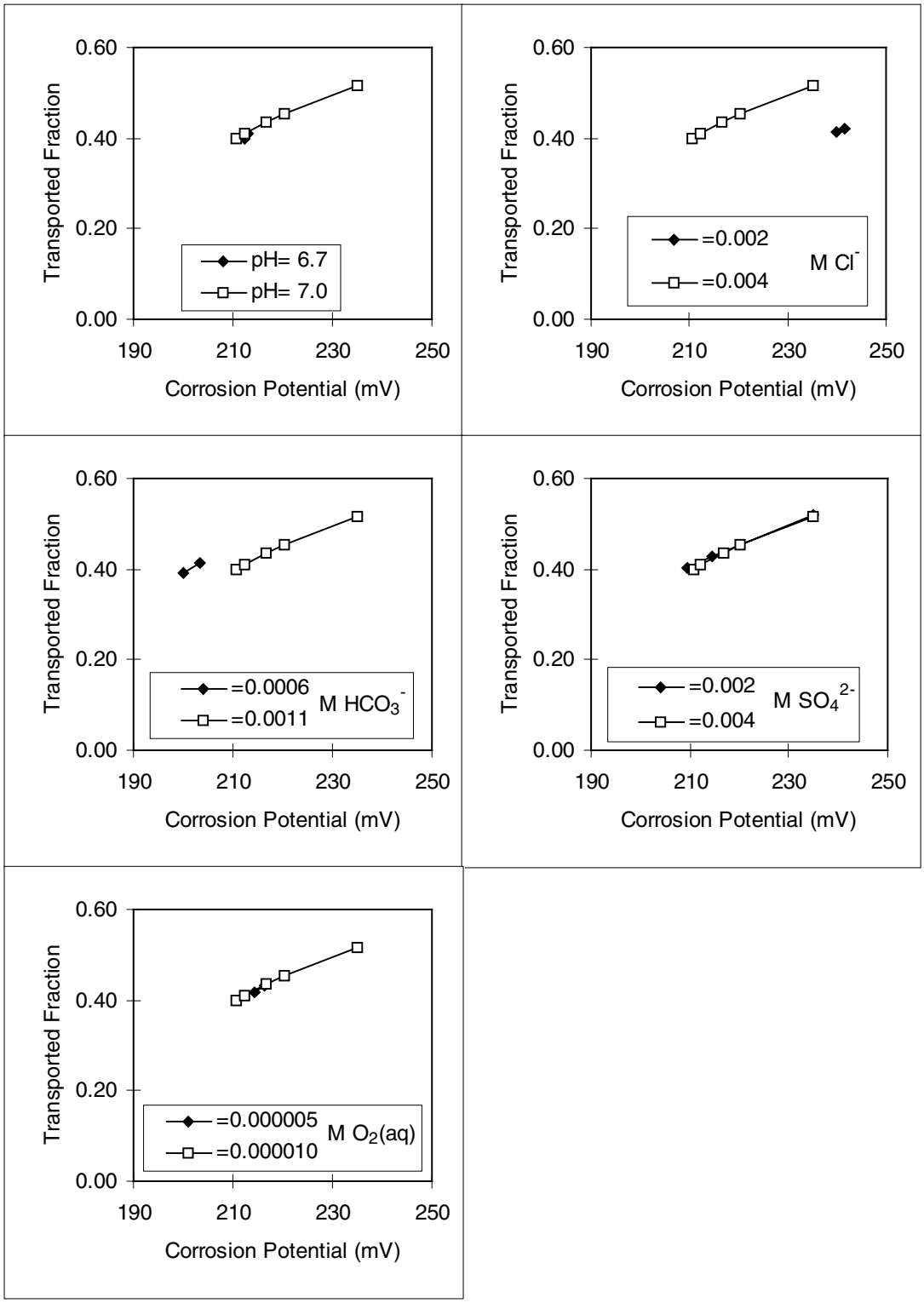

Figure 4-55. Transported fraction of the oxidised copper at the site of the metal dissolution as a function of the corrosion potential. Water B (open symbols) at 75°C with variations in one parameter at the time (filled symbols). Total concentrations in moles/litre

5 About the assumptions

The assumptions used in the calculation of the chemistry and mass transport in and around a corrosion pit are summarised in section 3.4. In this section we discuss the validity and implications of some of the assumptions.

5.1 Modes of transport

Diffusion and migration are the only modes of transport considered. Convective processes are likely to be of importance outside the crust of a corrosion pit in a fluid system. The conditions we simulate agree best with a stagnant solution and not with water streaming in a copper tube. Although the mass transport at a tube wall may be described as diffusion through an effective diffusion layer the rate is not proportional to the diffusion coefficient but to the diffusion coefficient raised to a power less than unity.

Extrusion of corrosion products from the cavity by mechanical forces is not considered. Mechanical forces similar to those, which may be exerted during corrosion of ferrous metals, have to our knowledge, with the possible exception of stress corrosion cracking, never been observed during pitting corrosion of copper. However, cases where an inner layer of corrosion products in a pit seems to have extruded through an outer layer of corrosion products have been reported /5-1/.

5.2 Metallic conductivity of cuprous oxide

5.2.1 Effects of a potential drop in solution on a redox couple

Cuprous oxide is a relatively good electronic conductor and $Cu_2O(s)$ is here treated as a metallic conductor. This metallic conductivity is of importance if, and only if, reductions or oxidations take place at the surface. Under the assumption of a fast reaction kinetics, $Cu_2O(s)$ may in a corrosion pit act as a redox electrode. The potential of this redox electrode may respond to or control equilibria such as:

$$Cu^{2+}(aq) + e^{-}(Cu_2O) <=> Cu^{+}(aq)$$

The potential of a continuous phase of $Cu_2O(s)$ is, due to the high electronic conductivity, the same everywhere in the pit and the same as the underlying copper metal. The potential of the solution in contact with the oxide varies along the pit, due to the transport of anodic current through the solution with limited conductivity.

The molar free energies of the charged species are affected by the potential of the phase in which they are present. The higher potential of the aqueous phase towards the bottom of the pit cause an increase in the electrostatic part of the molar free energy for all positive ions. For divalent ions the effect is twice that of univalent ions. At a constant activity ratio between Cu^{2+} and Cu^{+} , the higher increase in chemical potential of Cu^{2+} relative to Cu^{+} towards the bottom of the pit would impose a higher potential on the copper oxide towards the bottom of the pit than towards the mouth of the pit. However, the potential of a continuous phase of high conductivity is practically the same everywhere in the pit. The effect of a metallic conductor is therefore not to impose a

constant redox potential but to cause the local redox potential to vary according to the local potential of the aqueous phase. As the potential in the solution decreases from the bottom of the pit towards the mouth of the pit, the redox potential increases from the bottom to the mouth of the pit so that a constant electron activity in the metallic Cu_2O phase is maintained.

5.2.2 Non-conductive cuprous oxide

We have made calculations of pitting processes also for the assumption that the cuprous oxide formed in the pit is a poor conductor. We find that there is a driving force for the reduction of divalent copper, formed at the site of the metal dissolution, to monovalent copper in the regions of the pit where cuprous oxide is present. With the assumption of a conducting oxide we allow the divalent copper to be reduced electrochemically on cuprous oxide. A non-conductive cuprous oxide does not allow electrochemical redox reactions to take place at the oxide. Provided that cuprous oxide at external cathodic surfaces is a good electronic conductor, our results would not be drastically changed by the assumption of a non-conducting cuprous oxide in the pit. The transport of divalent copper in relation to corrosion rate illustrated in figures 4-3, 4-20 and 4-37 would be independent of the pH until increased by the chemical oxidation of monovalent copper by oxygen and decreased when precipitation of basic cupric salts takes place. The effect would be that more basic salts are formed and less cuprous oxide but the conditions at the site of the metal dissolution would not change drastically.

5.3 Alternative stability constant for $Cu_2O(s)$

In order to estimate the sensitivity of our results to variations in the stability constants used, calculations were made also for an alternative value of the stability constant for cuprous oxide. The relative stability of this oxide was judged to be the most important for the behaviour of a corrosion pit. Figure 5-1 shows the maximum transported fraction of the oxidised copper as a function of the corrosion potential. A value of the stability constant of 0.8 is used at 25°C. Data for water *A* are compared to results in the same water for pits calculated using a value of 0.5 instead of 0.8. The higher solubility associated with the lower value of the stability constant allows higher fractions of the oxidised copper to be transported away from the site of the metal dissolution, at a given potential. Pitting is possible at lower potentials if the lower value of the stability constant of cuprous oxide is used.

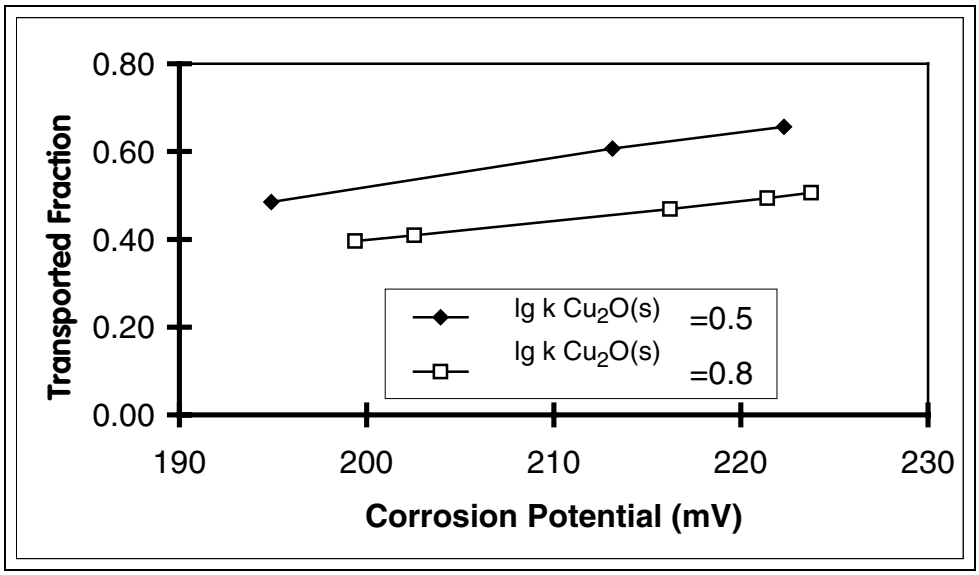

Figure 5-1. Transported fraction of the oxidised copper at the site of the metal dissolution as a function of the corrosion potential. Water A (open symbols) at 25°C with an alternative value for the stability constant of cuprous oxide (filled symbols).

Table 5-1 shows that the decrease in the value of the minimum pitting potential is about 19 mV for a decrease in the stability constant of 0.3. The decreased stability of the monovalent oxide relative to the divalent oxide results in a shift also for the coexistence potential of the oxides. The margin against pitting is almost independent of small variations in the stability constant of cuprous oxide.

Table 5-1. minimum potentials for pitting and maximum potentials for stability of cuprous oxide at conditions of the bulk solution. Results for two alternative values of the stability constant for $Cu_2O(s)$. Water *A*, 25°C.

lg k $Cu_2O(s)$	Minimum pitting potential (mV)	Most stable Cu(II)solid at bulk pH	Coexistence potential for $Cu_2O(s)$ with most stable Cu(II)solid (mV)	Margin against pitting (mV)
0.80	200	CuO	213	-13
0.50	181	CuO	195	-14

5.4 Precipitation of CuO(s)

Divalent copper can precipitate as cupric oxide and as cupric hydroxide. These phases are stoichiometrically equivalent in table 3-1. CuO(s) is according to the equilibrium constants the most stable at both temperatures considered and $Cu(OH)_2$(s) is not stable under any conditions.

It has however been found that $Cu(OH)_2$(s) has a lower surface energy than CuO(s) /5-2/. This implies that small particles of $Cu(OH)_2$(s) can be more stable than small particles of CuO(s) and that precipitation does not initiate until saturation with respect to the hydroxide occurs. Once formed, the small particles of $Cu(OH)_2$(s) may grow and the effect of the lower molar free energy of the phase CuO(s) is, at some particle size, likely to dominate so that a phase transition occurs. On the basis of the lower surface energy of the dihydroxide we have chosen to suppress the precipitation of cupric oxide outside corrosion pits at moderate levels of supersaturation. We have, however, not been consistent but consider precipitation of CuO(s) in the crust as a possible reaction for water *D*.

At a surface of a solid such as cuprous oxide, the influence of the lower surface energy of $Cu(OH)_2$(s) compared with CuO(s) is likely to be smaller and the upper stability region of Cu_2O(s) is determined as the coexistence potential for the cuprous oxide with CuO(s).

5.5 Reversible behaviour during copper dissolution

Relatively high concentrations of aqueous copper species arise at the bottom of a corrosion pit. During propagation of a pit, cuprous and cupric species are produced through electrochemical oxidation of copper metal with a net rate balanced by the rate of precipitation and the rate of transport out of the pit. The higher molar volume for copper in corrosion products than in copper metal imply that a large fraction of the oxidised copper must diffuse and migrate out from the restricted volume of a concave corrosion pit. The transport of the aqueous copper species out of the pit through diffusion and migration requires high concentrations at the bottom of the pit and concentration gradients away from the site of oxidation and out from the pit. A high local concentration of positive ions favours rapid migration. High concentrations of aqueous copper species at the bottom of the pit are a consequence of the high concentration gradients required for rapid diffusion. The higher the concentrations and the concentration gradients, the higher the transport rate. High concentrations of aqueous copper species at the bottom of the pit are therefore a necessary condition for a high propagation rate.

5.5.1 The exchange current density

In an equilibrium system, where a metal is in equilibrium with ions of the same metal, there is no net reaction. Oxidative dissolution of the metal occurs but is balanced by the reductive deposition of aqueous metal species. The rate of this exchange is often expressed in terms of an exchange current density. In an open system, as in a corrosion pit, there is a net dissolution of the metal but reductive precipitation of aqueous metal species is still possible. If the net rate is low compared with the exchange rate the system may still behave reversibly. Exchange current densities for redox reactions between a metal and its ions are in general much higher at low pH, presumably because of the inhibiting and blocking effect of surface oxides in alkaline or neutral solutions. At the bottom of a corrosion pit in copper the metal surface may be partly covered by

oxide. The sites, which are covered by oxide, are probably not the same at all times but oxide at one site may dissolve while oxide may form at another previously bare metal site. If we want to estimate the exchange current density at the bare metal sites from literature data we should use a determination made at a lower pH rather than a determination made in neutral solution.

5.5.2 Literature data

Kinetic data for heterogeneous redox reactions at solid electrodes is often connected with a high degree of uncertainty and depend very much on the experimental procedure used. Kinetic literature data is therefore here used only to show that observed rates of the oxidative dissolution of copper are very high compared with the net rates during pit propagation.

Figure 5-2 shows a Tafel diagram constructed for anodic dissolution of copper metal and cathodic reduction of 1 mM Cu^{2+} at copper metal in 0.1 N H_2SO_4 using literature data. The Tafel diagram is drawn for a standard exchange current density of $80 \cdot 10^{-3}$ A/cm^2 and a transfer coefficient a= 0.5 /5-3/, giving an exchange current density of about 2.6 mA/cm^2 at a copper ion concentration of 1 mM. At negative potentials, relative to the equilibrium potential, copper ions are reduced to copper metal on copper metal and at positive potentials copper metal is oxidized to copper ions. The current densities for these individual processes follow the straight lines with a slope of about -60 mV and +60 mV, respectively, per logarithmic unit of current density. The 60 mV slopes here are a result of the symmetric two electron transfer with a=0.5 at 25°C. The two straight lines cross at the exchange current density at the equilibrium potential. The net current density is the difference between the anodic and the cathodic current density and follows the curved lines with asymptotic approaches to the straight lines at high and low potential, respectively. A pitting rate of 1 mm per year corresponds to a net current density in the pit of about 10^{-4} A/cm^2. The intersection between the line for this current density and the curve for the net anodic current density, as a function of the potential, in figure 5-2 shows that the departure from the equilibrium potential is less than one millivolt. This very simplified treatment shows that relatively large anodic currents can be drawn from a bare copper metal surface without significantly disturbing the local electrochemical equilibrium at the surface.

In a corrosion pit, only a fraction of the copper metal may be free from oxide and the local current densities at the active free sites on the metal may be much higher than the average current density calculated from a pitting rate. If 90% of the copper surface at the bottom of a pit is covered by oxide, the local anodic current density is ten times higher than the average. As can be seen from figure 5-2, an increase in the current density from the line corresponding to a pitting rate of one millimetre per year by one logarithmic unit would still give a polarisation in the order of one millivolt. In this simplified treatment we have so far neglected the influence of univalent copper ions. The equilibrium potential for copper in 1 mM Cu^{2+} is about +250 mV on the hydrogen scale which gives a concentration of Cu^+ of about 30 mM. The influence of these cuprous ions, which in chloride containing pit solutions may attain concentrations of the same magnitude as the cupric ions, is likely to increase the exchange current density to higher values than observed in the study cited above where the concentration of Cu^+ was very low. The approximation of the corrosion potential of copper during pitting as a local equilibrium potential in a corrosion pit is thus a very good one. Although the relation between cause and effect may be the reversed, copper metal can be said to behave as a redox sensor for the solution in immediate contact with the bare metal at the

bottom of a corrosion pit. This discussion indicates that mass transport of copper away from the site of the oxidation and out of the pit is the major rate-limiting step also for rapidly growing corrosion pits. The copper electrode, that the bare metal at the bottom of a corrosion pit constitutes, is under almost total concentration polarisation with respect to the bulk of the solution outside the pit.

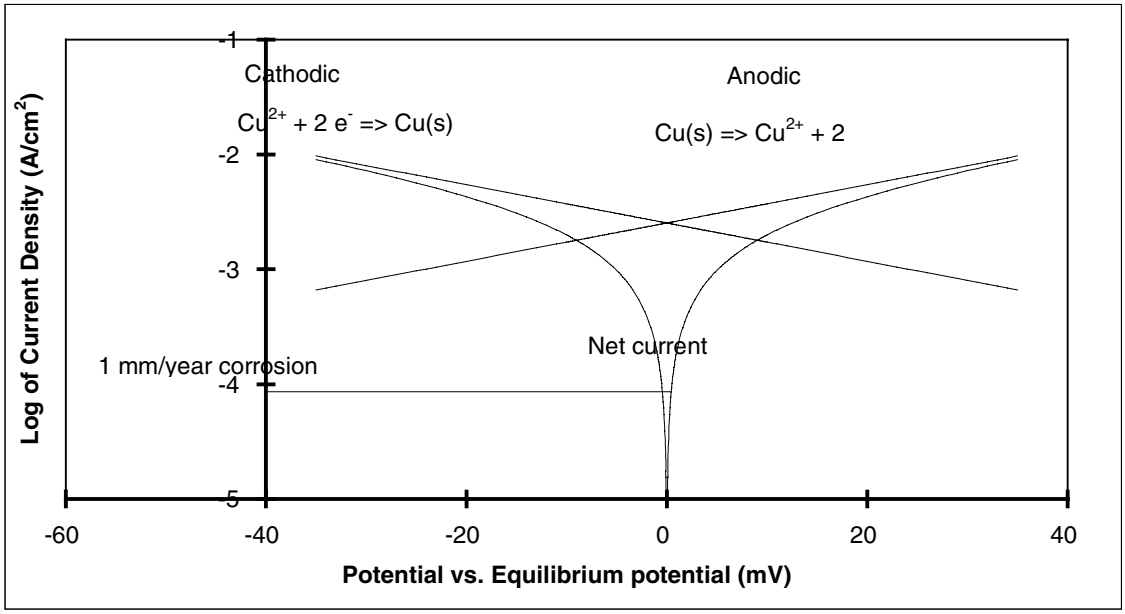

Figure 5-2. Tafel diagram showing the anodic and cathodic Tafel lines constructed from literature data for the dissolution-deposition reaction between copper metal and cupric ions in solution. The net, observable current density and the current density corresponding to a corrosion rate of 1.0 mm/year are shown

5.6 Oxidation of aqueous monovalent copper by oxygen

Monovalent copper is produced at the site of the metal oxidation at the bottom of a corrosion pit. In the bulk of the solution outside the pit the concentration of monovalent copper is zero, so there is a transport out towards the bulk solution where dissolved oxygen is present. Monovalent copper and molecular oxygen are not compatible. At equilibrium, any finite concentration of monovalent copper gives a negligible concentration of molecular oxygen and vice versa.

In our model for the chemistry in and around a corrosion pit in copper, we assumed that the reaction rate between aqueous monovalent copper and dissolved oxygen is very high so that there is practically no overlap between the concentration profiles. Monovalent copper from the bottom of the pit and dissolved oxygen from the bulk meet at one point where all monovalent copper is oxidised to divalent and all oxygen is reduced to water or to hydroxide.

In reality, the reaction rates are not infinite and an overlap between the concentration profiles must be expected so that there is a range where dissolved oxygen and monovalent copper are both present at significant concentrations.

5.6.1 Literature data

Sharma and Millero /5-4/ studied the oxidation of monovalent copper by molecular oxygen in seawater. They found that the rate can be described by an expression where the rate is proportional to the concentration of oxygen and to the concentration of the free cuprous ion. Complexation of the free cuprous ion by chloride decreased the rate so that the rate constant for the monochloride complex is lower than for the free cuprous ion and the di- and tri-chlorocomplexes do not significantly contribute to the rate. Values for the second order rate constants are $2.1 \cdot 10^4$ and $8.7 \cdot 10^2$ M^{-1} s^{-1} for Cu^+ and for CuCl, respectively.

5.6.2 Effects of the limited reaction rate on the pitting model.

The rate equations can not be incorporated directly into the model for the chemistry in a corrosion pit. A comparison between the rates of diffusion and the rates of reaction can be made only when the physical dimensions of the system are known. By assuming a diffusion limited rate for the reaction we find the site of the reaction in the crust of corrosion products formed by divalent copper outside the pit or in the solution between the crust and an underlying cuprous oxide.

Estimates of the rate of the reaction based on the experimentally determined rate constants, indicate that the kinetic limitation of the rate of oxidation of monovalent copper by dissolved oxygen in homogenous solution may be of importance. Diffusion of the reactants is not necessarily the slow step in the process. However, in many of the modelled corrosion pits, we find the site of reaction in the porous basic salt phase in the crust outside the pit. Parallel to the homogenous reaction path we then expect a heterogeneous catalysis reaction. The presence of a solid phase, particularly a porous solid with a large surface area, is likely to increase the rate of the redox reaction between oxygen and monovalent copper. It is frequently found that adsorption on, or interaction with, a solid catalyses reactions by lowering the activation energy.

While the rate of the homogenous reaction is not infinite, it is also not negligible. The kinetic limitation of the rate causes the concentration profiles to overlap. Depending on the particular pit considered, a concentration of the reaction either to the porous crust of basic cupric salts or to the underlying cuprous oxide may be expected.

If the flux of monovalent copper to the crust is not high enough to consume the flux of oxygen from the bulk, the remaining part of the oxygen flux will be reduced by the reaction with monovalent copper in the solution or at the cuprous oxide surface or undergo electrochemical reduction on cuprous oxide. A concentration of the reaction to the crust outside the pit would give an increased consumption of oxygen since the diffusion path is shorter. This behaviour would be in agreement the mechanism suggested by Lucey/5-5/.

5.7 Cathode at the site of the pit

In all our calculated corrosion pits we find that current for the anodic processes in the pit must be supplied from external cathodic areas. Cuprous oxide as a cathode material has a decreasing stability at higher pH values. The effect of the electrochemical reduction of oxygen is to increase the pH locally. The pH at the site of the cathode is likely to be higher than the pH of the bulk or in any case not lower. If the site of the oxygen reduction is at the site of the pit, at the outer parts of the crust as Lucey /5-5/ suggests or at a cuprous oxide covering the cavity, the pH might by influenced by the

acidifying reactions in the pit. The net corrosion process is however slightly alkalising and it seems improbable that the site of the cathode should be more influenced by the acidifying processes than by the alkalising processes associated the cathodic reduction. Also for cases where the cathodic reactions take place at the sit of the pit we find that the stability of the cuprous oxide at the pH of the bulk is relevant as a cathodic condition for propagation of corrosion pits.

6 Discussion

In this section we discuss the influence of various environmental factors on a pitting process on copper. Conditions, which in practice have lead to pitting, are results of a number of factors of which we have considered only a few. We have made a detailed model of the anodic processes in a corrosion pit. The cathodic processes required to drive the processes in the pit have been included only to the extent that we have considered the stability of cuprous oxide at external areas as a cathode material. These cathodic processes must be able to deliver current for the anodic processes at a potential higher than the minimum pitting potential. The anodic dissolution of copper in a corrosion pit consumes a part of the current delivered from the cathodic reactions. General corrosion of the cuprous oxide and renewal of the cuprous oxide layer on copper are processes likely to consume the rest of the cathodic current. The general corrosion of cuprous oxide involve the oxidation to aqueous divalent copper species, under some conditions also to solid cupric phases but also the chemical dissolution of the oxide to monovalent copper. At stationary conditions, the thickness of the cuprous oxide layer may be kept constant by corrosion of the underlying copper metal.

For a freely corroding copper specimen the corrosion potential is controlled by the relative rates of the electrochemical processes. A facile kinetics for the reduction of an oxidising agent tends to give high values of the corrosion potential. Rapid dissolution or oxidation of cuprous oxide, with the associated renewal through oxidation of the underlying copper metal, tends to give low values of the corrosion potential. Pitting corrosion, if the corrosion potential is high enough to support pitting, also tends to decrease the value of the corrosion potential. In this section we discuss the influence of various parameters on the pitting process including the influence on the conditions at cathodic sites and on the competing general corrosion.

6.1 The influence of temperature

The difference in chemistry and mass transport in and around a corrosion pit in copper we find when the temperature is increased from 25°C to 75°C is mainly a result of changes in the equilibrium constants. Other factors influenced by an increased temperature are, the activity coefficients, the diffusion coefficients and the influence of migration relative to the diffusion.

Table 3-1 shows the equilibrium constants used for 25°C and for 75°C, respectively. Among the changes are increased self-ionisation of water, a shift in the stability region of hydrogen carbonate to lower pH values, an increased strength of cupric complexes with hydroxide, with chloride and with carbonate. The sulphate complex with divalent copper shows a decrease in the stability as the temperature is increased. For the solid oxides the main changes are an increased solubility of $Cu_2O(s)$ and an increased stability of CuO(s).

The effects of the increase in the solubility of cuprous oxide on corrosion pits in water *B* is shown in figure 4.21 for 25°C and 4-38 for 75°C. The same total concentration of monovalent copper is found at a higher pH for 75°C than for 25°C. Figure 4.21 and 4-38 show also the shift from a cupric dominated aqueous chemistry at 25°C to the cuprous domination found at low pH values for 75°C. We find that the anodic pitting

behaviour of water *B* at 75°C is similar to that of water *A* at 25°C. For water *A* at 75°C the copper transport is totally dominated by monovalent copper at the site of metal dissolution.

The increase in the stability of CuO(s) and the decrease in the stability of Cu_2O(s) is illustrated as a smaller stability region for Cu_2O(s) in the potential- pH diagram for 75°C in figure 4-36 than for 25°C in figure 4-19. For all calculated corrosion pits in water *A* and water *B* at 75°C , the solution is super-saturated with respect to CuO(s) at some location. We have chosen to suppress precipitation of that oxide as a crust outside a corrosion pit for these waters. However, on top of cuprous oxide at an oxidised copper surface some distance away from a corrosion pit, the formation of CuO(s) is considered. Figure 4-51 illustrates that at conditions where a corrosion pit at 75°C can barely propagate, the corrosion potential is in a region where CuO(s) is the most stable copper solid at the pH of the bulk.

6.2 The influence of the water composition

The study of the aqueous chemistry and mass transport in and around a propagating corrosion pit allows an examination of the role of a specific water component in the pitting of copper. The influence of a component in the water on the pitting process is separated into the effects on the anodic dissolution of copper in the pit and the effects on the stability of cuprous oxide as a cathode material at pitting potentials.

6.2.1 pH

The influence of the pH of the bulk water on the minimum pitting potential is relatively small in the cases we have studied. The pH at the site of metal oxidation, necessary for propagation of a corrosion pit, is almost independent of the pH of the bulk outside the pit.

A high pH value of the bulk water favours precipitation of cupric oxide rather than the basic salts in a crust outside the cavity. All basic salts of divalent copper have decreasing solubilities with increasing pH and the fraction of the oxidised copper, which is transported out into the bulk water, is lower at higher pH values. Larger crust of corrosion products are therefore predicted at higher pH values of the bulk water. The relative stability of the basic salts is, at higher pH values, favoured according to increasing hydroxide character and decreasing salt contents.

Outside the pit and some distance away at an oxidised copper surface the pH is approximately the same as in the bulk water. The pH at the oxidised surface has a big influence on the stability of cuprous oxide at a given potential. The coexistence potential for Cu_2O(s) with CuO(s) shifts to about 60 mV higher values for a decrease of the pH by one unit at 25°C and to about 70 mV higher at 75°C. Lower values of the margin against pitting is therefore found in all cases where the pH has been decreased in tables 4-8 and 4-10 to 4-12.

6.2.2 Chloride

The main influence of chloride on the anodic dissolution of copper in a corrosion pit is that it forms strong complexes with monovalent copper. As shown in figures 4.8, 4.25 and 4.42 monovalent copper in solution in the corrosion pits considered is predominantly present as chloride complexes. The dominating species is the dichloride complex, which has a stability proportional to the square of the chloride concentration. Cuprous complexes, however, constitute only a small fraction of the total chloride

concentration. Unless oxidised by dissolved oxygen the monovalent copper precipitates as cuprous -oxide as the alkaline gradient from the bulk is encountered. This precipitation occurs in the pit but may also extent outside the plane of the unpitted copper surface. In a corrosion pit where the transport of copper is dominated by monovalent copper the pitting process may be described as a dissolution of copper through a porous cuprous oxide.

For water *A* at 25°C, figure 4-3 shows that the aqueous transport of copper away from the site of metal dissolution is equally divided between monovalent and divalent copper. Since the monovalent copper is present mostly as chloride complexes, a strong sensitivity of the minimum pitting potential on the chloride concentration of the bulk water would be expected. Figure 4-52 confirms that when the chloride concentration of the bulk is decreased to 50%, we find a value of the minimum pitting potential about 20 millivolts higher.

For water *B*, which has a lower chloride concentration than water *A*, figure 4-20 shows that the aqueous transport of copper away from the site of metal dissolution is dominated by divalent copper. Figure 4-53 confirms that the minimum pitting potential, is less sensitive to a decrease in the chloride content of the bulk water in water *B* than in water *A* at the same temperature.

However, for 75°C figure 4-37 shows that the aqueous transport of copper away from the site of metal dissolution is dominated by monovalent copper also for water *B*. Monovalent copper in aqueous solution is present predominantly as chloride complexes also at this temperature. The dependence of the minimum pitting potential on the chloride concentration in figure 4-55 is accordingly stronger than for the same water at 25°C and stronger also than for water *A* at 25°C. An increase in temperature from 25°C to 75°C shifts the behaviour of the corrosion pit from the cupric dominated copper transport in water *B* at 25°C to the cuprous dominated copper transport found at 75°C and found also for the more chloride rich water *A* at 25°C.

Solid cuprous chloride is frequently found in real corrosion pits of types I and III. For the water compositions we have considered there is a wide gap between the minimum pitting potential and the potential where solid cuprous chloride is formed. Figure 4-5 for water *A* at 25°C and figure 4-22 for water *B* at the same temperature show the calculated activities for the solids considered. The potential is in both cases only slightly higher than the minimum pitting potential for that water composition. Although water *A* has a higher chloride content than water *B*, the maximum activity for CuCl(s) is higher for water *B* than for water *A* under comparable conditions. An explanation for this is that the minimum pitting potential is greatly influenced by the solubility of monovalent copper, which is dominated by the dichloride complex. The dependence of the stability of the dichloride complex on the chloride concentration is stronger than the dependence of the stability of the solid cuprous chloride. A comparison at conditions of similar pitting severity may therefore show that solid cuprous chloride is more likely to be observed in the water with the lower chloride concentration than in the water with the higher.

We have calculated corrosion pits where solid cuprous chloride is formed for water *B* at 25°C with a chloride concentration decreased to 50%. Where CuCl(s) is formed, we find that its stability is confined to a region close to the site of metal dissolution and that cuprous oxide is formed simultaneously.

A basic chloride salt of divalent copper is formed in water *D* at 25°C. At a pH slightly more acidic than the pH 7.5 of the bulk, the basic chloride is the most stable cupric solid in a water with this very high chloride concentration. At higher pH values or at higher temperature cupric oxide is more stable.

At an oxidised copper surface without corrosion pits, a high concentration of chloride in the bulk water may increase the rate of dissolution of cuprous oxide. At uniform corrosion where the anodic and the cathodic processes take place at approximately the same sites, only small changes in the pH at the oxidised surface from the pH of the bulk water, is expected. For bulk waters with near neutral pH, the cuprous ion has a very low maximum concentration. A high chloride concentration in the water increases the maximum concentration of monovalent copper sharply above about 1.0 mM chloride. Bare copper metal is seldom observed in contact with oxygenated waters. A high rate of dissolution of cuprous oxide therefore implies a high corrosion rate such that the layer of cuprous oxide is renewed continuously. Waters with high chloride concentrations are likely to give high rates of the uniform corrosion. This uniform corrosion consumes oxidising power from the oxidising agent and polarises the corrosion potential of a specimen in the negative direction. Chloride may play the same role at a cuprous oxide surface outside the pit as in a corrosion pit. A high concentration of chloride in the bulk water lowers the minimum pitting potential while the corrosion potential of a specimen or a construction decreases simultaneously. Thus, chloride is aggressive towards copper at the lower pH values in a corrosion pit as well as at the higher pH of the bulk of a natural water.

6.2.3 Carbonate

The role of carbonate in the pitting of copper is complex. Carbonate forms relatively strong aqueous complexes with divalent copper. Basic carbonate salts of divalent copper are formed at most of our calculated corrosion pits. A large part of the acidity produced in the corrosion by the formation of cuprous oxide is transported out from the pit by carbonate species.

Waters *A* and *B* have similar carbonate contents and figures 4-9 and 4-26 show that at 25°C at pH values above pH 7.0 a carbonate complex is the most stable aqueous form of divalent copper. At 75°C in water *B*, the cupric carbonate is the most stable aqueous cupric species down to pH 5.5. While precipitation of the basic carbonate salts may limit the aqueous concentration of divalent copper, carbonate may also increase the total concentration of divalent copper in regions where the concentration is limited by precipitation of a cupric phase not containing carbonate.

The dominating carbonate species are the hydrogen carbonate and the carbonic acid or dissolved carbon dioxide, which we have regarded as equivalent. The complexes formed with divalent copper and with calcium do not significantly decrease the free carbonate concentration. Figure 4-15 for water *A* at 25°C and figure 4-32 for water *B* at the same temperature, show that hydrogen carbonate is the dominating current transporting species at pH values above 5.5. Inside the crust of basic carbonate salts there is no net transport of carbonate but the transport of hydrogen carbonate inwards is balanced by a transport of carbonic acid, with a small contribution of copper carbonate, outwards. The result being that acidity and charge is transported outwards. For 75°C in water *B*, figure 4-49 shows that the hydrogen carbonate is a significant charge transporting species also at the low pH at the site of the metal dissolution. While this

transporting capacity of carbonate may facilitate the corrosion processes in the pit, the transport of acidity out from the pit facilitates the formation of cuprous oxide most.

The effect of a change in the carbonate concentration of the bulk water on the minimum pitting potential is small in waters *A* and *B* at 25°C. For 75°C figures 4-54 and 4-55 show that a decrease of the carbonate concentration to 50% in waters *A* and *B*, respectively, shifts the minimum pitting potentials to lower values. The small effects observed at 25°C probably underestimates the beneficial influence of carbonate in these waters. The concentration of carbonate may have a small influence on the pH, which must be attained at the site of metal dissolution for propagation to be possible, and thereby on the minimum pitting potential. The pH at the site of the metal dissolution is too low for the hydrogen carbonate - carbonic acid couple to behave as efficient carriers of acidity. For the initiation process before the low pH-values have been established, a high carbonate concentration is likely to counteract the acidification so that the low pH required for propagation does not establish and pitting may not initiate.

Outside the pit, formation of basic carbonate salts may limit the stability of cuprous oxide as a cathode material. Table 4-10 shows that as the salt contents of water *A* increases to a level where a basic carbonate salt is more stable than cupric oxide at the pH of the bulk solution, the maximum potential for stability of the cuprous oxide decreases. Although the effect in this case can not compensate for the decrease in the minimum pitting potential caused by the simultaneous increase in the chloride contents, the influence of the decrease in the maximum potential of stability for cuprous oxide is to increase the value of the margin against pitting.

Carbonate is not aggressive against copper at the low pH values where the metal dissolution occurs in a corrosion pit. Particularly at the lower temperature complex formation with copper is negligible at a pitting pH. At higher pH values such as the pH of the bulk for a natural water, complex formation is strong and oxidative dissolution of cuprous oxide may well be increased by high carbonate concentrations.

6.2.4 Sulphate

Similar to carbonate, sulphate forms a neutral aqueous complex with divalent copper. Although a comparison at the same concentrations of sulphate ion and carbonate ion shows that the sulphate complex is much weaker, the stronger protolysis of hydrogen sulphate relative to hydrogen carbonate results in that the sulphate complex is stronger at low pH values.

Divalent copper, in contrast to monovalent copper, stays in solution until relatively high pH values are encountered. The speciation changes from the free cupric ion and the sulphate complex to hydroxide complexes and carbonate complexes but precipitation does not take place until saturation with respect to the least soluble basic salt occurs. Because of the strong hydroxide and carbonate complexes, divalent copper can remain in solution until a pH much higher than the pH at the site of the metal dissolution. Precipitation of divalent copper therefore occurs outside the plane of the unpitted copper surface where the solid corrosion products does not impede the mass transport between the bulk water and the solution at the site of metal dissolution to the same extent as precipitation of monovalent copper inside the pit does.

Figures 4-9 and 4-26 illustrate the increasing relative stability of the sulphate complex at low pH values for water *A*, and water *B*, respectively, at 25°C. One effect of a high sulphate concentration is that higher total concentrations of divalent copper can form at

a given corrosion potential. The higher concentration of divalent copper enables a faster transport away from the site of the metal oxidation and a decrease in the value of the minimum pitting potential. This effect is shown for water *A* at 25°C in figure 4-52 and for water *B* at the same temperature in figure 4-53.

However, at 75°C we do not see an increase of the minimum pitting potential when the sulphate concentration is decreased to 50%. On the contrary, Figures 4-54 and 4-55 show slight decreases in the potentials required to obtain a transported fraction around the pitting limit, for water *A* and water *B*, respectively. An explanation to the apparent absence of the detrimental influence of sulphate at the higher temperature is given by figure 4-49 which shows that the fraction of the current which is transported by sulphate is negligible in water *B* at 75°C. A decrease in the sulphate concentration causes a decrease in a factor which is already negligible. An explanation to the apparent beneficial influence of sulphate lies in the influence of sulphate on the iR-drop in the solution between the bulk of the water and the solution at the site of metal dissolution. Tables 4-3 and 4-5 show that the iR-drops are higher at the lower sulphate concentrations. One effect of the iR-drop is to increase the concentration of the negatively charged species. The higher the value of the iR-drop, the higher the value of the concentration ratio between the site of metal dissolution and the bulk. Although this effect in the case of chloride is complicated by complex formation with monovalent copper, it is clear that the higher iR-drop results in a higher value of the concentration ratio between the site of the metal dissolution and the bulk water. The solubility of the cuprous oxide increases strongly with an increase in the local chloride concentration. The influence of the increases in the concentration of free chloride at the site of metal dissolution on the pitting potential is stronger than the contribution of the iR-drop to the corrosion potential so that pitting conditions may be established at a lower corrosion potential. Decreases in the concentration of sulphate for waters *A* and *B* at 75°C cause negligible changes in the speciation and transport of divalent copper. The decreased concentrations result in higher values of the iR-drop and cause stronger tendencies for accumulation of chloride at the site of metal dissolution. These higher concentrations of free chloride decrease the value of the potential required to obtain a local solubility of copper such that a corrosion pit can propagate. At an increase, rather than a decrease in the sulphate concentration, particularly in a water where the transport of copper, at the site of metal dissolution, is less dominated by the monovalent copper, we predict that an increase in the sulphate concentration should give a decrease in the value of the minimum pitting potential also at 75°C.

Sulphate, similar to carbonate, also forms basic salts of divalent copper. Two of these are considered for 25°C and one at 75°C. In our calculated corrosion pits, we find a basic sulphate in the crust for some variations in the composition of water *A* at 75°C and for some variations in the composition of water *B* at 25°C. Table 4-3 shows that precipitation of basic sulphate in the crust occurs in water *A* at 75°C when the carbonate content has been reduced to 50%. Table 4-4 shows that simultaneous precipitation of basic sulphate and basic carbonate occurs when the chloride or the carbonate contents of water *B* has been reduced to 50%. When more than one basic salt of divalent copper precipitates we find the sulphate inside the carbonate. Basic carbonate forms an outer crust covering an inner layer of basic sulphate. This tendency of the basic sulphate to form at lower pH values than the basic carbonates appears also as a low relative stability at the pH of the bulk water. In no case we have considered do we find basic sulphate as the most stable cupric solid at the pH of the bulk.

Sulphate is aggressive towards copper at low pH values. At the pH of the bulk of a natural water the sulphate complex with divalent copper is insignificant.

6.2.5 Oxygen

Oxygen is probably the most common oxidising agent in aqueous systems where cases of pitting of copper have been observed. Reduction of dissolved oxygen or another oxidising agent at external cathodic areas is a prerequisite for the anodic dissolution of copper in all corrosion pits we have modelled.

However, the diffusion path from bulk solution to the site of the metal oxidation at the bottom of a corrosion pit is open also for dissolved oxygen and the influence of the oxygen on the chemistry in a corrosion pit should not be neglected. In our model we assume a fast reaction between aqueous oxygen and monovalent copper. This fast reaction may result in a peak in the concentration of divalent copper and the site of this peak, which is influenced by the concentration of oxygen in the bulk water, may determine which of the basic salts or oxides of divalent copper is precipitated and where precipitation occurs. At 25°C this reaction between monovalent copper predominantly in the form of the dichloride complex and oxygen yields divalent copper predominantly in the forms of cupric carbonate, cupric sulphate and cupric ions. This reaction is coupled to a release of alkalinity or consumption of acidity. At 75°C however, as shown in figure 4-43 for water *B*, the product is dominated by the carbonate complex and by the dihydroxide complex of divalent copper. The homogenous reaction between monovalent copper and oxygen is then coupled to a release of acidity.

The influence of the concentration of aqueous oxygen in the bulk water on the minimum pitting potentials is small in all cases we have studied. However, in some cases we have not found a solution to the equilibrium and mass transport problem, which is consistent with the assumptions, for one oxygen concentration, while we have found a solution for a different, usually lower, oxygen concentration.

The chemical oxidation of monovalent copper by oxygen is important to the formation of a crust of cupric salts. Particularly for corrosion pits where the transport of dissolved copper is dominated by monovalent copper, the concentration of divalent copper would, in the absence of oxygen, be lower than the saturation level with respect to any cupric solid.

The redox potential is also at low oxygen concentrations high enough to drive a pitting process. Unless the reduction process is polarised by other anodic processes, pitting is likely to occur.

6.2.6 Calcium

The effect of calcium on the pitting of copper was studied only for water *B* at 25°C. Figure 4-53 shows that when almost all sodium in water *B* was exchanged with calcium, a slightly higher potential is required to obtain the same transported fraction. The explanation for this effect is the complex formation between calcium and sulphate, which decreases the concentration of free sulphate enough to decrease the extent of complex formation between divalent copper and carbonate. Figure 4-30 shows that for water *B* at 25°C where the sulphate concentration is much higher than that of calcium, a large fraction of the total calcium is present as the calcium sulphate complex. When the concentration of calcium has been increased to a value higher than that of sulphate, large amounts of the total sulphate is present as the calcium sulphate complex. In the

bulk water with the high calcium concentration, about 26% of the total sulphate is present as the calcium complex.

Table 4-12 shows that in the high calcium water the cupric oxide is the most stable cupric solid at the pH of the bulk whereas in the water with the lower calcium content a basic carbonate is the stable phase. This is an effect of the complex formation between calcium and carbonate, which decreases the concentration of carbonate slightly. In the bulk water with the high calcium concentration about 3% of the total carbonate is present as aqueous calcium complexes. A possible detrimental effect of calcium is that when present at higher concentrations than carbonate, precipitation of calcium carbonate in response to a local alkalisation, may precipitate most of the carbonate from the solution and favour initiation of type I pitting as described by Lucey/6-1/.

6.3 Effects of an iR drop in the solution

The difference in potential in the aqueous phase between the bulk solution and the solution at the site of metal dissolution at the bottom of a corrosion pit causes a tendency for ions with negative charge to accumulate at the bottom of the pit. Aggressive anions such as chloride and sulphate may therefore have higher concentrations at the site of the metal dissolution than in the bulk water outside the pit. We explain the aggressive influence by chloride with the complex formation with monovalent copper. Monovalent copper is present in the pit as a result of the electrochemical oxidation of copper metal but also at external areas in the form of cuprous oxide. Chloride may be equally aggressive towards copper metal in a pit, enhancing the local corrosion rate, as towards cuprous oxide at an external surface, increasing the rate of the general corrosion. Once a corrosion pit is initiated and an iR-drop is established chloride may become more aggressive towards copper in the pit than towards the cuprous oxide at external sites. The appearance of corrosion pits is likely to be an effect of a difference in the aggressive behaviour of the solution in a corrosion pit relative to the behaviour at external sites. The iR-drop is one factor, which causes a solution to be more aggressive in a corrosion pit than at external areas.

The magnitude of the iR-drops, which may arise, is a direct function of the conductivity of the bulk water. The increase in aggressive behaviour is therefore greater in waters with low ionic contents.

6.4 The importance of a crust

From our modelling we find that a pitting process could be operative also without the formation of a crust of salts of divalent copper outside the cavity. Particularly at higher temperatures, the acidification associated with the precipitation of basic salts seems to be relatively small since divalent copper, in the pH range where precipitation occurs is present mainly as the dihydroxide complex and as a carbonate complex. However, without a crust of corrosion products, the solution in contact with the cuprous oxide would probably be influenced by convective processes so that dissolution from the outside would occur. The effect would be to cause general corrosion and not pitting.

6.5 Growth rates

Our estimates of the development or the depth of a corrosion pit with time are based on a method described in Appendix 1. For cavities with a hemispherical shape the corroding surface increases with increasing depth of the pit. The site of the pit consumes more and more current, which must be delivered by a cathodic process. At some point

the corrosion potential would be influenced by the increasing consumption of anodic current and the potential would shift in the negative direction.

For a pit, which, for some reason, grows preferentially deeper and not wider, the current would not increase with time. For the limiting case of a cylindrical pit the current consumed would decrease with time. For pits with hemispherical shape as well as for pits with a cylindrical shape we predict a maximum depth which increases with the square root of time at constant potential. Tables 4-2 to 4-8 show the predicted times to reach a depth of 0.5 cm for cavities with hemispherical shapes only. A pit, which grows only deeper and not wider, would reach this depth faster. The time required would in all cases be longer than half the time in tables 4-2 to 4-8.

7 Experience of copper

In this section we compare our results to published experimental observations and to practical experience of copper. Studies of the anodic dissolution of copper by electrochemical experiments give useful material in an attempt to validate our results. Solution composition and temperature are usually controlled while the anodic dissolution is stimulated by imposed anodic potentials.

The real test of the predictive capacity of our model is however by comparing our results to the practical experience of copper and to case studies where pitting of copper has occurred under service conditions. This comparison is made more difficult because of an uncertainty of the conditions prevailing when pitting occurred. A hot water pipe may frequently be cold and periods of stagnation and turbulence lead to variations in water compositions. Few if any observations of a corrosion pit during growth have been made. Examinations by optical or electron microscopy are frequently made a long time after the specimen has been removed from the pitting environment. Elements found at trace amounts may not have been present as solid compounds during the pitting process.

First, we compare results from electrochemical experiments to our results. We compare our predicted values for the minimum pitting potentials to published values. Finally, we discuss the types of pitting described in the literature and their characteristics. The corrosion products identified in case studies and the shapes of the cavities are discussed in relation to our results.

7.1 Electrochemical experiences of copper

Potential scans are frequently used to study the pitting of copper in electrolyte solutions. The resulting polarisation curves are sometimes quantified as a breakdown potential defined as a the potential at which the current increases from an almost constant value and as a repassivation potential defined as the potential at which the lower constant value is regained on the return sweep. Another measure used is the pitting potential defined as the potential at which the current at a fixed potential increases with time.

7.1.1 At 25°C or lower

For solutions of only one salt at pH 8.0, Shalaby and coworkers /7-1/ found that 60 ppm sulphate gave higher dissolution rates of copper than 60 ppm chloride or 15 ppm hydrogen carbonate. In their results there is a potential window where the chloride solution gives a dissolution current almost a decade higher than the sulphate solution. The carbonate solution gives the lowest dissolution current at high potentials, but in the potential range where chloride solution gives the higher current, the carbonate is second and the sulphate gives the lowest dissolution currents. We interpret their results as support for our conclusion that sulphate is aggressive towards copper only at high potentials. At exposure up to 50 hours at 150 mV (SCE), which is in the potential range where sulphate gave the highest current of the single salt solutions, the single salt sulphate solution gave a dissolution current several times higher than the single salt chloride and mixed sulphate, carbonate, chloride solution. Analysis of the surfaces after exposure in single salt solutions revealed predominantly general corrosion with intergranular attack in the sulphate solution, pitting in the chloride solution and an adherent oxide film in the carbonate solution. After exposure in solutions containing

carbonate and sulphate or chloride, the surface analysis showed a stronger beneficial effect of carbonate in the chloride solution than in the sulphate solution. Severe grain boundary corrosion was found on the specimen exposed in the sulphate containing solution whereas the specimen exposed in the chloride containing solution had suffered little corrosion. From these observation we find support for our conclusions that the beneficial effect of carbonate is stronger in cases where the copper transport is dominated by monovalent copper.

Further support is found by comparing results of Francis /7-2/ to those of Thomas and Tiller /7-3/. In solutions of sulphate with concentrations from 10^{-4} M to 10^{-2} M SO_4^{2-} Francis found that additions of carbonate from 10^{-4} M to 10^{-2} M HCO_3^- increased the dissolution current. A decreased dissolution current was observed when 10^{-1} M HCO_3^- was added.

Thomas and Tiller /7-3/ studied the anodic dissolution of copper in solutions of carbonate and chloride. They found that the addition of 10^{-2} M HCO_3^- to solutions of 10^{-2} M and 10^{-1} M NaCl decreased the dissolution current up to a potential where breakdown occurs. The value of the breakdown potential was not significantly affected by the carbonate addition.

Thomas and Tiller /7-4/ also studied the pH dependence of the breakdown potentials. They found, in agreement with our results that, a decrease from pH 8.6 to pH 7.3 did no change the value of the breakdown potential.

Edwards /7-5, 7-6/ in a study of copper dissolution in single salt solutions found that sulphate gave increasing currents and chloride gave decreasing currents when polarised to a high anodic value (+125 mM vs Ag/AgCl). Chloride and sulphate gave initially high dissolution currents. In the chloride solution, the current generally decreased after a few hours whereas in the sulphate solution, the current remained at the high value. Corrosion potentials and corrosion currents at the corrosion potential determined before and after such exposures showed that the corrosion rate had increased by the anodic polarisation period in the sulphate solution and decreased in the chloride solution. This was found for pH 10, pH 8.5 and pH 7.0 but for pH 5.5 the corrosion rate had increased also for the chloride solution. The change in corrosion potential by the anodic polarisation period seems unsystematic but the corrosion potential was at all pH values lower in the chloride solution. The combination of a lower corrosion potential and a lower corrosion rate, which was observed in the chloride solution relative to the sulphate solution, indicates that the rate of the cathodic reduction of oxygen is also lower in the chloride solution. Pitting was observed in the sulphate solution at all pH values except pH 10. In the chloride solution pitting was indicated only at pH 10. Notable is that in carbonate solutions pitting was observed at all pH values except pH 7.0.

7.1.2 At higher temperatures

Thomas and Tiller /7-4/ found from their experiments with solutions of carbonate and chloride at 25°C, 60°C and 90°C that the breakdown potentials for copper decreased with increasing temperature. Thicker layers of cuprous oxide were formed at 60°C than at 25°C and the breakdown potential, defined as the potential at which the current increases with time, was about 80 millivolts lower at 60°C than at 25°C. Comparing the difference between breakdown potentials and corrosion potentials they find that the

difference increases from 130 millivolts at 25°C to 260 mV at 60°C. These observations are, at least qualitatively, in accordance with our results.

Sridhar and Cragnolino /7-7/ studied the breakdown and repassivation potentials of copper in solutions mixed electrolytes at 30°C, 60°C and 95°C. At 95°C localised corrosion was observed only for the solutions with low salt contents. At 30°C the lowest value of the repassivation potential was found in sulphate containing solutions and the value was not affected by chloride addition.

Mattsson and Fredriksson /7-8/ studied the anodic dissolution of copper in solutions containing carbonate and sulphate or chloride at 75°C. A voltage of 500 mV was applied between a large copper counter electrode and a small copper specimen in the form of a rod with a diameter of 0.5 mm. The circular end surface of the rod was exposed, face downwards, in a glass tube so that about 1.5 mm of the about 4 mm distance between the electrodes was essentially free from forced convection.

Given the geometry of the experimental set-up it is clear that the specimen was subjected to high anodic polarisation and that the iR-drop in the glass tube caused an accumulation of negatively charged species at the specimen surface. For inert anions we estimate the accumulation as a factor of ten per 70 mV iR- drop for monovalent ions and two factors of ten for divalent ions. While neither chloride nor sulphate are inert with respect to copper, it seems clear that the magnitude of the iR-drop is controlled by the anion concentration so that a change in the bulk concentration does not cause a proportional change in the concentration at the corroding copper surface.

For pH 7, Mattsson and Fredriksson found higher dissolution currents in waters where the sulphate concentration was between 0.2 mM and 2.0 mM than in waters where the chloride concentration was 4 mM. For pH 8 they found the same high current for the sulphate containing solution and that carbonate below a certain level increased the dissolution rate.

While we have not modelled any corrosion pit at 75°C for so high corrosion potentials that the aqueous chemistry and mass transport is dominated by divalent copper the situation seems to be comparable to our results for water *B* at 25°C. In this water we find that the copper transport in the pit is dominated by divalent copper and in agreement with the results of Mattsson and Fredriksson we find that carbonate at low concentrations, under these conditions, has a small if any beneficial influence.

Mattsson and Fredriksson concluded that the crusts of corrosion products formed in and at the anode compartment contained basic copper sulphate in the sulphate containing waters and basic copper carbonate in waters free from sulphate. They found the basic sulphate crust at the end of the capillary and the basic carbonate crust in the capillary or at the corroding copper surface.

In all cases we have modelled where simultaneous precipitation of basic sulphate and basic carbonate occurs, we invariably find the sulphate salt inside an outer crust of basic carbonate salt. We find the basic sulphate at a lower pH than the pH where we find the basic carbonate. Mattsson and Fredriksson find the sulphate further away from the copper metal than they find the carbonate, although the simultaneous precipitation of the two basic salts was not observed. One explanation is probably that in the experiments with sulphate containing waters, the solution at the corroding copper becomes much more acid than in the experiments without sulphate. Sulphate is, as

Mattsson and Fredriksson state, likely to decrease the transport number of the hydrogen carbonate. The transport of acidity away from the site of copper oxidation is, in the presence of sulphate, less facilitated by carbonate migrating into the anode compartment and diffusing out in the form of carbonic acid.

In our modelling we found the corresponding influence of sulphate also on the chloride. The presence of sulphate decreases the transport number of chloride so that less monovalent copper is transported away from the site of metal oxidation in the form of chloride complexes.

7.2 Experiences of the pitting of copper

7.2.1 Pitting potentials

Pourbaix /7-9/ found for cold Brussels water that pitting occurred when the potential of copper exceeds about 270 mV (NHE). To this value an iR-drop should be added so that the measurable potential is about 420 mV for a concave tube surface and about 350 mV for the convex surface of a thin wire /7-9/. Pourbaix concludes that copper does not attain these high values spontaneously but only in the presence of a galvanic coupling to a more noble phase such as carbon, gold or platinum.

Cornwell and coworkers/7-10, 7-11/ found that in cold British tap waters, no pitting occurred at potentials below about 350 mV (NHE). Severe pitting occurred at potentials higher than about 420 mV. These potentials were attained by copper tubes with an internal contamination of carbon remaining from the manufacture. After cleaning of the tubes the corrosion potentials settled at about 260 mV, almost 100 mV below the pitting limit.

For hot water Fujii and coworkers /7-12/ found that severe pitting of copper tubes occurred at potentials higher than about 400 mV (NHE). These values were in chlorinated water attained also in the absence of internal carbon films.

7.2.2 Solids observed

In the actual cavity, only cuprous oxide and frequently also cuprous chloride have been observed in case studies. These findings agree well with results from electrochemical studies and also with our results. Outside the cavity in a crust of corrosion products a number of cupric solids have been identified. To our knowledge no pitting has been observed in a natural water without precipitation of at least one of the basic salts of sulphate, carbonate or chloride with divalent copper.

Vinka /7-13/ has in a recent report summarised the identified corrosion products associated with various types of pitting. The so called type I pitting, observed in cold waters with high alkalinity, is associated with precipitation of basic carbonates malachite $Cu_2(OH)_2CO_3$ and more rarely azurite $Cu_3(OH)_2(CO_3)_2$ in a crust outside the cavity. Basic chloride, atacamite, $Cu_2(OH)_3Cl$ and cupric oxide, tenorite CuO have also been found. These observations agree well with our results although we find the basic chloride salt only in water D where the chloride concentration is similar to that in seawater. The precipitation of calcium carbonate found outside cavities in type I pitting does not agree with our results where we invariably find a monotonous decrease in the product of the activities of calcium and carbonate ions from the bulk towards the pit.

The presence of the calcium carbonate is frequently an indication of the site for the oxygen reduction. Precipitation of calcium carbonate outside corrosion pits in type I

seems to be the strongest evidence for Lucey's membrane cell theory for type I pitting. By assuming that the cathodic reaction required to drive the pitting process takes place in the crust of corrosion products outside the cavity, Lucey can explain the precipitation of calcium carbonate as a result of an alkalisation caused by the reduction of oxygen. Type I pitting may therefore contain elements which we have not accounted for in our model.

Type II pitting, observed in hot water systems, is characterised by the presence of basic sulphate salt of divalent copper. Brochantite $Cu_4(OH)_6SO_4$ and antlerite $Cu_3(OH)_4SO_4$ are found in the crust.

In some cases only the basic sulphates have been identified as the main components. In other cases basic carbonate or basic chloride salts of divalent copper have been observed together with a basic sulphate in the crust /7-8/. The shift in crust composition from basic carbonates to basic sulphates as the temperature increases agrees well with our results. We have also found that precipitation of more than one cupric solid outside the cavity is likely.

Pitting type III, observed in cold water pits, is similar to type II in that basic sulphates are observed in the crust. Basic carbonate, basic chloride and cupric oxide have also been identified.

The diversity in the composition of the corrosion products accumulated outside the cavity indicate that while a crust is necessary for the build up of an aggressive solution, no single phase is necessary. The composition of the crust more reflects the composition of the water in which pitting occurs than the precipitation of a specific solid that creates the pitting conditions.

7.2.3 Shapes of the cavities

Types I and III seem to give rise to cavities with approximately hemispherical shapes whereas type II gives rise to cavities with irregular shape. Type III differs from type I and II in that several small pits may be concentrated in a relatively small area. Cuprous oxide is found in all three types of cavities. Pits of type I and III contain some cuprous chloride whereas pits of type II may be almost completely filled with cuprous oxide.

A hemispherically shaped cavity indicate that the pitting process is governed by mass transport towards a small opening. An irregularly shaped cavity may indicate that the copper surface in the cavity is partly covered by an adherent and protecting layer of cuprous oxide. In relation to our results we would explain the hemispherically shaped pits as occurring under conditions such that a large fraction of the oxidised copper is transported away from the site of metal dissolution as divalent copper. The irregularly shaped cavities filled with cuprous oxide indicates that monovalent copper is the dominating corrosion product. Monovalent copper, in contrast to divalent copper, may precipitate also at low pH.

Calculated corrosion pits for water *B* at 25°C agree best with the growth condition deduced for a hemispherical shape. Table 4-5 includes results for pits in water *B* with a chloride contents reduced to 50% at 25°C where solid cuprous chloride also is precipitated at the bottom of the cavity.

Growth conditions deduced for the irregularly shaped cavities agree best with pits calculated for 75°C. Both water *A* and water *B* give predominantly monovalent copper

as corrosion product at this temperature. Thus the growth conditions we find from our calculations agree well with the shapes of the cavities found in practice.

7.3 Detrimental factors

7.3.1 Carbon films

Cornwell and coworkers /7-10,7-11/ have shown that much higher corrosion potentials are obtained for copper pipes with an internal contamination of elementary carbon remaining from the manufacture. The adoption of special procedures to remove any carbon films than might have been formed during manufacture produced a drastic decrease in the number of failures of copper water pipes by pitting corrosion /7-14/.

7.3.2 Photo-negative cuprous oxide

Cuprous oxide is a semiconductor and may be non-stoichiometric in composition so that some copper is missing in the crystal structure. Stoichiometric cuprous oxide is an n-type semiconductor. A copper electrode covered with the n-type oxide responds to illumination with a decrease in corrosion potential. Copper deficient cuprous oxide is a p-type semiconductor and responds to illumination with an increase in potential /7-16/. Copper deficient cuprous oxide is photopositive. Lucey /7-15/ has shown that in Dartford tap water, the photonegative cuprous oxide does not form at potentials below +90 mV (NHE). Lucey correlates the formation of the photonegative oxide to the incidence of pitting and considers +90 mV as a potential limit, which should not be exceeded in order to avoid pitting. Di Quarto and coworkers /7-16/ studied the photorespons of copper in aerated solutions of sodium sulphate. They found that photopositive cuprous oxide formed at pH 5.0 and that photonegative oxide formed at lower pH-values.

Although the link between the n-type or p-type behaviour of the cuprous oxide and pitting corrosion does not seem clear, there seems to be a correlation between the formation of n-type oxide and cold water pitting of copper /7-22/.

7.3.3 Biological activity

Organic substances in water have been found to have a beneficial effect on the pitting of copper. Surface water have been found to contain an inhibiting agent which is absent in deep well waters.

However it has also been found that components of biological origin deposited in copper tubes are aggressive towards copper. Films containing polysaccharides, and proteins formed on copper tubes have been associated with cold water pitting of copper/7-13, 7-17, 7-18,7-23/.

7.3.4 Thermally formed oxides

It has been found that copper oxides formed during brazing of copper tubes may enhance cold water pitting /7-20/. Soldering, which is made at lower temperatures, does not enhance the tendency for pitting, provided that the soldering flux is removed /7-20/. Billi and coworkers /7-21/ studied the electrochemical behaviour of copper oxidised in air at various temperatures. Specimen oxidised at temperatures above about 473 K showed a higher corrosion rate, as indicated by a lower corrosion potential and a lower

polarisation resistance in a dilute carbonate, sulphate, chloride solution at 298 K, than specimen oxidised at lower temperatures.

7.4 Copper in seawater

Campbell /7-14/ and Gilbert /7-19/ state that copper may pit in seawater. Seawater containing sulphide is concluded to be more aggressive. Films of copper sulphide may form and these may have a detrimental influence. Carbon films on copper is reported to cause pitting also in seawater /7-14/

7.5 Discrepancies

The anodic processes and the influence of the various water components seem to be adequately described by our model. However, for many of the waters where pitting has been observed in practice we find that the minimum pitting potential is in a potential range where cuprous oxide is not the stable copper phase at the pH of the bulk water.

8 Conclusions

- There is a minimum potential for pitting corrosion of copper. This minimum potential must be exceeded in order to allow the acidifying reactions, which produce a sufficiently low pH in the pit. A low pH in the pit is a prerequisite for high concentrations of copper in the local solution in the pit. A high concentration of copper in the local solution is necessary for a sufficient fraction of the oxidised copper to be transported away from the site of metal dissolution as aqueous species. The composition of the bulk water has a big influence on the value of the minimum pitting potential.

- For propagation of a corrosion pit to be possible, there must be a cathode material, which is stable at potentials where pitting is possible. Copper metal is in all practical cases in contact with cuprous oxide as an inner layer of corrosion products. An outer layer of oxide or salts of divalent copper may exist on top of the cuprous oxide. The reduction of oxygen at an outer layer of corrosion products with electronic conduction through the poorly conducting cupric phases, through the cuprous oxide to the copper metal seems an unlikely process. Cuprous oxide has high electronic conductivity and we regard cuprous oxide as the cathode material where reduction of oxygen or other oxidising agents takes place. The stability of cuprous oxide compared with the solid cupric phases defines an upper potential above which the anodic dissolution of copper metal in a corrosion pit cannot be sustained by a reduction process on cuprous oxide.

- The pH of the bulk water outside a corrosion pit has a small influence on the minimum potential where pitting is possible. The stability of the cuprous oxide against oxidation decreases with increasing pH. The potential window where reduction at a cuprous oxide surface can drive the anodic dissolution in a corrosion pit therefore decreases with increasing pH. Pitting of copper is less likely to occur at high pH values.

- Expressing the difference between the minimum potential for propagation of a corrosion pit and the upper potential for stability of cuprous oxide as a margin against pitting, we find that for a water with given composition, the value of this margin increases with temperature. Pitting is less likely to occur at higher temperatures.

- Of the common anions, chloride is the most aggressive species towards copper. A strong complex formation of chloride with monovalent copper allows high copper concentrations in contact with corroding copper metal. The chloride concentration is decisive for the value of the minimum pitting potential of copper. However, chloride is likely to be equally aggressive towards cuprous oxide. A high dissolution rate of the cuprous oxide at the pH of the bulk is likely to decrease the corrosion potential through an increased polarisation of the cathodic processes. However, using the margins against pitting as criteria, we find that the value of this margin decreases with increasing chloride concentration. Pitting is, according to this criterion, more likely to occur in waters with high chloride concentrations.

- Carbonate forms strong complexes with divalent copper. The pH dependence of the concentration of the carbonate ion makes carbonate more aggressive at the higher pH of the bulk than at the lower pH in a corrosion pit. A high carbonate concentration may therefore facilitate the anodic reactions in general corrosion. Precipitation of basic carbonate salts with divalent copper at cuprous oxide may however also decrease the rate of the cathodic reactions. The buffering capacity of hydrogen carbonate at moderately low pH values facilitates the transport of acidity out from the pit. An increased transport rate for protons, in the form of carbonic acid, favours the formation of cuprous oxide in the pit rather than the competing formation of aqueous copper species. If there is any detrimental effect of carbonate, with respect to pitting, it would be that an increased concentration may enable the formation of a crust of corrosion products outside a corrosion pit where at a lower concentration there would be none. A high carbonate concentration may increase the value of the minimum pitting potential and decrease the value of the upper stability potential for cuprous oxide. Pitting is less likely to occur in waters with high carbonate concentrations.

- Sulphate forms a complex with divalent copper. This complex may be a major copper species at the low pH in a corrosion pit while, because of the increased stability of the carbonate and hydroxide complexes, it is a minor copper species at the pH of an external surface. Sulphate may therefore be aggressive towards copper in a corrosion pit and almost inert with respect to the general corrosion. Although a small beneficial effect may be found in waters with relatively high chloride concentrations, the effect of an increased concentration of sulphate is generally to decrease the value of the minimum pitting potential. Pitting is more likely to occur in waters with high sulphate concentrations.

- Calcium may have an indirect beneficial effect. The strong complex formation with sulphate decreases the concentration of free sulphate and thereby the extent of complex formation between sulphate and divalent copper. For a water with a high sulphate concentration, pitting is less likely to occur if the calcium concentration is of the same magnitude or higher.

- For cold water pitting calcium, when present at higher concentration than carbonate, may have a detrimental effect. Large fractions of the carbonate may be removed from the solution by precipitation of calcium carbonate.

- Oxygen can also at low concentrations give potentials higher than the minimum pitting potential. The influence at the site of the pit of the direct oxidation of monovalent copper to divalent has a small influence on the minimum pitting potential. This direct oxidation may however cause a smaller fraction of the corrosion products to precipitate in the cavity and a higher fraction outside the cavity.

- Corrosion pits where the transport of copper is dominated by monovalent copper may lead to precipitation of large amounts of porous cuprous oxide in and outside the cavity. Where the transport is dominated by divalent copper, precipitation, in the form of basic salts, occurs at higher pH values and outside the cavity.

- Precipitation in the cavity decreases the aqueous cross sectional area available for diffusion and migration to a higher extent than precipitation outside the cavity. A certain volume of corrosion products may outside the cavity take the form of a hemispherical shell with a large area and a small thickness. In the cavity the area is restricted and the thickness has to be greater. Pits where the precipitation occurs mainly outside the cavity therefore have higher growth rates.

- Factors favouring the type of pits dominated by monovalent copper are high chloride contents in the bulk water and high temperatures. Factors favouring the type of pits dominated by divalent copper are a high sulphate concentration, low concentrations of other salts and high potential.

- Pitting of copper has been observed in waters with a composition and temperature such that we find the minimum pitting potential in a range where cuprous oxide is not stable relative to solid cupric phases at the pH of the bulk water. Many of these observations have been explained by the presence of foreign phases such as carbon films where the reduction of oxygen has taken place.

- Pitting of copper is possible in all waters we have studied. In some waters a corrosion pit will not propagate unless the cuprous oxide at external surfaces is stabilised or if there is electronic contact with a conducting more noble phase.

- Limits of the propagation rates for corrosion pits in copper can be given only as conditional of the corrosion potentials.

- In waters with chloride contents approaching that of seawater, pitting is possible with high propagation rates also at high pH values. Cuprous oxide is, at pitting potentials, in these waters stable against oxidation to solid cupric phases. Small amounts of oxygen may oxidise the monovalent copper in the cavity to divalent copper, which does not precipitate inside the cavity and therefore does not significantly impede the mass transport and rapid growth of the pit.

9 Recommendations

On the basis of this study the following recommendations for a copper canister in compacted bentonite clay can be made.

- The surface of the copper should be as uniform as possible. If the canister is to be welded, the oxides formed should be removed. Such thermally formed oxides have been found to be a likely cause of pitting of copper.
- The pressure exerted by the compacted bentonite should also be as uniform as possible. A non-uniform pressure may stabilise the cuprous oxide at one site while allowing precipitation of less dense oxides and salts of copper at another site.

10 Future work

The results presented here should be further validated by comparison to published observations and possibly also to new experiments designed to support or to reject the conclusions. For waters with compositions similar to that of seawater, we found that pitting is possible also at high pH values. The only solid precipitating outside the cavity then is the cupric oxide. To our knowledge pitting of copper has never been observed without precipitation of at least one basic salt of divalent copper. If it can be substantiated that precipitation of a basic salt is a prerequisite for pitting and that a crust consisting of only cupric oxide has properties which do not allow propagation of corrosion pit, an upper pH limit for pitting can be set.

We have found that waters with moderate chloride concentrations will not cause pitting because the potentials required can not be supported by a reduction process on cuprous oxide. Pitting has been observed in such waters. In many of these cases the high potentials have found an explanation in the presence of a carbon film or other noble cathode material. For some of the observed cases there remains an uncertainty as to the cause to the high potentials. Most of the observations com from tap water systems where cupric phases may have scaled off the underlying cuprous oxide thus baring a new surface for the oxygen reduction. Although explanations to the high potentials can be found, further investigations into the stability of cuprous oxide as a prerequisite for pitting is desirable. Should the stability limit for cuprous oxide be found to be an acceptable criterion for pitting, the effect of pressure on the relative stability of the cuprous oxide versus the cupric oxide and the basic salts of divalent copper should be investigated. Since a certain amount of copper occupies a smaller volume in the monovalent oxide than in the divalent oxide and in the basic salts, the effect of an increased pressure is to stabilise the more dense cuprous oxide.

The method we use to predict the maximum growth rate is relatively crude and could be refined. The good agreement between our results and the experience of copper shows that modelling is a fruitful approach to the problem of pitting corrosion on copper. A limitation of our model is that no exact shape of the cavity can be predicted and since no dimensions are fixed, the relatively slow kinetics of the reduction of dissolved oxygen by monovalent copper has not been accounted for. A solution to these shortcomings would be to use a dynamic model instead of this static. A simulation of the growth of an initially small corrosion pit with time can be made.

11 Acknowledgement

This work was commissioned by the Swedish Nuclear Fuel and Waste Management Co.

12 References

3-1 **Wallin T and Lewis D**

Thermodynamic calculations of equilibrium concentrations for the system Cu-H_2O-Cl^-- CO_3^{2-}-SO_4^{2-}-F^-. Appendix B1 in Corrosion resistance of a copper canister for spent nuclear waste, SKB Technical Report 82-24

3-2 **Lewis D**

The Thermodynamics for the system Cu-H_2O-Cl^--CO_3^{2-} at elevated temperatures - A prestudy, Appendix B2 in KBS 90, SKB Technical Report

3-3 **Sillén L-G and Martell A F**

Stability constants of metal ion complexes, The Chemical Society Special Publication No 17

3-4 **Sillén L-G and Martell A F**

Stability constants of metal ion complexes, The Chemical Society Special Publication No 25

3-5 **Smith M and Martell E**

Critical stability constants volume 4: Inorganic complexes, Plenum Press, New York 1976

3-6 **Lewis D**

Studies of redox equilibria at elevated temperatures. I. The Estimation of equilibrium constants and standard potentials for aqueous systems up to 374°C, Arkiv för Kemi Band 32 nr 32 1971, p.385

3-7 **Stumm W and Morgan J J**

Aquatic chemistry. An introduction emphasizing chemical equilibria in natural waters, 2nd ed. Wiley, New York 1981

3-8 **Koryta J and Dvorak J**

Principles of Electrochemistry, Wiley, Chichester 1987

3-9 **Lide D R**

Handbook of Chemistry and Physics 71:st ed. CRC, Boca Raton, Florida 1990

5-1 Taylor R J and Cannington P H

Control of pitting corrosion in potable waters, Research Report No 64 1993 Urban Water Research Association of Australia

5-2 Baes F and Mesmer R E

The Hydrolysis of Cations Wiley, New York 1976

5-3 Tanaka N and Tamamushi R

Kinetic Parameters of Electrode reactions, Electrochimica Acta Vol 9 1964, p 963

5-4 Sharma V K and Millero F J

Effect of Ionic Interactions on the Rates of Oxidation of Cu(I) with O_2 in Natural Waters, Mar. Chem. Vol 25 p141 1988 as quoted by B. Werli in *Redox Reactions of Metal ions at Mineral Surfaces* in Aquatic Chemical Kinetics. Reaction rates of Processes in Natural Waters Ed. W Stumm, Wiley, New York 1990

5-5 Lucey V F

Developments leading to the Present Understanding of the Mechanism of Pitting Corrosion of Copper, British Corrosion Journal Vol. 7 1972, p 36

6-1 See reference 5-5 and reference 7-15

7-1 Shalaby H M, Al-Kharafi F M and Said A J

Corrosion morphology of copper in dilute sulphate, chloride and bicarbonate solutions, British Corrosion Journal Vol. 25 1990, No 4, p 292

7-2 Francis P. E., Cheung W. K., Pemberton R. C.

Electrochemical measurements of the influence of sulphate/hydrogen carbonate ion ratio on the pit initiation process on copper, Proceedings of the 11th International Corrosion Congress, Florence, April 1990, Associazione Italiana di Metallurgia. p 5.363

7-3 Thomas J G N, Tiller A K

Formation and breakdown of surface films on copper in sodium hydrogen carbonate and sodium chloride solutions, I. Effects of anion concentration, British Corrosion Journal Vol 7 1972 p 256

7-4 Thomas J G N, Tiller A K

Formation and breakdown of surface films on copper in sodium hydrogen carbonate and sodium chloride solutions, II. Effects of temperature and pH, British Corrosion Journal Vol 7 1972 p 263

7-5 Edwards M, Meyer T and Rehring J

Effect of various anions on copper corrosion rates, Preprint from the authors, to be published in Journal of American Water Works Association

7-6 Edwards M, Rehring J and Meyer T

Inorganic ions and copper pitting, Preprint from the authors, to be published in Journal of American Water Works Association

7-7 Sridhar N and Cragnolino G A

The effect of environment on localized corrosion of copper based high-level waste container materials, Corrosion 92, Paper 121, NACE

7-8 Mattsson E and Fredriksson A M

Pitting corrosion on copper tubes- Cause of corrosion and countermeasures, British Corrosion Journal Vol 3 1968, p 246

7-9 Pourbaix M

Recent applications of electrode potential measurements in the thermodynamics and kinetics of corrosion of metals, Corrosion Vol 25 1969, p 267, NACE

7-10 Cornwell F J, Wildsmith G and Gilbert P T

Pitting corrosion in copper tubes in cold water service, British Corrosion Journal Vol 8 1973, p 202

7-11 Cornwell F J, Wildsmith G and Gilbert P T

Pitting corrosion in copper tubes in cold water service in galvanic and pitting corrosion - Field and laboratory studies, ASTM STP 576 1976, American Society for Testing and Materials p 155

7-12 Fuji T, Kodama T and Baba H

The effect of water quality on pitting corrosion of copper tube in hot soft water, Corrosion Science Vol 24 1984, p 901

7-13 Vinka T-G

Composition of corrosion products and biofilm on copper tubes in tap water, Swedish Council for Building Research (BFR) Research Project 881020-5, 1994 (In Swedish)

7-14 Campbell H

A Review: pitting corrosion of copper and its alloys, Localized Corrosion, NACE Houston 1979 Editors: R W Staehle, B F Brown, J Kruger, A Agrawal

7-15 Lucey V F

Mechanism of pitting corrosion of copper in supply waters, British Corrosion Journal Vol. 2 1967, p175

7-16 Di Quarto F, Piazza S and Sunseri C

Photoelectrochemical study of the corrosion product layers on copper in weakly acidic solutions, Electrochem Acta Vol 30 1985, p315

7-17 Fischer W R, Wagner D H J and Paradies H H

An evaluation of countermeasures to microbially influenced corrosion (MIC) in copper Potable water Supplies, Microbially Influenced Corrosion Testing, ASTM STP 1232, Editors : J R Kearns and B Little American Society for Testing and Materials, Philadelphia, p 275, 1994

7-18 Geesey G G, Bremer P J, Fischer W R, Wagner D, Keevil C W, Walker J, Chamberlain A H L and Angell P

Unusual types of pitting corrosion of copper tubes used for water service in institutional buildings, Summary Paper to be published in Biofouling/Biocorrosion in Industrial Water Systems Editors: G G Geesey, Z Lewandowski and H-C Flemming 1993

7-19 Gilbert P T

Copper and its alloys in Corrosion Vol 1: Metal/Environment Reactions 2nd ed. Editor: L L Shrier, Newnes-Butterworth 1976

7-20 Baukloh A, Protzer H and Reiter U

Kupferrohre in der Hausinstallation- Einfluss von Produktqualität, Verarbeitungs- und Installationsbedingungen auf die Beständigkeit gegen Lochfrass Typ I, Metallwissenschaft und Technik 43 Jahrgang January 1989 p 26

7-21 Billi A, Marinelli E, Pedocchi L and Rovida G

Surface characterisation and corrosion behaviour of Cu-Cu_2O-CuO systems, Proceedings of the 11th International Corrosion Congress, Florence, April 1990, Associazione Italiana di Metallurgia. p5.129

7-22 Taylor R J and Cannington P H

Control of pitting corrosion in potable waters, Research Report No 64 1993Urban Water Research Association of Australia

7-23 Wagner D, Peinemann H, Siedlarek H, Fischer W R, Arens P and Tuschewitz G J

Microbially influenced pitting corrosion of copper pipes, International Copper Association ICA Report No 453-A, Iserlohn March 1994

13 Appendix 1

A1 Pitting rate on copper

Mass transport in a corrosion pit is governed partly by migration and partly by diffusion. In order to estimate the flux of matter and charge in the pit the potential and the concentrations of all participating species have to be known at all locations. To simplify the analysis of the chemistry and the mass transport in the pit that problem is solved for a very simple model geometry. The results from this analysis is then translated to a corrosion pit with a more realistic geometry. The problem of the pit chemistry and the mass transport can thereby be separated from the geometrical problems associated with the propagation of a corrosion pit.

A1.1 The model geometry

To make the analysis of the chemistry and the mass transport as simple as possible, the analysis is made for a normalised geometry. This geometry can be regarded as consisting of N elements in series, all having an aqueous cross sectional area equal to A_{norm} and an element length of Δx_{norm}. A corrosion current i_{norm} is calculated for the normalised geometry.

This current is the local current at the site of the metal dissolution. We treat the copper(I)oxide formed in the pit as a metallic conductor so that redox reactions may take place in the porous oxide. We find that some divalent copper is reduced to monovalent copper as the alkaline influence from the bulk solution is encountered. The current from the reduction is carried back to the copper metal by electronic conduction in a local galvanic element. Reduction of divalent copper at a slightly higher pH may contribute to the rate of the metal dissolution. The current carried by aqueous species may therefore not be constant in the domain where copper(I)oxide is present. The corrosion rate is proportional to the aqueous flux of charge at the site of the metal dissolution. The proportionality factor has a value between one and two moles copper per mole electrons, depending on the distribution between monovalent and divalent copper formed at the corroding metal.

The distribution of the corrosion current on the ionic species in the pit as a function of the local pH is calculated for the normalised geometry. However, to obtain the propagation rate for a pit of a given size and shape the geometry of that particular pit must be regarded.

The propagating pit is segmented into the same number of elements as the normalised geometry. The dimensions of the elements are selected so that the ratio of the length of an element to the cross sectional area available for mass transport for that element is the same for all elements representing the propagating pit.

$$\frac{\Delta x_n}{A_n \ fp_n} = constant(t) \qquad \text{A1-1}$$

A porosity factor *fp* is introduced since a part of the cross sectional area may be occupied by solid corrosion products and not available for aqueous mass transport. The value of the ratio for the propagating pit may be different from the value of the ratio for the normalised geometry.

The corrosion current can be calculated for any suitable dimensions of the normalised elements and be related to the current for any other pit geometry such that the condition of a unidirectional mass transport is fulfilled.

The site of the corrosion pit, including the crust of corrosion products deposited outside the plane of the original copper surface, is as all times represented by a fixed number of elements, *N*. As the reaction propagates and the dimensions of the pit increase, the dimensions of the elements also increase. The corrosion current for the pit changes with the dimensions of the elements according to equation A1-2.

$$i = i_{norm} \frac{A_n \; fp_n}{A_{norm}} \frac{\Delta x_{norm}}{\Delta x_n} \qquad \text{A1-2}$$

A1.2 Volume increase during corrosion

$Cu_2O(s)$ is the major corrosion product under the conditions investigated and the volume of the solid product is larger than that of the solid reactant. The corrosion of copper in a restricted geometry under stationary conditions requires that a certain fraction of the corroded copper is transported away from the site of the oxidation.

1 cm^3 Cu(s)	8.92	g	0.140	moles Cu
1 cm^3 $Cu_2O(s)$	6.00	"	0.084	"
difference			0.057	"

The mole fraction of Cu(I) which would have to be transported out from a restricted volume to keep the volume of the formed $Cu_2O(s)$ equal to the volume of the corroded copper is about 40 %.

A1.3 Conditions for propagation

At a time when the pitting reaction has caused a cavity in a copper surface an amount of corrosion products will have been deposited outside the cavity. For stationary conditions, the volume of copper oxide deposited inside the plane of the original copper surface may not be larger than the original copper volume. A condition for propagation is thus that the transported fraction of the oxidized copper at the plane of the original surface is 40 % or higher since some porosity in the copper oxide is required for propagation. If the pH at the plane of the original copper surface is low enough to obtain

a transported fraction higher than 40 %, the pH at the bottom of the pit is even lower. The potential required for propagation of a corrosion pit is therefore higher than the potential required for the formation of an occluded cell. Occluded cells may form but be unable to propagate, propagate for a short time, or propagate with an extremely low rate because of the formation of a covering layer of corrosion products with a porosity approaching zero.

A1.4 Propagation rates

A complication in the calculation of a propagation rate for this system is the precipitation of solid corrosion products. Moreover, the corrosion products precipitate also outside the cavity so an assumption of the geometry and porosity of the actual cavity is not enough to describe the total resistance to diffusion and migration. The approximations needed to estimate a pitting rate are therefore rather coarse.

A stable mode of propagation is considered where the shape of the cavity is conserved and the same fraction of the corroded copper is deposited in the cavity at all times. The propagation rate of a pit with a given geometry is determined by the rate of the stationary mass transport for that particular geometry. The depth of the pit may be obtained through an integration in time over a series of stationary states.

A1.4.1 A geometric model of a corrosion pit and crust

The site of the corrosion pit, including the crust of corrosion products deposited outside the plane of the original copper surface, is as all times represented by a fixed number of elements, N. As the reaction propagates and the dimensions of the pit increase the dimensions of the elements also increase.

We express the corrosion current at the site of the metal dissolution , in terms of the dimensions of the cavity as:

$$i = N \frac{i_{norm}\ \Delta x_{norm}}{A_{norm}} \quad \frac{N_{cav}}{N} \quad \frac{A_p\ fp_p - A_0\ fp_0}{p \ln \frac{A_p\ fp_p}{A_0\ fp_0}} \qquad \text{A1-3}$$

The right hand side of expression A1-3 may be regarded as an average aqueous cross section area divided by the depth of the cavity.

A1.4.2 The dependence of the pit current on the shape of the cavity

For a cylindrical cavity of depth p and constant radius the area terms are constant and equation 3 predicts a pit current decreasing with time. For a hemispherical cavity the radius is represented by p. With a hemispherical growth the corroding area A_p increases with the square of the radius of the cavity and an increase of the pit current with time is predicted. Such an increase in the pit current with time can in a real system not be maintained forever. As the pit propagates the pit current would eventually begin to increase the polarisation of the cathodic reaction outside the pit. Together with a possible increase in the iR drop outside the pit the increased polarisation of the oxygen reduction would have the effect of decreasing the corrosion potential of the system. On the other hand, the current density at the corroding surface decreases with time for both a cylindrical and a hemispherical cavity. The activation over potential for the corrosion process in the cavity is therefore likely to decrease with time.

A1.4.3 Pitting rate

The corrosion of a small volume dV can be regarded as an increase in the pit depth dp over the corroding area A_p. The growth rate in centimetres per second can then be described by:

$$\frac{dp}{dt} = \frac{M_{Cu}}{\rho_{Cu}} N_{cav} \frac{i_{norm} \Delta x_{norm}}{\nu F A_{norm}} \frac{fp_p - fp_0 \frac{A_0}{A_p}}{p \ln \frac{fp_p A_p}{fp_0 A_0}} \qquad \text{A1-4}$$

M_{Cu}	g/mole	= the molar weight of copper
ρ_{Cu}	g/cm^3	= the density of metallic copper
ν		= average oxidation state for copper at the site of metal dissolution

A1.4.4 Pit geometries

In order to calculate the ratio between the area at the plane of the original copper surface to the corroding area at the bottom of the cavity the shapes of the elements representing these parts of the pit have to be known. Mass transport in a hemispherical cavity implies curved elements and linear mass transport implies elements with plane surfaces perpendicular to the flux.

For a cylindrical cavity, where both elements are plane, the ratio between the areas is unity. For a hemispherical pit the ratio would have the value of 1/2 if the mass transport across the plane of the original copper surface is linear.

A1.4.5 Pit depth

For pit geometries such that the ratio between the corroding area at the bottom of the pit and the area at the plane of the original copper surface is constant and the same fraction of the oxidized copper is precipitated as $Cu_2O(s)$ at all times equation A1-4 can be integrated directly. An expression for the time, t, required for a cavity which is p_1 cm deep at time t_1 to propagate to the depth p is given by equation A1-5.

$$t - t_1 = \frac{p^2 - p_1^2}{2} x \frac{\rho_{Cu}}{M_{Cu}} \frac{\ln \frac{fp_p A_p}{fp_0 A_0}}{N_{cav} (fp_p - fp_0 \frac{A_0}{A_p}) \frac{i_{norm} \Delta x_{norm}}{\nu F A_{norm}}} \qquad \text{A1-5}$$

In order to use equation A1-5, the porosity at the plane of the original copper surface, fp_0, and the fraction of the geometric resistance, which represents the cavity, N_{cav}/N, have to be determined. If the porosity at the plane of the original copper surface is allowed to tend towards zero the rate of growth would also tend towards zero. If the porosity at the plane of the original copper surface is very close to the porosity at the corroding wall of the cavity the fraction of the resistance attributed to the cavity would

be very small and the rate of growth would tend towards zero. It seems appropriate to look for a maximum in the function describing the growth. The result would then to some extent be that for a worst case. The relevant factor to maximise is:

$$\frac{N_{cav}}{N} \frac{fp_p - fp_0 \frac{A_0}{A_p}}{\ln \frac{fp_p}{fp_0} \frac{A_p}{A_0}} \qquad \text{A1-6}$$

The porosity at the plane of the original copper surface, fp_0, is however not directly accessible. Accessible is the fraction of the oxidized copper, which is transported as aqueous copper species for each element. The transported fraction of the oxidized copper at the pit bottom defines the porosity at the pit bottom, fp_p, whereas the transported fraction at the plane of the original copper surface defines the fraction of the oxidized copper which is deposited in the cavity. The value of the fraction of the oxidized copper which, at the original copper surface, is transported as aqueous species can be used to calculate the average porosity in the cavity as the ratio of the volume of the precipitated copper oxide in the cavity to the total volume of the cavity. Assuming that the average porosity in the cavity is an arithmetic mean of the porosity at the pit bottom and the porosity at the plane of the original copper surface, respectively, the unknown porosity, fp_0 can be evaluated.

We determine the maximum value of the expression A1-6 from the output file of the program used to calculate the concentration profiles in and around a propagating corrosion pit. The value is calculated for various alternative locations of the plane of the unpitted surface. The maximum value of expression 6 is used to calculate the development of a corrosion pit with time by equation A1-5. Different maxima are obtained for hemispherical cavities and for cylindrical pits. A hemispherical cavity may give a maximum propagation rate if the plane of the unpitted surface is at one location while a cylindrical pit may give a maximum propagation rate if the location of the unpitted copper surface is at another location corresponding to a slightly different local pH.